FUNCTIONAL ANALYSIS OF ENTEROCYTE-FATTY ACID BINDING PROTEINS

By

HIBA RADHWAN TAWFEEQ

A dissertation submitted to the

Graduate School-New Brunswick

Rutgers, The State University of New Jersey

In partial fulfillment of the requirements

For the degree of

Doctor of Philosophy

Graduate Program in Nutritional Sciences

Written under the direction of

Dr. Judith Storch

And approved by

_____

_____

_____

_____

_____

New Brunswick, New Jersey

October, 2022

ABSTRACT OF THE DISSERTATION

Functional Analysis of Enterocyte-Fatty Acid Binding Proteins

By Hiba Radhwan Tawfeeq

Dissertation Director:

Dr. Judith Storch

The enterocyte fatty acid binding proteins (FABP), the liver FABP (LFABP, FABP1) and intestinal FABP (IFABP, FABP2) are members of small molecular weight 14-15kDa FABP family that are expressed in various mammalian tissues. LFABP is expressed in both the liver and the intestine while IFABP is solely expressed in the intestine. Previous studies in chow fed mice null for either LFABP ($LFABP^{-/-}$) or IFABP ($IFABP^{-/-}$) suggested that the two proteins are functionally distinct. Challenging $LFABP^{-/-}$ and $IFABP^{-/-}$ mice with high fat diet (HFD) revealed a divergent phenotype, underscoring functional differences. $LFABP^{-/-}$ mice appear to be a model for a metabolically healthy obese (MHO) phenotype, while $IFABP^{-/-}$ mice remained lean when compared to their respective wild-type (WT) control mice. In the present studies, the luminal bacteria content and its metabolite the short chain fatty acid (SCFA) were examined to assess whether there is a relationship between the observed dramatic whole-body phenotypic divergence of $IFABP^{-/-}$ and $LFABP^{-/-}$ mice and the gut microbiome. We found that the lean $IFABP^{-/-}$ mice had the shortest intestinal transit time, and higher fecal output and abundance of potentially beneficial bacterial guilds. By contrast, $LFABP^{-/-}$ mice were found to have a longer intestinal transit time, less fecal output and more bacterial guilds containing bacteria associated with obesity. Both $IFABP^{-/-}$ and

LFABP$^{-/-}$ mice under both chow diet and HFD were found to have a higher levels of fecal SCFAs compared to the WT control mice. Thus, the alterations in gut bacterial communities and their metabolites are associated with many of the phenotypic changes observed in LFABP$^{-/-}$ and IFABP$^{-/-}$ mice. Since LFABP is expressed both in the liver and in the intestine, it is not clear whether the ablation of liver-LFABP, intestine-LFABP or the ablation of LFABP from both tissues is required to induce the MHO phenotype. In order to get a further insight into the role of liver-LFABP in the observed MHO phenotype, a conditional knock out LFABP mice (LFABP cKO) in which the gene was ablated only in the liver, was generated. Like HF fed whole-body LFABP$^{-/-}$ mice, liver-specific LFABP$^{-/-}$ (LFABP$^{liv-/-}$) mice were found to have better capacity for endurance exercise when compared to their WT “floxed” controls (LFABP$^{fl/fl}$) mice. Female LFABP$^{liv-/-}$ mice were found to be more obese after the HF feeding challenge, with greater body weight gain and fat mass (FM). However, despite their obesity, female LFABP$^{liv-/-}$ mice were protected against HFD induced hepatic steatosis. Thus, in female mice the liver specific ablation of LFABP is enough to induce the MHO phenotype observed in the whole body knockout mouse. Males, however, may require the ablation of either intestine-LFABP or both liver- and intestine-LFABP to induce the full MHO phenotype. Taken together, this work has revealed a role of the enterocyte FABPs in modulating intestinal bacterial content and its metabolites. Furthermore, these studies demonstrate a role of liver-LFABP in efficient hepatic uptake and trafficking of lipid in mice fed HFD.

Acknowledgements

I would like to thank Dr. Judith Storch for being my graduate mentor through the years of my research project. I feel very privileged to have had the opportunity to work in her lab and learn from her and from the other lab members. I am very grateful for the financial and emotional support that Dr. Storch has offered me during Covid-19 outbreak when I was struggling with three kids without my husband. I am also thankful for the members of my committee, Dr. Harini Sampath, Dr. Joseph Dixon and Dr. William Blaner for offering helpful criticisms, suggestions and advices which helped me to structure my thesis.

I have been fortunate to work with wonderful people in Storch laboratory during my PhD journey. Great thanks to our senior lab technician Yinxiu Zhou. I really appreciate all the help and the time she spent training me when I first joined the lab; she taught me all what I need in animal surgery and was generous with her expertise in all the experiments that I conducted during my research work. I would also like to thank our former post doc Dr. Olga Ilnytska and our former PhD student Dr. Heli Xu for all of the advice and guidance that they have provided me. I am so grateful to our former PhD student Dr. Atreju Lackey for his endless support and for all the advices and suggestions that he has provided me even before I joined the lab and till this moment while I am writing my thesis. I would like to thank the other graduate student in the lab, Anastasia Diolintzi, who is also doing research on the FABP project but different aspects. I really enjoyed working with all the people in the lab and got benefit from our conversations and friendly talks in the past few years.

I would also like to thank all the undergraduate students that I have had the opportunity working with in the lab. All were hard workers and dedicated students who helped me in different parts of this project and hopefully the experience they got while working in the

lab will help them in their future career. I also appreciate all the help and support that I received from staff and faculty members in the Graduate School and Nutritional Sciences Department. I would like also to thank Dr. Liping Zhao and his lab members Dr. Yan Lam and Guojun Wu for helping us in doing fecal microbiome analysis; Deepth Kumaraswamy from Dr. Harini Sampath lab for helping us in analyzing fecal short chain fatty acids.

I would like to show my gratitude to my country, and to the enormous effort that the Higher Committee for Educational Development in Iraq (HCED) has done to award the Iraqi students this great opportunity to study in the United States. I highly appreciate the scholarship honor and the financial support that HCED has given me.

Last but not least, my forever cheerleaders, my family, remind me that I am not alone in my journey. From the bottom of my heart I would like to thank my mother for supporting me and for taking care of my kids during the hardships and obstacles I have encountered especially at the time of Covid-19 outbreak. My brother, my sister, and all of the other members in my family, thank you for the warm feelings and wishes you send me cross the continents. My husband, Thamer Omar, I am very grateful and appreciative to you, none of this would have been possible without your kindness, patience and support during this endeavor.

Dedication

I would definitely dedicate this achievement to my kids; my father (may Allah have mercy on his soul), who has always been my source of inspiration.

Table of Contents

List of Tables

Chapter 1

Chapter 2

Chapter 3

List of Figures

Chapter 1

Chapter 2

Chapter 3

List of Abbreviations

2-AG	2-arachidinoylglycerol
Acaa1b	Acetyl-CoA acyl transferase 1b
ACBP	Acyl-CoA-binding protein
ACC1	Acetyl-CoA carboxylase 1
Acox1	Acyl-CoA oxidase-1
ACSL	Acyl-CoA synthetase long chain
AEA	Arachidinoylethanolamide
AMPs	Antimicrobial peptides
ASM	Acid soluble metabolite
AUC	Area under the curve
Cav-1	Caveolin1
CB1R and CB2R	Cannabinoid 1 and 2 receptors
CCK	Cholecystokinin
CD36	Cluster of differentiation 36
CE	Cholesteryl esters
cKO	Conditional knockout
CPT1 and CPT2	Carnitine palmitoyl transferase I and II
DG	Diglycerides
DGAT1 and 2	Diacylglycerol acyltransferases 1 and 2
DNL	*De novo* lipogenesis
ECs	Endocannabinoids
EECs	Enteroendocrine cells
eWAT	Epidedmal white adipose tissue

FABPpm	Plasma membrane fatty acid binging protein
FABPs	Fatty acid-binding proteins
FAs	Fatty acids
FASN	Fatty acid synthase
FATP4	Fatty acid transport protein 4
FFA	Free fatty acid
Fgf21	Fibroblast growth factor 21
FM	Fat mass
G3P	Glycerol-3-phosphate
GIP	Gastric inhibitory polypeptide
GLP-1	Glucagon-like peptide 1
GOT	Glutamic oxaloacetic transaminase
GPAT	Glycerol-3-phosphate acyltransferase
GPRs	G-protein coupled receptors
HFD	High fat diet
Hmgcs	3-hydroxy-3-methylglutaryl-CoA synthase
HNF4α	Hepatocyte nuclear factor 4α
HSCs	Hepatic stellate cells
IECs	Intestinal epithelial cells
IFABP	Intestinal Fatty acid binding protein
LCFA	Long chain fatty acid
LFABP	liver Fatty acid binding protein
Lipc	Hepatic TG lipase
LPL	Lipoprotein lipase
LPS	Lipopolysaccharide

MCFA	Medium chain fatty acid
MG; MAG	Monoglycerides; monoacylglycerol
MGAT	Monoacylglycerol acyltransferase
MTTP	Microsomal triglyceride transfer protein
PCTVs	Prechylomicron transport vesicles
PL	Phospholipids
PPRE	Peroxisome proliferator response element
PRRs	Pattern recognition receptors
PUFA	Poly unsaturated fatty acids
PYY	Peptide tyrosine tyrosine
RER	Respiratory exchange ratio
SCFAs	Short chain fatty acids
SCP2	Sterol carrier protein 2
SFA	Saturated fatty acids
TG	Triglycerides
TLRs	Toll-like receptors
UFA	Unsaturated fatty acid
VLDL	Very low-density lipoprotein

Chapter 1

Introduction and Review of the Literature

Introduction

Dietary Lipids

Lipids are hydrophobic small molecules that can be dissolved in non-polar solvents. They include fatty acids (FAs) (which fall into two categories, saturated FA (SFA) and unsaturated FA (UFA)), sterols, fat-soluble vitamins (vitamins A, D, E, and K), certain hormones, waxes, monoglycerides (MGs), diglycerides (DGs), triglycerides (TGs), and phospholipids (PL) [1]. The three main important functions of lipids in the body are regulating signaling pathways (e.g. steroid hormones and FA amides), storing energy (primarily TGs), and forming structural components of cell membranes (primarily PLs and cholesterol) [1,2]. The most abundant form of dietary lipid is TG, which is considered both a major source of energy as well as the essential FAs linoleic and linolenic acid [3].

A Westernized diet is high in calories and rich in SFA, cholesterol and simple sugars (sucrose and fructose), and may be low in essential poly unsaturated FAs (PUFAs), i.e., linoleic acid (18:2,ω6) and γ-linolenic acid (18:3,ω3) and low in fiber; this may result in a positive energy balance and body weight gain [4,5]. A positive correlation has been noted between high dietary fat intake and the increase in adiposity; many studies have shown that diets rich in fat, in which fat provides about 30 % of the total energy, can easily induce obesity in humans [6]. High fat diet (HFD) not only induces obesity in humans but also promotes adiposity in animals. In both mice and rats a positive relationship has been found between the amount of fat ingested and body weight or fat tissue gain [7], thus rodent models have been used to gain insight into human obesity.

Obesity is considered to be a major risk factor for chronic diseases such as coronary heart disease, hypertension, type 2 diabetes, fatty liver disease, osteoarthritis and some types of cancer [8,9]. The prevalence of obesity around the world is increasing, with 650 million

(13%) adults being obese and 1·9 billion (39%) overweight in 2016 [10]. It is estimated that the prevalence of obesity in the United States in 2017-2018 was 42.4% in adults and 19.3% in children and adolescents [11]. Although dietary fat is one of the factors inducing obesity, it is also of integral importance to human health, and its ingestion and absorption have many effects on metabolically active tissues, including the liver, gastrointestinal tract and even adipose tissue. Therefore, it has become a necessity to understand how dietary lipids are digested, absorbed, metabolized and processed by the body tissues, allowing for more effective strategies to be developed to properly manage weight and maintain health by nutritional and/or pharmacological interventions.

Overall, the studies described in this dissertation aimed to investigate the functions of two important fatty acid-binding proteins (FABPs); the liver-FABP (LFABP or FABP1) which is expressed in the liver and the intestine, and the intestinal-FABP (IFABP or FABP2) which is solely expressed in the intestine. Additionally, the studies provide novel information about the influence of LFABP and IFABP on the gut microbiota composition, and whether this influence is associated with the observed dramatic whole-body phenotypic divergence observed in IFABP$^{-/-}$ and LFABP$^{-/-}$ mice.

Lipid Digestion

The digestive system is composed of the gastrointestinal tract (mouth, pharynx, esophagus, stomach, small intestine, large intestine, and anus) and accessory organs (salivary gland, liver, pancreas, and gallbladder) [12]. The first step of lipid digestion begins in the oral cavity. The chewing process helps to mechanically break large aggregates of lipids and other macro nutrients into smaller particles. In humans, the saliva contains low levels of the enzyme lingual lipase, which is secreted by the lingual serous (von Ebner) glands of the tongue where it causes a simple enzymatic digestion of lipids [13,14]. Despite

the low amounts of lipolysis that occurs in the oral cavity, however, it plays an important role in dietary fat sensing [15]. The pH optimum of the enzyme lingual lipase is 3.5-6 and most of its action occurs in the stomach [14,16]. Additional mechanical mixing by the gut helps to disperse fat molecules into emulsion particles, making them more accessible to the lipase produced by the stomach, i.e. gastric lipase which is secreted by chief cells and acts at the acidic pH in the stomach [14]. Lingual and gastric lipases play a minor role in total fat digestion, and the majority of enzymatic digestion of TG and other lipids mainly occurs in the intestinal lumen [16,17].

Peristaltic movement of the gut helps to emulsify lipid particles and forms chyme that moves down to the small intestine for further digestion. When chyme reaches the first section of the small intestine, the duodenum, additional organs participate in lipid digestion, including the gallbladder, which stores bile that is made in the liver, and the pancreas that secretes pancreatic juice. Bile salts are an effective emulsifier that act as detergents due to their amphipathic structure, having both a hydrophobic side attached to the lipid droplets and a hydrophilic side facing luminal liquid contents. Bile salts help break large lipid globules into smaller droplets to optimize the surface area of the particles to expose them to digestive lipases [18-20].

Pancreatic lipase is the most effective lipase, responsible for up to 70% of dietary TG hydrolysis. It is secreted from the pancreas together with a small protein cofactor, co-lipase, into the small intestine for further enzymatic digestion of TG in the lipid emulsion. Breaking down of the remaining TG yields two free FAs (FFAs), and one MG which has one FA still attached to the glycerol backbone at the sn-2 position. The lipid droplets now contain MG, and FA, in addition to cholesterol and PLs, and these key lipid components combine and package themselves into micelles which are particles in colloidal solution

[20,21]; the increased surface area of the micelles promotes the absorption of their component lipids by the small intestine.

Small Intestinal Structure

The largest part of the gastrointestinal tract includes the small and large intestines. The small intestine, where most of digestion and absorption of nutrients take place, can be divided into three sections: duodenum, jejunum, and ileum. The intestine has four layers: mucosa which has three sublayers (epithelium, lamina propria and musclaris mucosa), submucosa, muscular layer, and serosa (adventitia) (Fig. 1-1). Jejunum is the main site for lipid absorption while bile acid reabsorption occurs in the ileum [22,23].

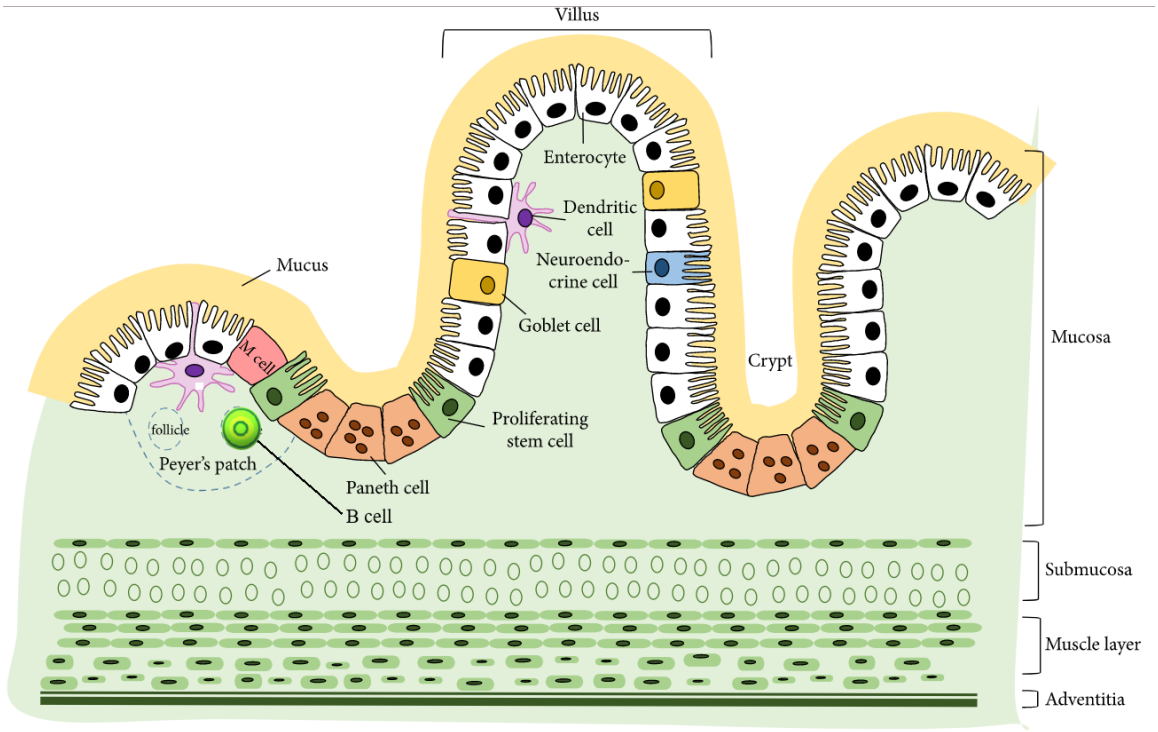

Figure 1-1: Small intestine structure. The main four layers of the small intestine are mucosa, submucosa, muscle layer, and adventitia. The major epithelial cells of the gastrointestinal tract that are present in the small intestine include enterocytes, goblet cells, enteroendocrine cells, Paneth cells, B cells, M cells, dendritic cells, stem cells, and others. These cells are arranged in a single layer within the mucosal layer. The illustration is adapted with edit from Kong *et al.*, 2018 [23].

The mucosal lining of the intestine at the luminal (apical) surface forms fingerlike projections called villi surrounded by crypt structures (Fig. 1-1). The intestinal epithelial cells (IECs) in the mucosal layer, arranged in a single layer, are composed primarily of the enterocytes (in the small intestine) and colonocytes (in the large intestine) and interspaced by other specialized cells [24,25]. The aged IECs undergo apoptosis, shedding off the top of the villi, and are replaced every 2-6 days by new cells produced by differentiation of stem cells located at the base of the crypts which migrate up across the villi-crypt axis.

The stem cells give rise to progenitor stem cells that have the ability to differentiate into other mature IECs [25]. Different cell types are present in the apical intestinal epithelium, including enterocytes, goblet cells, Paneth cells, microfold (M) cells, hormone-producing enteroendocrine cells (EECs) and many others (Fig. 1-1) [26]. IECs are tightly connected by paracellular proteins called tight junction proteins which regulate the permeability of the epithelium [27].

Enterocytes are the most abundant intestinal epithelial cells (representing up to 80 % of the small IECs) where they play a pivotal role in the absorption of nutrients and secretion of immunoglobulins. Goblet cells are less abundant and secrete a variety of mucin glycoproteins which form the mucus layer. In addition to its function in protection against invading bacteria, mucus act as a lubricant to facilitate food passage through the intestines while also protecting the intestinal walls from the effects of digestive enzymes [28,29]. Paneth cells are only expressed in the small intestine, mainly in the ileum, and are located at the base of the crypts. They have a longer lifespan than the other epithelial cells and their function is to produce antimicrobial peptides (AMPs) and proteins like α-defensins and C-type lectins. IECs express microbe-associated molecular pattern or what are called pattern recognition receptors (PRRs). Their function is to sense the presence of microbial antigens. Toll-like receptors (TLRs) are a type of PRR that is expressed on Paneth cells and used for pathogen detection. The activation of TLR4 by lipopolysaccharide (LPS), the major gram-negative bacterial product, stimulates Paneth cells to produce AMPs [28,30,31]. The follicle-associated epithelial cells, the M cells, also express a high levels of TLR4, and together with the dendritic cells (DC) facilitate antigen uptake from the intestinal lumen. Additionally, B cells residing in the intestinal mucosa within Peyer's patches, produce mucosal immunoglobulin A, which helps to add further protection to the epithelium against bacterial overgrowth [24]. EECs include several cell types, such as I, L,

Mo, N and others; are involved in nutrients sensing, modulating food intake and intestinal motility via hormones production (to be discussed below). In addition to their expression in Paneth cells and M cells, TLR 1, 2, and 4 are expressed in EECs. Stimulation of TLRs promote IECs to secrete inflammatory cytokines which play a role in intestinal disease progression [32].

The mucosal layer adds structural support to the intestine via the muscularis mucosa which consists of a thin layer of muscle. The other layer of the small intestine beneath the mucosa is the submucosa where the lymphatic capillaries are embedded. After this layer comes the muscularis layer which is composed of an inner circular layer and a longitudinal outer muscular layer. Stimulation of afferent sensory neurons by intestinal wall tension due to the presence of chyme, results in peristaltic contraction of muscularis layer which assists in the movement of foodstuffs distally. The serosal layer is located underneath the muscularis layer, and helps in the movement of the intestine within the peritoneal cavity through lubricant secretion [22,23].

Lipids Sensing by EECs and Intestinal Motility

EECs act as chemoreceptors (Fig. 1-1); in response to various stimuli and nutrients they release intestinal peptide hormones into the bloodstream to activate nervous responses. They express several types of receptors such as the G-protein coupled receptors (GPRs) FFAR1/GPR40 and FFAR4/GPR120 which are stimulated by medium and long chain FAs (MCFA and LCFA) and other nutrients. Furthermore, EECs express carbohydrate receptors, and peptide and amino acids receptors. Most interestingly, they express GPR41/43 which has the ability to sense bacterial metabolites such as short chain FAs (SCFAs), thus in turn modulating energy homeostasis, immunity and intestinal barrier function [32,33].

The activation of L cells, one of the EECs, results in the secretion of glucagon-like peptide 1 (GLP-1) and peptide tyrosine tyrosine (PYY). These hormones assist in controlling glucose homeostasis, appetite, promote satiety and reduce gut motility [32,34]. Other hormones secreted by EECs include gastric inhibitory polypeptide (GIP) secreted by K cells, motilin secreted by Mo cells, secretin from S cells and neurotensin secreted by N cells. All of the aforementioned hormones function to control intestinal motility. Cholecystokinin (CCK) is another peptide hormone released by I cells when stimulated by lipids entering the small intestine [35]. CCK assists in lipids digestion by stimulating the pancreas and gallbladder to release pancreatic enzymes and bile acids, respectively. While CCK and serotonin reduce food intake, ghrelin produced by the stomach increases food intake in response to fasting [33]. Leptin is made in both adipose tissue and P cells of the intestinal epithelium; leptin acts to regulate energy balance by inhibiting food intake [32]. There is also Somatostatin which is secreted by endcrine D cells and regulates a wide variety of physiological functions [36]. Gastrointestinal hormones released by EECs have their receptors on the vagus nerve endings that are embedded in the intestinal mucosa and can directly stimulate vagal afferent neurons resulting in the regulation of food intake and intestinal motility [33,37].

In addition to the effect on food intake and intestinal motility of gut hormones, it has been found that a class of lipid metabolites, the endocannabinoids (EC), have similar effects. Anandamide (arachidinoylethanolamide, AEA) and 2-arachidinoylglycerol (2-AG, which is a 2-MG) are agonist of two GPRs known as cannabinoid 1 and 2 receptors (CB1R and CB2R). These receptors are abundantly expressed in the brain and gastrointestinal tract. Activation of CB1R by an agonist such as 2-AG results in inhibition of gastric acid

secretion, promotion of food intake, and slowing of gastric emptying rate and intestinal motility, while antagonists such as Rimonabant reverses these actions [38-41].

Large Intestine

Unlike the small intestine, the large intestine does not have villi; instead it has a surface epithelium that is interspaced by colonic glandular crypts that have the same function as the small intestinal crypts. The epithelium of the mucosal layer in the large intestine is composed of enterocytes (colonocytes), EECs, and goblet cells [24,42]. Paneth cells do not exist in the colon, therefore there are no Paneth cells' α-defensin secretions [43]. For this reason, the mucous secreted by goblet cells plays an important role in separating the epithelium from luminal microbes; the amount of goblet cells reaches a maximum in the distal colon [42,44]. The large intestine has a smaller surface area but larger diameter than the small intestine. It functions to ferment the remaining chyme that reaches it following processing by the small intestine; the luminal microbiota ferment the chyme and the large intestinal colonocytes absorb the fermentation products like SCFAs [42]. Additionally, the large intestine helps to reabsorb water, leading to chyme condensation and feces formation [45]. While the mucus is thin, penetrable and discontinuous in the small intestine, the large intestine has two mucus layers the inner tightly adherent layer that is sterile and free of bacteria and rich with other AMPs such as cathelicidin, and the outer loosely adherent layer which is colonized by commensal bacteria [43,46].

Gut Microbiome

Because of the similarity at the genus level, and the apparently similar functions, mouse gut microbiota is used as a model to study the human gut microbiota, typically by investigating the prevalence of bacteria in the mice feces [47]. The gut microbiome consists of commensal (beneficial) and detrimental (pathobionts) microorganisms, which

are usually in neutral state within the gut ecosystem [48]. As in humans, more than 90% of the bacterial phyla that reside in the distal part of the intestine are composed of 2 main bacterial divisions, the *Bacteroidetes* and the *Firmicutes* which are in a state of symbiosis [49-51]. Studies in human subjects and genetically obese C57BL/6J ob/ob mice revealed that obesity is associated with higher relative abundance of the *Firmicutes* and lower relative abundance of the *Bacteroidetes* than their lean controls [50,51].

The epithelium of the gut is considered the first line of defense, transmitting information to the immune system of the lamina propria and secreting different compounds like mucus and defensins [52]. Microbial interaction can help in the development of innate and adaptive immune systems. This communication with the gut microbes is mediated by TLRs and nucleotide oligomerization domain-like receptors which are components of the PRRs [53]. These receptors are able to recognize a pathogen related substances like LPS or damaged parts from the microorganisms. Thus, the immune cells in the gastrointestinal tract are always exposed to a large number of microbial antigens and metabolites [53]. A disturbance of the gut barrier integrity as a result of microbiota dysbiosis is associated with an increase in intestinal permeability and attenuation of the mucus layer; as a consequence antigens and endotoxins can enter the systemic circulation causing low grade inflammation, and subsequently obesity and insulin resistance [54].

Despite the detrimental effects of some of the bacterial species on gut integrity, there are many other bacteria that have beneficial effects on the host. Lactic acid producing bacteria, *Lactobacillus*, have many beneficial effects including protection against peptic ulcer and diarrhea, enhancing the immune system, prevention of colon cancer and other functions [55]. Gut microbes can ferment the indigestible dietary fiber resulting in the liberation of SCFAs, mainly butyrate, propionate, and acetate. SCFAs are also known to

modulate intestinal epithelium integrity via stimulating the production of mucus by the goblet cells [56]. They also have the ability to stimulate the production of gut peptides such as GLP-1 by L-cells, which is involved in the regulation of energy balance and glucose homeostasis [34]. Butyrate, produced mainly by *Faecalibacterium prausnitzii*, has an important role in decreasing mucosal inflammation and reducing the oxidative stress, and is the primary energy source for the colonic epithelium, thereby enhancing the intestinal epithelial barrier integrity and promoting immune system homeostasis [57,58]. Propionate and acetate are also known to have the same activity as butyrate but to a lesser extent [59]. It has been found that chronic inflammatory bowel disease is associated with lower levels of butyrate, supporting its essential role in maintaining gut barrier integrity [60].

Also of interest regarding the gut microbiome is the proposed crosstalk between gut microbiota and the EC system. In this interaction LPS released from the bacteria causes robust production of AEA in adipose tissue macrophages [61] which in turn activates intestinal EC receptor CB1R, leading to increased gut permeability, endotoxenimea, as well as increased appetite and fat mass (FM) development [62,63]. Additionally, it has been found that providing mice with oral inulin (an indigestible fiber) was associated with both the higher levels of fecal SCFAs and enhanced endurance exercise capacity, further supporting the crosstalk between organs, i.e. gut and muscle [64]. Recent studies have indicated that SCFAs and secondary bile acids produced by commensal bacteria can protect against mitochondrial dysfunctions caused by reactive oxygen species accumulation and inflammation that occurs in response to endurance exercise training [65].

In order to understand the contributions of gut microbiome, many studies have employed germ free mice. These mice were unhealthy and have a compromised immunity because

of the absence of commensal bacteria that help to shape the immune system. However, they were resistant to diet induced obesity [66,67]. This resistance to obesity, due to the absence of their gut microbiota, is thought to be caused by alterations in the expression of genes involved in energy oxidation and fat storage [66,67]. It has been found that transplanting germ-free mice with human gut microbiota coupled with a high fat or high sugar diet resulted in induction of obesity [66,67]. Studies such as this suggest that diet composition can promote alterations in gut microbiome composition [68]; it is important to note that these alterations can be beneficial or detrimental.

It is well established that HFD induced obesity is associated with disturbances in the gut microbial community which cause an increase in intestinal bacterial species that produce endotoxins like LPSs and trigger low grade chronic inflammation by the activation of TLRs signaling pathways [69]. Subsequently, this alters the intestinal barrier structure via a reduction of tight junction proteins [70], and elevation of inflammatory mediators in the ileum and colon of conventionally raised mice but not in germ free mice [71]. Many groups have reported that a HFD is capable of modulating gut microbiota severely enough to cause dysbiosis, which occurs in association with increased body weight, inflammation, and insulin resistance [70,72-74].

Intestinal Lipid Metabolism

While a minor amount of chyme passes through the gastrointestinal tract and reaches the colon for bacterial fermentation of the indigestible fiber to produce SCFAs, a majority of the products of dietary nutrient digestion are absorbed in the proximal part of the small intestine. About 95% of ingested fat is absorbed with remaining 5% being excreted in the feces [75]. Micelle formation in the proximal intestinal lumen by the action of bile and pancreatic secretions is important in facilitating efficient fat absorption [76]. Due to their

amphipathic nature, lipid micelles are able to diffuse across the unstirred water layer between villi. This promotes the dissociation of the products of dietary lipid digestion, primarily FAs and MG, and their uptake across the apical membrane of the absorptive enterocytes in the jejunal mucosa, where the majority of LCFAs absorption takes place [76-78]. Most of the bile acids are reabsorbed in the ileum and transported back to the liver to be stored in the gall bladder, and used again for emulsifying new fat emulsion particles entering the proximal intestine, for the induction of micelle formation [76].

The transport of lipid across the plasma membrane occurs by two major mechanisms, the passive diffusion mechanism, and the active protein-dependent mechanism. FA transport protein 4 (FATP4), cluster of differentiation 36 (CD36), plasma membrane FA binging protein (FABPpm) and Caveolin 1 (Cav-1) are highly expressed in the enterocyte and have been proposed to play a role in facilitating the uptake and transport of LCFAs from the intestinal lumen into the enterocytes [19,79]. The uptake of 2-MGs into the enterocyte is thought to be the same as for FAs; in addition to simple diffusion, it may be mediated via membrane transport proteins. Cell culture studies in Caco-2 cells demonstrated the saturable mechanism for MG uptake [80,81]. Also, it has been found that adding excess FA to Caco-2 cells medium resulted in lower uptake of 2-MG and vice versa. These findings suggested that FA and 2-MG compete each other for the same transport protein(s) for their uptake into the enterocyte. However, the other intermediate product of TG hydrolysis, DG, has no inhibitory effect on the intestinal uptake of FA or 2-MG [80,81].

When FA and MG are within the enterocytes, they are directed into different organelles for further metabolism [19]. TG is resynthesized in the endoplasmic reticulum (ER) to avoid building up of excessive intracellular FA, which can result in cytotoxicity [82,83]. In order to reach the ER, the TG hydrolysis products have to be carried in the cytoplasm by specific

binding proteins. The two major lipid binding proteins found in enterocytes are the FABPs, LFABP and IFABP [84] (to be discussed in more details later). The predominant pathway for enterocyte TG biosynthesis is the monoacylglycerol (MAG) pathway or it is called the monoacylglycerol acyltransferase pathway (MGAT). The first step of this pathway is the acylation of FA by the action of acyl-CoA synthetase long chain family members 3 and 5 (ACSL3, ACSL5) [85], or FATP4 [86], to ensure trapping of FA within the cell. Then, fatty acyl-CoA is covalently joined with MGs to form DGs in a reaction catalyzed by MGAT2 [87,88]. DGs can be further acylated by diacylglycerol acyltransferases-1 and -2 (DGAT1 and 2) leading to the reformation of TG [88,89]. This route accounts for more than 75% of the TG that is synthesized in the enterocytes. The other pathway for intestinal TG synthesis is the glycerol 3-phosphate (G3P) pathway which only accounts for 20–30% of TG synthesis [88]. In the ER, TG is then packed along with cholesterol, apolipoproteins and other lipids into prechylomicrons which are enclosed inside vesicles, forming what is called prechylomicron transport vesicles (PCTV). A multiprotein complex is required for PCTV budding from the ER and traveling to the Golgi apparatus, including CD36, apoB48, LFABP and other proteins [90,91]. The PCTV fuse with the Golgi apparatus for final lipidation into ApoB-containing mature chylomicrons. Then, the chylomicrons are exported through the basolateral membrane, and reach the general circulation via lymphatic system within one to two hours after consuming a meal [79,92].

TG that is synthesized from FA and MGs in the enterocytes can also be stored as cytosolic lipid droplets to be used when it is needed [93]. Some of the FAs that were acylated by ACSLs can be incorporated into membrane PLs, where the composition of FAs can influence membrane fluidity [94]. FA entering the enterocytes from basolateral membranes can be directed to disposal pathways other than chylomicron secretion, like mitochondrial or peroxisomal oxidation or it can be used in PL synthesis while luminal FAs are primarily

incorporated into TG [95,96]. Furthermore, FAs in the enterocyte serve as ligands for peroxisome proliferator-activated receptors (PPARs) which are involved in regulating gene expression and cell signaling [97].

When chylomicrons reach the systemic circulation, lipoprotein lipase (LPL), which is located on the surface of endothelial cells in capillaries, acts to hydrolyze chylomicron bound TGs, resulting in the release of FA for local cellular uptake by adipose tissues and muscle for storage and/or to provide energy substrates, respectively, during the fed state [98,99]. The residuals of chylomicron, called chylomicron remnants, will be recognized by their receptors leading to endocytic uptake by hepatocytes [100]. In contrast to LCFAs which are usually incorporated into chylomicron in the enterocyte before entering the circulation, SCFAs and MCFAs that have 14 carbons or less, enter directly to the liver from the intestinal tract via the portal vein as FFAs [101,102].

Liver Structure

The liver is a metabolically active organ that performs many functions including bile formation and excretion, regulation of carbohydrate homeostasis, lipid metabolism, and synthesis and secretion of plasma lipoproteins. Furthermore, it is the place for the production of urea, clotting factors, albumin, and antibody production. It also plays an important role in drug metabolism or detoxification, defending the body against foreign substances [103,104].

As shown in figure 1-2, each lobe of the liver has around 50,000 to 100,000 lobules, which are the basic structural subunits. Hepatocytes, the functional cells in the liver, are arranged in radial hepatic cords known as the cellular plates which are comprised of two hepatocytes in thickness [105,106]. These cellular plates are arranged around a central

vein, forming the lobules, and are separated from each other by the sinosuidal capillaries that receive their blood from the portal vein and hepatic artery. The portal vein supplies the liver with nutrients from the intestine. Within the hepatic cellular plates there are the cannaliculi which are the bile transporting channels that drain to form bile ducts. Together, the hepatic artery, the portal vein and the bile duct form what is called a portal triad which borders the hepatocytes [106]. A second group of cells, called macrophage (Kupffer) cells, play an important role in antibody production, and phagocytosis of foreign particles and bacteria transported to the liver via the portal vein [107]. Lymphocytes are another cell type in the liver; they contribute to immunity and include several immune cells, such as natural killer T cells and other innate immune cells [108]. Under normal conditions hepatic stellate cells (HSCs), the lipid storing cells, assist in retinol uptake and storage in the form of esters. In addition to retinyl easters the lipid droplets in HSCs store other neutral lipids, FFA and other lipids as well. HSCs also produce the extracellular matrix (collagen) and play a major role in fibrinogenesis and in repairing hepatic tissues after injury [109,110].

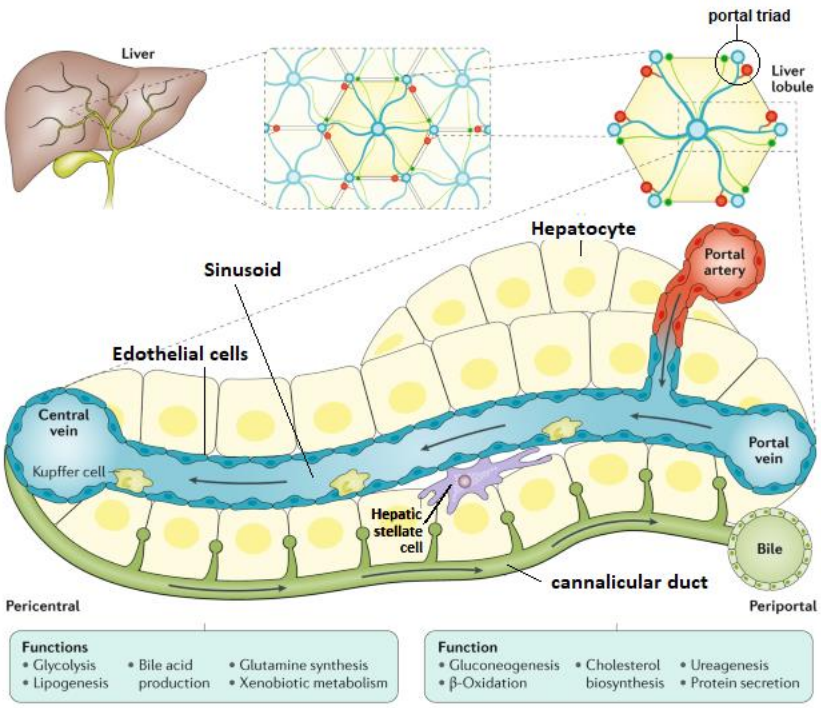

Figure 1-2: Liver structure and functions. The hepatic cellular plates contain, in addition to the hepatocytes, other cell types including endothelial cells which surround the sinusoid, Kupffer cells attached to the sinusoidal wall, HSCs and other cells. The illustration is adapted with permission from ref. [104]. Copyright 2019, Springer Nature.

Liver Lipid Metabolism

The liver plays a major role in lipid metabolism, importing FFA, as well as synthesizing, storing, and exporting lipids [8,111,112]. The remnant receptors on the surface of the liver recognize chylomicron remnants through their apoE content. Then, following endocytosis, chylomicron remnants are digested within the lysosomes releasing glycerol, FA, cholesterol, amino acids, and phosphate [98,100]. This happens during the fed state and it is considered an exogenous or dietary source of hepatic FA (Fig. 1-3A).

Other sources of hepatic FA are the endogenous sources, which occur between meals (Fig. 1-3B). FFA enter the liver from the circulation after TG breakdown in adipose tissues. Uptake is either via simple diffusion depending on the concentration gradient, or by active transport by plasma membrane-associated proteins such as FABPpm, FATPs (2 and 5), glutamic oxaloacetic transaminase (GOT), or CD36 [113-115]. Another endogenous FA source, which occurs in the cytosol, is *de novo* lipogenesis (DNL) of FA from non-lipid sources (glucose, fructose, amino acids or acetate), where the starting molecule is acetyl-CoA [116]. Acetyl-CoA carboxylase 1 (ACC1) catalyzes the rate limiting step in this pathway, and leads to the formation of malonyl-CoA which undergoes a series of reactions including condensation, reduction, dehydration and reduction again [117]. For the elongation purpose of the newly formed FA the previous reaction cycle will be repeated. The entire reaction for FA synthesis is catalyzed by the action of the FA synthase (FASN)

complex which is present at high levels in lipogenic tissues, such as the liver [117]. Its activity is under the control of hormones (insulin and glucagon) and nutritional status [118].

In order to prevent lipotoxicity caused by high levels of exogenous or endogenously synthesized FA, the intracellular FFA and fatty acyl-CoAs in the hepatic cytosol require carrier proteins, the same as in the enterocytes. LFABP, in addition to its expression in the intestine, is also present in the liver and plays a potential role in enhancing the uptake of several hydrophobic molecules such as LCFAs and fatty acyl-CoA, and is thought to traffic them to different metabolic or signaling pathways [119-122]. In addition to its function in intracellular cholesterol transfer, sterol carrier protein2 (SCP2), is another lipid binding protein that has been reported to bind both FA and fatty acyl-CoAs [123]. Furthermore, there is acyl-CoA-binding protein (ACBP) that binds acyl-CoAs in the cytosol [124-126]. ACSL isoforms 1 and 5 mediate the activation of a LCFA to a fatty acyl Co-A, and determine the metabolic fate of FA by channeling them into various metabolic pathways for elimination. Depending on which isoform catalyzes the reaction, the elimination of FA will occur either by oxidation or by incorporating FA into TG to be secreted into the plasma as TG-enriched very low-density lipoprotein (TG-VLDL) [127-129].

Hepatic FA whether from plasma, dietary sources or DNL are esterified to generate TG and other glycerolipids on the microsomal membrane [130]. The G3P pathway is dominant in the liver for TG synthesis. The enzymes that are involved in this pathway include glycerol-3-phosphate acyltransferase (GPAT), acylglycerol-3-phosphate acyltransferase, lipins/PA phosphatases and DGAT, leading to TG synthesis from G3P [131]. Additionally, FA can be used for the synthesis of other complex lipids like PL, and are also esterified to cholesterol to generate cholesteryl esters (CE). TG, PLs, CE and other lipids are either

stored in cytoplasmic lipid droplets, or secreted into the bloodstream as VLDL particles [132].

VLDL assembly begins in the ER where the microsomal TG transfer protein (MTTP) incorporates TG into apoB100-containing particles, then it is transferred into the Golgi apparatus for further lipidation into more mature VLDL particles, which involves the activity of apoCIII and other apolipoproteins [126,133,134]. During fasting, VLDL is considered an important source of concentrated FA supply to be used by the muscle for oxidation and producing energy (Fig. 1-2B) [135]. LPL is the key molecule that directs TG-VLDL to muscle and adipose tissues, and hydrolyzes TG, allowing the release of FFA [136]. VLDL production relies on exogenous FA rather than endogenously synthesized FA; less than 5% of the TG incorporated in VLDL particles is derived from FA synthesized by DNL pathway [137,138]. The enhancement of DNL that was seen in ob/ob mice or caused by the inhibition of glucose-6-phosphatase was not associated with increased VLDL production [139,140].

Another pathway for FA disposal in the liver is β-oxidation which occurs in both the mitochondria and peroxisomes. The non-esterified form of SCFA and MCFA permeate the mitochondrial membranes and then are activated by acyl-CoA synthetase into their fatty acyl-CoA derivatives. In contrast, LCFA (FA of 14-22 carbons) are activated into their fatty acyl-CoA derivatives in the cytosol and are imported into the mitochondrial interior via carnitine palmitoyl transferase I and II shuttle (CPT1/CPT2) [102].

Higher uptake of LCFA can overwhelm the mitochondrial β-oxidation machinery, leading to incomplete oxidation and shifting acetyl-CoA toward ketogenesis where it is converted into ketone bodies (acetoacetate, β-hydroxybutyrate and acetone) instead of entering the

tricarboxylic acid (TCA) cycle [141]. The β-oxidation of very LCFA which are composed of 24-26 carbon, takes place in the peroxisomes, and is associated with heat and hydrogen peroxide production rather than production of ATP [142,143]. The end product of peroxisomal oxidation of VLCFA, octanoyl-CoA, is taken up by the mitochondria for further oxidation into acetyl-CoA [143,144]. Peroxisomal α-oxidation is specialized for the degradation of phytanic acid, a branched chain FA that can be obtained from dairy products [142]. Hepatic FA ω-oxidation occurs in the ER and produces long chain dicarboxylic acids which are further metabolized by peroxisomal β-oxidation into SCFA that can be taken up by the mitochondria for complete oxidation or directed toward the ketogenesis pathway [145]. In addition to its action in facilitating the hepatic uptake and transport of FA and acyl-CoAs to different organelles, LFABP interacts with and delivers FA and other ligands to transcription factors such as the nuclear peroxisome proliferator-activated receptor alpha (PPARα) [146]. The expression of PPARα is high in the liver because of its role in regulating hepatic lipid metabolism by inducing the expression of enzymes involved in peroxisomal and mitochondrial FA β-oxidation [147].

As mentioned previously, lipid uptake, synthesis, and disposal in the liver are usually in balance and tightly regulated. Accumulation of hepatic lipids as a result of increased FA delivery, increased synthesis, or reduced disposal via oxidation, and/or reduced fat export as VLDL particle, enhances the development of fatty liver and eventually leads to hepatic steatosis (Fig. 1-3C). Many studies have shown that the excessive accumulation of hepatic TGs is mainly due to the excessive delivery of FFA from adipose tissues and higher rate of hepatic DNL of FA, rather than a reduction in β-oxidation or VLDL export [148,149].

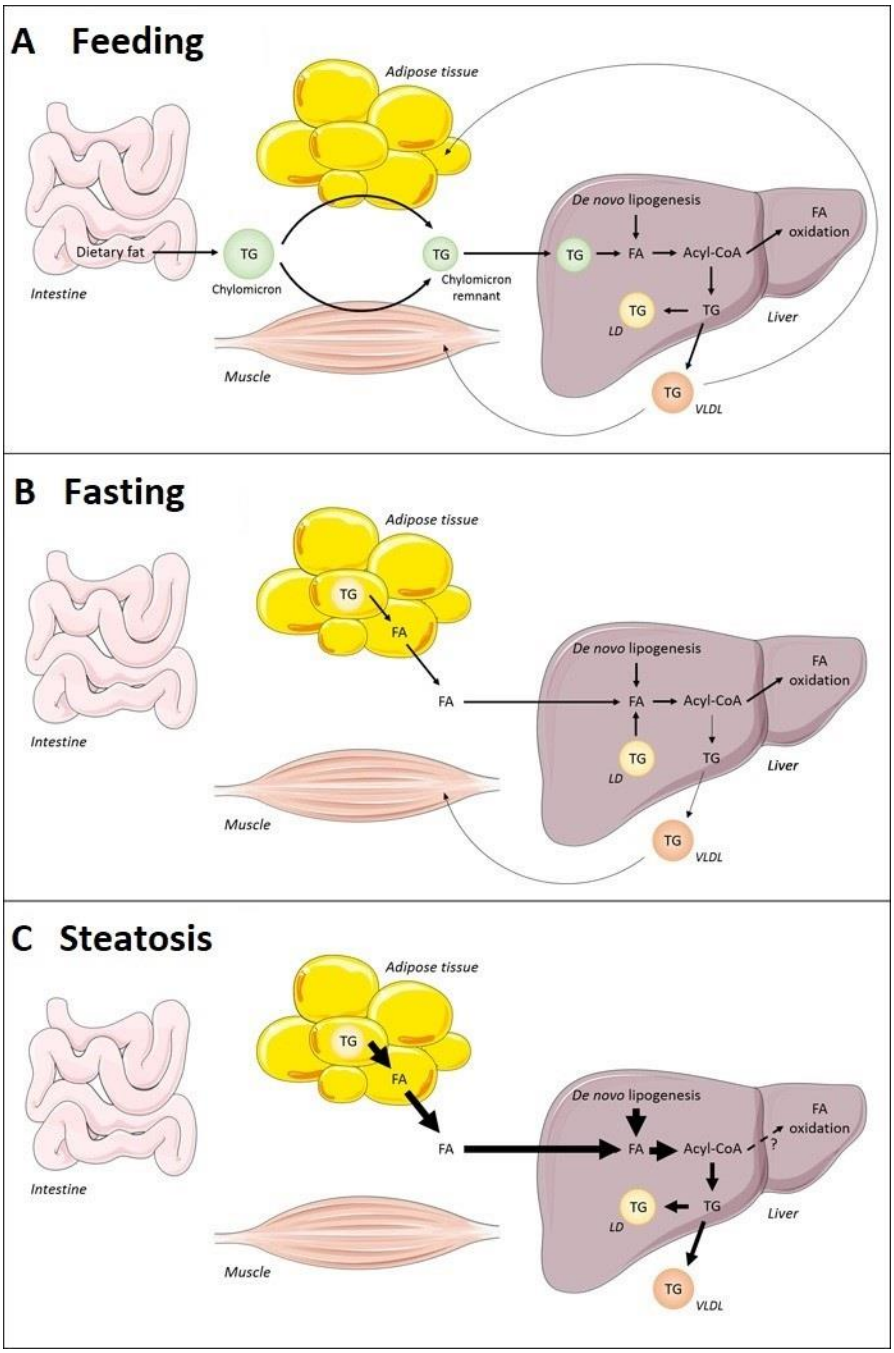

Figure 1-3: Major sources for hepatic fatty acids during feeding, fasting and hepatic liver disease. A, During the feeding state the dietary FAs are esterified into TG which is packed into chylomicrons and released into the circulation to supply lipids to muscle and adipose tissue. The resultant chylomicron remnants are taken up by the liver, releasing FAs within hepatocytes. Other source of FA in the liver is DNL where carbohydrates, such

as glucose, are utilized to produce FA. In order to metabolize FAs, they should be activated to form fatty acyl-CoA molecules, which can be directed either to oxidation or be incorporated into complex lipids, such as TG, which can be stored as lipid droplets or packed into VLDL for secretion. B, During the fasting state, TG stores in adipose tissues and hepatocytes are mobilized to release FA. DNL also contributes to FA source during fasting. C, Fatty liver disease can result from overnutrition and insulin resistance, leading to higher blood levels of FA due to the increased rate of adipose tissues lipolysis. Hepatic FA uptake and DNL will be increased, and the extra supply of FA cannot be consumed by oxidation, therefore, it will be directed towards TG synthesis leading to its accumulation in lipid droplets and VLDL overproduction. Bold arrows indicate the higher rates of metabolic activities. The illustration is adapted with permission from ref. [126]. Copyright 2018, American Physiological Society.

FABPs

As FA, of hydrophobic nature, are going to be transported within the hydrophilic cytoplasm, they will need to be carried by intracellular proteins to ensure efficient transportation and trafficking. The FABP family of proteins, discovered for the first time in the 1970s and have since been identified as cytosolic proteins that can bind not only FA but many other hydrophobic ligands as well [122,150]. These 14-15kDa proteins have highly conserved tertiary structures that are composed of 2 small α-helices and 2 antiparallel β-sheets composed of 10 β-strands, forming a “clam shell” necessary for ligand binding [151] (Fig. 1-4).

The mammalian FABP family is composed of 9 FABPs (Table 1-1) that are members of a superfamily of lipid-binding proteins which contains also retinol/retinoic acid binding proteins [152]. Unlike retinoid binding proteins which are expressed in both fully differentiated and developing tissues, FABPs are expressed only in fully differentiated tissues [153]. While most tissues express one FABP, there are some tissues having more than one type [84]. FABPs of the same type but from different mammalian species share ~ 90% homologies [154] and have high binding affinity for LCFAs (>14C) and other hydrophobic ligands [155]. FABPs play a fundamental function in facilitating the uptake and the transport of lipids to different cellular compartments, for example to the ER for synthesis and secretion of TG-rich chylomicron and for membrane synthesis; to lipid droplets for storage; they also can traffic FA to the mitochondria or peroxisomes for oxidation; or to the nucleus for signaling and regulation of gene transcription [156]. Furthermore, FABPs have an important role in maintaining membrane integrity by being reservoirs for FA in the cytoplasm, preventing lipotoxicity and protecting the cell from the detergent effects caused by high concentrations of non-protein bound FA, by trafficking

FA to enzymes involved in their synthetic incorporation into TGs and PLs, or to be directed to oxidation pathways (Fig 1-4) [156,157].

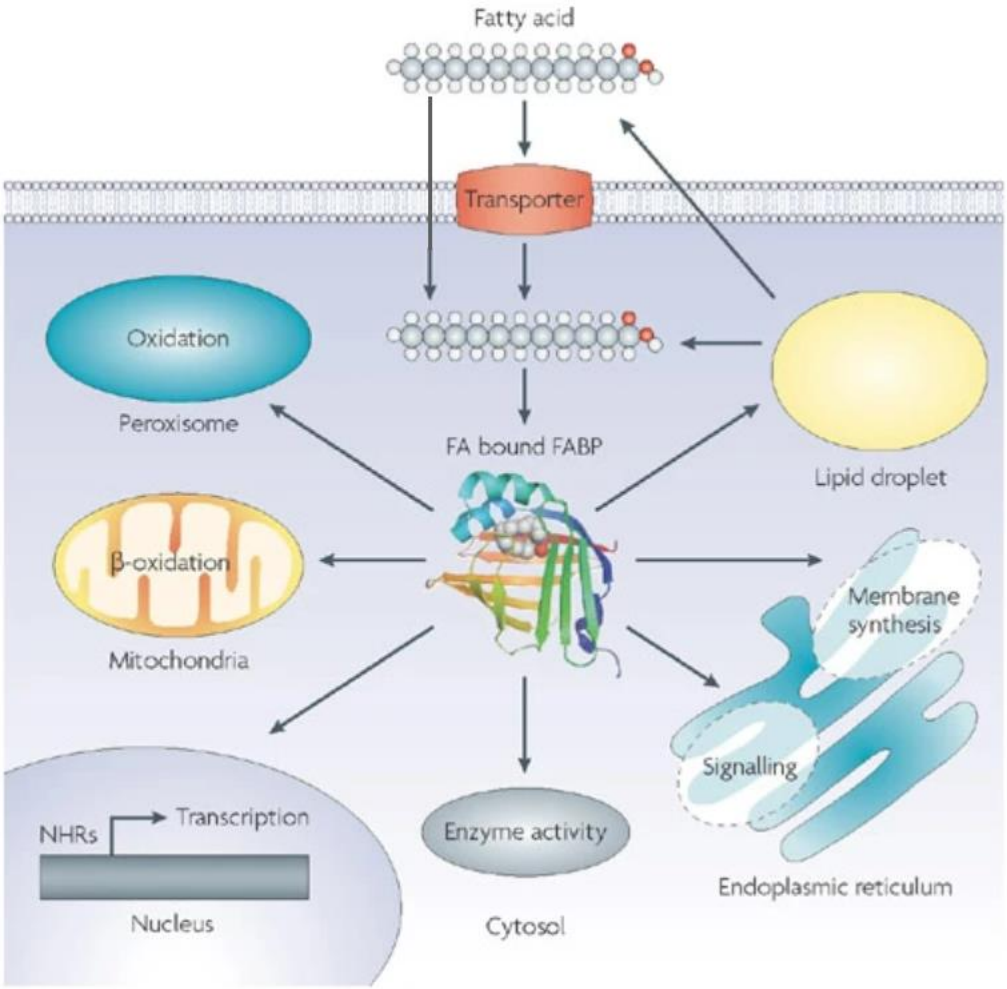

Figure 1-4: Structure and functions of FABPs. FABPs are intracellular lipid binding proteins that have been proposed to play important roles in the uptake and trafficking lipids to different compartments: for example to lipid droplets for storage; to the mitochondria or peroxisomes for oxidation; to the ER for signaling and membrane synthesis; to cytosol for regulating enzymes activity; to the nucleus for regulating the expression of genes involved in lipids metabolism via interaction with nuclear hormone receptors (NHRs). The illustration is adapted with permission from ref. [156]. Copyright 2008, Nature Publishing Group.

Table 1-1: FABPs family members [158].

Common name	Abbreviation	Expression site(s)
Liver FABP	Fabp1 (LFABP)	Liver, intestine, kidney
Intestinal FABP	Fabp2 (IFABP)	Intestine
Heart FABP	Fabp3 (HFABP)	Heart, skeletal muscle, brain, kidney, adrenal gland, mammary gland
Adipocyte FABP	Fabp4 (AFABP)	Adipocyte, macrophage
Epidermal FABP	Fabp5 (EFABP, KFABP)	Skin, adipose tissue, mammary gland, brain, intestine, kidney, liver
Ileal FABP	Fabp6 (ILBP)	Ileum, ovary
Brain FABP	Fabp7 (BFABP)	Brain
Myelin FABP	Fabp8 (MFABP)	Peripheral nervous system
Testis FABP	Fabp9 (TFABP)	Testis

The table is adapted with permission from ref. [158]. Copyright 2008, Annual Reviews.

FABP expression is high (2-5% of the total cytoplasmic proteins) in the tissues and cells that have high rates of lipid metabolism such as intestine, liver, adipose tissue and muscle. The binding affinity of FABPs to LCFAs helps to keep the concentration gradient for LCFAs uptake in the favor of passive diffusion. However, the expression of FABPs is greatly affected by intracellular FA concentration, increasing dramatically after chronic feeding of dietary lipids [159]. Also, it has been found that LFABP expression is affected by gender; being higher in female rat liver than male rat liver [160,161].

Two of these lipid binding proteins, the LFABP and IFABP, are co-expressed in the proximal part of the small intestine. Based on our previous studies, it is suggested that these two proteins do not share the same exact functions, indicating the differential role they might have [162,163]. Therefore, in the current studies, we are focusing on the functions of these two proximal enterocyte FABPs, to better understand not only their role in liver and intestinal lipid processing, but also their interaction with other lumenal content such as the microbiota and its metabolites, and its impact on the whole body responses. Thus, we are going to discuss these two enterocyte FABPs in more detail.

LFABP

LFABP was the first identified FABP. Initially it was discovered in the liver (hepatocytes and HSCs), but was later found in the enterocyte, and expressed to a lesser extent in the human kidney [122,164-166]. The presence of LFABP in the plasma is considered to be a marker for hepatocellular injury [167]. LFABP has a higher binding capacity than the other FABPs; it has two binding sites that can bind two FA ligands instead of one, with a higher affinity towards SFA relative to UFA [168,169] and two MGs [170]. In addition to FA binding, LFABP is able to bind other types of lipid species, including but not limited to prostaglandins, lysophospholipids, ECs, cholesterol, and bile acids [168,169,171-174]. In contrast to all other FABPs, which transfer their ligands by a collisional mechanism, LFABP transfers the ligands to and from PL membranes by a diffusional mechanism [158,175].

In liver cytosol, LFABP is one of the most abundant proteins, constituting 2-5% of the soluble proteins [176]. LFABP has been proposed to have several functions, starting with facilitating the uptake and intracellular trafficking of FA to different organelles [119,177-180]. Hepatic LFABP acts to direct dietary derived FA to the ER for the synthesis of TGs,

PLs and CE, and also to mitochondrial and peroxisomal oxidation [180-182]. Additionally, LFABP acts to bind and direct the exogenously derived FA into the nucleus. Inside the nucleus LFABP traffics FA to PPARα to induce the transcription of many genes that are involved in FA uptake and oxidation, including LFABP itself, which has a peroxisome proliferator response element (PPRE) [183-185]. Hepatocyte nuclear factor 4α (HNF4α) is another NHR that interacts with LFABP; it regulates a wide range of physiological activities including the expression of several hepatic genes that are involved in metabolism, cell junctions, anti-inflammatory effects, cell differentiation and organ development [186,187]. Hepatic and intestinal FA oxidation is reported to be reduced in the absence of LFABP; this reduction is thought to be due to decreased FA uptake, transport and availability without affecting the FA oxidative capacity [119,162,163,179,188,189]. Additionally, it has been reported that in Chang liver cells LFABP has an antioxidant activity that protects against cellular damage caused by reactive oxygen species [190].

In addition to its expression in the liver, LFABP is also abundantly expressed in the intestinal enterocyte. It is present in the intestinal segments where most of dietary lipid absorption takes place, i.e. in the duodenum and jejunum [191]. In rat enterocytes, it has been found that the localization of LFABP is affected by the nutritional status. During the fasting state LFABP localizes near the luminal membrane, while during feeding LFABP distributes though out the cytoplasm [192]. LFABP has a crucial role in the budding of prechylomicron transport vesicles (PCTVs) from the ER. These PCTVs are then directed to the Golgi apparatus where the prechylomicrons are further processed to form mature chylomicrons, which then leave the enterocytes and are carried through the lymphatic vessels into the general circulation [90,91,193]. Via this way, dietary lipid will reach different body compartments, and this emphasizes the important role that LFABP has in affecting

the availability of dietary lipid for other body tissues in addition to the small intestine and liver where it is expressed.

Polymorphism of LFABP

T94A LFABP, in which threonine is replaced by alanine at position 94, is one of the most common polymorphisms in LFABP. This replacement induces alteration in LFABP secondary structure, thermal stability, and conformational and functional responses to fibrates [194]. Expression of the T94A LFABP variant in human is associated with increased liver TG levels, nonalcoholic fatty liver disease and reduction in the effectiveness of fenofibrate, a PPARα agonist that is used to lower human plasma TG levels [195-197]. Additionally, transcription of LCFA β-oxidative enzymes was attenuated in human hepatocytes expressing the LFABP T94A variant relative to the predominant LFABP [196]. However, another study has shown that cultured cells expressing the T94A variant have the same antioxidant activity as the predominant LFABP [198].

IFABP

The other FABP that is expressed abundantly in the proximal intestine is the IFABP (FABP2). Unlike LFABP, IFABP is solely expressed in the small intestine (mature enterocytes) with highest levels in the jejunum [167,199,200]. Like LFABP, the localization of IFABP is more at the apical membrane of the enterocytes than the basolateral membrane and in the villi rather than crypts [201]. IFABP localization is also affected by nutritional status, being localized at the apical side rather than basolateral side during fasting [192]. IFABP has a high affinity for both saturated and unsaturated LCFA with a single ligand binding site [168,169,202], and recently it has been shown to bind ECs as well [203]. IFABP transfers FA ligands to PL bilayer membranes by a direct protein-membrane collisional mechanism that is typical of other members of the FABP family [175]. In contrast

to LFABP, IFABP is not involved in chylomicron formation [90-92,193]. However, IFABP is proposed to have a role in the uptake and transportation of luminal FA to different enterocyte organelles [192]. IFABP gene expression is regulated by mechanisms other than what was found for LFABP. Expression of the IFABP gene is induced by PYY and down regulated by the epidermal growth factor [204].

Polymorphism of IFABP

In humans, no deletions of the IFABP or LFABP genes have been reported. However, like in LFABP, a single nucleotide polymorphism has been identified in IFABP, in which alanine is replaced by threonine at position 54 (A54T) [205]. The A54T polymorphism has been reported to have a higher binding affinity for LCFA than the predominant IFABP [205]. The expression of A54T variant in humans was associated with insulin resistance, increased TG synthesis and secretion, elevated plasma TG level, and higher susceptibility to atherosclerosis [205-208]. Interestingly, a recent study has shown that IFABP serum concentration is less in patients diagnosed with Covid-19 when compared to other patients that had a non-Covid pulmonary diseases or abdominal pain [209]. The functional significance of this finding, if any, is unknown. Both IFABP and LFABP appear in the circulation as well as in the urine, when there is intestinal membrane damage or enterocyte turnover [210,211].

To study the functions of LFABP and IFABP at the whole-body physiological level, mouse models have been used.

LFABP$^{-/-}$ mice

A global knockout (KO) of LFABP (LFABP$^{-/-}$) was generated by two groups independently on the C57BL/6 background [179,189]. Schroeder and Binas group's LFABP whole-body KO mice were generated by a complete deletion of all four exons of the LFABP gene along

with the promoter region and had their first report on those mice published in 2003 [179]. These mice were backcrossed to the C57BL/6N mouse strain six times [179]. From those mice our LFABP$^{-/-}$ mice were derived and they were further backcrossed to C57BL/6J [162,163]. The other laboratory, the Davidson group also published their first report in 2003 in which green fluorescent protein was “knocked in” to exons1 and 2 of the LFABP gene [189]. These mice were kept on the C57BL/6J background [189,212].

LFABP$^{-/-}$ mice from these two laboratories were shown to have differences in body weight under HFD feeding regimen. The Schroeder group found that their KO mice gained more weight than their counterpart control mice [213,214]. In contrast, the Davidson group found that their male and female LFABP$^{-/-}$ mice were protected against diet induced obesity, however the diet used for most of their studies was deficient in essential FAs [189,212]. Despite the body weight differences, both lines displayed a protection against hepatic steatosis, reduction in FA oxidation and VLDL secretion which is thought to be due to defects in FA uptake and availability [177-179,188,189,212,214,215]. The observed differences in the body weight phenotypes between the two groups’ mice could be attributed to the difference in the strategies that were used to generate the KO mice, HFD composition, strains background, caging environment or even the gut microbiome composition.

IFABP$^{-/-}$ mice

A single line of IFABP$^{-/-}$ mice was generated by the Agellon laboratory on the C56BL/6J background [216]. There was a sexual dimorphism in the body weight of IFABP$^{-/-}$ mice in response to a HFD. Both male and female were fed a 35% Kcal fat HFD as coconut oil with 1.25% cholesterol for 19 weeks. Male IFABP$^{-/-}$ mice were found to have increased body weight and hepatic lipid accumulation relative to male WT mice, while in female

IFABP$^{-/-}$ mice there was less body weight gain when compared to their WT control mice [216]. From the Agellon line of IFABP$^{-/-}$ mice our mice were derived and maintained on the C56BL/6J background, and this substrain has been used [162,163].

Comparing LFABP and IFABP Whole-Body Knockout Mice

In our laboratory, Lagakos *et al.* studied the intestinal phenotypes of LFABP$^{-/-}$ and IFABP$^{-/-}$ mice [163], providing the first direct comparison of KOs for these co-expressed proteins. For baseline phenotypic evaluation, LFABP$^{-/-}$ and IFABP$^{-/-}$ male mice were fed a chow diet. No dramatic changes in the body weight of either LFABP$^{-/-}$ and IFABP$^{-/-}$ mice were observed when they were compared to the WT control mice. The ablation of either IFABP or LFABP did not result in up-regulating the mucosal expression of the other intestinal FABPs. The studies revealed that LFABP has a role in directing FA towards oxidative pathways as seen by the impairment in FA oxidation caused by LFABP ablation. Additionally, there was a lower TG/PL ratio in the enterocytes of IFABP$^{-/-}$ after the dietary administration of ^{14}C oleate and a lower TG/PL ratio in the enterocytes of LFABP$^{-/-}$ mice after dietary administration of ^{3}H monoolien, suggesting that IFABP may play a role in directing dietary FA towards the synthesis of TG and LFABP is important in incorporating MG into TG relative to PL [163]. Feeding these mice with a semipurified 10% kcal low fat diet gave the same results as the chow diet and both IFABP$^{-/-}$ mice and LFABP$^{-/-}$ mice showed no dramatic whole-body phenotypic differences when they were compared to the WT control mice [162].

It was hypothesized that challenging those mice with a HFD may reveal phenotypic changes in the body weight. In a study by Gajda *et al.*, HFD was administered to 8 week old LFABP$^{-/-}$ and IFABP$^{-/-}$ male mice for 12 weeks. In response to this HF load, LFABP$^{-/-}$ mice displayed a higher body weight and FM than WT mice, and showed a lower

respiratory exchange ratio (RER) than WT mice, indicating that these mice utilized lipid as their primary energy source [162]. In contrast to LFABP$^{-/-}$ mice, IFABP$^{-/-}$ mice, upon HF feeding, gained less weight, less FM and remained lean relative to WT. IFABP$^{-/-}$ mice had higher RERs than WT mice, suggesting that these mice were using carbohydrate as a primary energy source [162]. Furthermore, there was an alteration in food intake of LFABP$^{-/-}$ and IFABP$^{-/-}$ mice. LFABP$^{-/-}$ mice showed a higher food intake which may be related to higher mucosal levels of two of the ECs, 2-AG and AEA, while IFABP$^{-/-}$ mice showed a lower food intake than WT mice [162]. However, an assessment of feeding efficiency did not fully explain the alterations in the body weight that have been observed in both LFABP$^{-/-}$ and IFABP$^{-/-}$ mice. Most interestingly, challenging those mice with chronic HF feeding revealed that the concentration of lipid in the feces did not differ between the three groups of mice suggesting that there is no lipid malabsorption accompanying the ablation of LFABP or IFABP.

Surprisingly, although LFABP$^{-/-}$ mice gained substantially more weight and FM than WT mice, they appeared to remain healthy, showing glucose, insulin and lipids levels that are comparable to the WT [162]. Although obese HF fed WT mice were shown to have slower intestinal TG secretion rates than the non-obese mice [217,218], the intestinal TG secretion rates were not different in LFABP$^{-/-}$ mice from that of the WT mice [162]. Additionally, despite their heavier body weight and increased FM, LFABP$^{-/-}$ mice were protected against HFD induced hepatic steatosis [213], had a higher spontaneous activity than the control mice [162], and were protected from HF feeding induced decline in exercise capacity, running about double the distance when compared to the WT mice [219]. After intraduodenal administration of ^{14}C oleate to IFABP$^{-/-}$ and LFABP$^{-/-}$ mice and ^{3}H monoolien to LFABP$^{-/-}$ mice, there was a lower TG/PL ratio in the enterocytes of both IFABP$^{-/-}$ and LFABP$^{-/-}$ mice, indicating that both IFABP and LFABP are important to incorporate FA into

TG relative to PL, and LFABP is important in directing MG towards TG synthesis rather than PL [162].

These findings further suggest that LFABP$^{-/-}$ mice can be considered a model of healthy obesity. It has been found that there is a group of overweight and obese population still considered to be healthy, showing a lower level of comorbidities that are usually associated with obesity; although those people have a high body mass index that is above 30, they do not have a metabolic syndrome. A new term has been given to this phenomenon, a “metabolically healthy obesity” (MHO) [220,221]. Because of LFABP expression in both the intestine and the liver, it is unknown whether these alterations and the observed MHO phenotype are due to its ablation from the intestine, the liver or whether simultaneous ablation from both the intestine and the liver is required.

It is also worth mentioning that in both LFABP$^{-/-}$ and IFABP$^{-/-}$ mice there was no compensatory up-regulation of the gene expression or protein abundance of other FABPs present in the intestine when challenged with either chow diet or HFD [162,163]. The overall studies strongly support the distinct functional role of LFABP and IFABP in the intestine regarding the modulation of lipid metabolism and transport and in whole body homeostasis.

As mentioned above, IFABP null mice were found to have a leaner phenotype when compared to the WT counterparts following HFD feeding. This might be explained in part by the reduced food intake [162]. No significant difference was found in the fecal lipid percentage, thus not explaining in full the observed phenotype of the IFABP$^{-/-}$ mice. However, we have recently found that HF fed IFABP$^{-/-}$ mice have a blunt villus phenotype, thinner muscularis layer, reduced goblet cell and Paneth cell densities, reduced transit

time and increased intestinal permeability. Furthermore, despite the comparable concentration of fecal lipids between IFABP$^{-/-}$ and WT mice, IFABP$^{-/-}$ mice excreted more feces than the WT mice. All of these findings are indicative of a general nutrient malabsorption, including lipid malabsorption, which might contribute to the lower body weight phenotypic changes that were observed in IFABP null mice [222].

Summary:

The proximal intestinal enterocyte FABPs, LFABP and IFABP, are highly abundant lipid binding proteins in the small intestine and the liver, two tissues with high lipid processing capacity. Both proteins have high affinities for FAs, and appear to serve as a buffer to control the uptake and trafficking of lipids within the cytoplasm into different metabolic pathways. Despite their similar tertiary structures, *in vitro* studies have shown differences in ligand binding, affinities to FAs, mechanisms of delivery, and interaction with transcriptional factors, suggesting their distinct roles in lipid transport and metabolism. *In vivo* studies in mice, revealed that LFABP$^{-/-}$ and IFABP$^{-/-}$ mice had a divergent phenotypes in response to long-term HF feeding. While IFABP$^{-/-}$ mice remain lean, LFABP$^{-/-}$ mice become more obese. In addition to the body weight differences, these mice were showing different intestinal lipids distribution. These findings have confirmed the different roles for each of these proteins in regulating whole-body energy homeostasis. Recently, it has been found that IFABP$^{-/-}$ mice have a disturbance in their intestinal structure, transit time and fecal output. There is a new emerging concept about the pivotal role and effect of gut microbiota on intestinal health and how it influences the whole-body energy homeostasis via organ crosstalk [223-225]. Therefore, it is of great interest to determine the intestinal bacterial composition in IFABP$^{-/-}$ and LFABP$^{-/-}$ mice and its relationship with the phenotypes that are observed in these mice.

Despite their obesity, whole-body LFABP$^{-/-}$ mice were a good model of MHO phenotype, displaying protection against a HFD induced decline in exercise activity and hepatic steatosis. It is important to remember that in addition to its expression in the intestine, LFABP is also expressed in the liver. As noted above, therefore, it is unknown whether the phenotypes observed in the HF fed LFABP$^{-/-}$ are a result of the ablation of liver-LFABP, intestinal-LFABP, or ablation of both is necessary. Therefore, the aims of this thesis project are:

Specific Aims:

Specific Aim 1: To assess the effect of whole-body ablation of LFABP and IFABP on gut microbiota composition

As mentioned above, the whole body KO of LFABP was associated with obesity. However, those mice were an example of MHO phenotype; the mice displayed a glucose tolerance, insulin and lipids levels that are comparable to their WT controls and they were protected against the HF feeding induced decrease in endurance exercise activity [162,219]. The intestinal morphology of LFABP$^{-/-}$ mice appears normal (unpublished data). On the other side, although IFABP$^{-/-}$ mice were fed the same HFD, they were leaner than their WT controls, have better glucose tolerance and comparable lipid profile to the WT control [162]. However, IFABP$^{-/-}$ mice also showed changes in their gut motility and signs of deterioration in gut barrier integrity [222]. Those effects may be related to the fact that the HFD induces alterations in intestinal microbiota, which can have either beneficial or detrimental effects on the host. Studies in chapter 2 will target this aim and investigate the microbiota composition in both genotypes in relation to the WT microbiota, in order to determine whether alterations in gut microbiota composition and its metabolites are associated with the whole-body phenotypes that have been observed in both LFABP$^{-/-}$ and IFABP$^{-/-}$ mice.

Specific Aim 2: To examine the contribution of liver-LFABP to the MHO phenotype that has been observed in HF-fed whole-body LFABP$^{-/-}$ mice

LFABP$^{-/-}$ mice seem to be a good model of MHO, being normoglycemic, normoinsulinemic and normolipidemic. Because LFABP is expressed in both the liver and the intestine, we need to understand the underlying causes of the phenotype that was noted in the global LFABP$^{-/-}$ mice and whether it is related to the ablation of LFABP in the intestine or in the liver, or whether concomitant ablation of both genes is required. Thus, the second aim (chapter 3) is focused on our LFABP conditional KO (cKO) to assess the role of LFABP specifically within the liver, and the impact of its ablation on whole-body energy homeostasis. Floxed LFABP (LFABP$^{fl/fl}$) WT mice were used to generate liver-specific LFABP null mice through mating with mice that express Cre recombinase driven by the albumin promoter which has its highest activity in the liver [226]. The resultant liver-specific LFABP null mice (LFABP$^{liv-/-}$) and control LFABP$^{fl/fl}$ mice were fed a 45% kcal fat HFD for 12 weeks. They were compared for body weight gain, body composition, food intake, indirect calorimetry, endurance capacity and plasma levels of glucose, insulin, lipids and other metabolic indicators that are used to assess whole-body energy homeostasis. Studies in this aim will establish the contribution of liver-LFABP to the phenotypic and metabolic changes observed in the global LFABP$^{-/-}$ mice.

Specific Aim 3: To determine the effect of liver-specific ablation of LFABP on hepatic steatosis, and whether there is shifting of FA uptake into tissues other than the liver

Previously, it has been shown that global LFABP$^{-/-}$ protected HF fed mice against hepatic steatosis [213], and reduced hepatic FA uptake and oxidation [179,189]. This may increase the availability of LCFAs to either be oxidized in the muscle or to be stored in adipose tissue [213,219]. Thus, in aim 3 (chapter 3), we tested whether the cKO of LFABP from the liver alone protects the liver against HFD induced hepatic steatosis, and also examined

the potential mechanisms underlying such potential protection, including increased hepatic TG secretion, reduced hepatic FA uptake and/or increased FA oxidation. We hypothesized that there will be a reduction in hepatic FA uptake, resulting in a protection against hepatic steatosis, and leading to FA clearance into other tissues like adipose tissue, intestine or muscle, secondary to higher concentration of circulating FA.

Chapter 2

Gut Microbiota and Phenotypic Changes Induced by Ablation of Liver- and Intestinal-Type Fatty Acid Binding Proteins (LFABP and IFABP)

Abstract

Intestinal fatty acid binding protein (IFABP; FABP2) and liver fatty acid binding protein (LFABP; FABP1) are small intracellular lipid binding proteins. Deficiency of either of these proteins in mice leads to differential changes in intestinal lipid transport and metabolism, and to markedly divergent changes in whole-body energy homeostasis. The gut microbiota has been reported to play a pivotal role in metabolic process in the host and can be affected by host genetic factors. Here, we examined the phenotypes of wild-type (WT), LFABP$^{-/-}$ and IFABP$^{-/-}$ mice before and after high fat diet (HFD) feeding and applied 16S rRNA gene V4 sequencing to explore the gut microbiota structure and its associations with the phenotypes. The results show that compared with WT and IFABP$^{-/-}$ mice, LFABP$^{-/-}$ mice gained more weight, had slower intestinal transit time, less fecal output and more bacterial guilds containing bacteria associated with obesity, such as the guild including *Desulfovibrionaceae.* By contrast, IFABP$^{-/-}$ mice were the leanest, had the fastest intestinal transit time, the most fecal output and the highest abundance of potentially beneficial bacterial guilds such as those including *Akkermansia*, *Lactobacillus* and *Bifidobacterium*. These genotype-related bacterial guilds were associated with body weight. Interestingly, compared with WT mice, the levels of short-chain fatty acids (SCFAs) in feces were significantly higher in LFABP$^{-/-}$ and IFABP$^{-/-}$ mice under both chow and HF diets. Collectively, these studies show that the ablation of LFABP or IFABP induced marked changes in the gut microbiota and these were associated with phenotypic changes found in these mice.

Introduction

Fatty acids binding proteins (FABPs) are a family of 14-15kDa intracellular proteins that are thought to transport fatty acids (FAs) and other lipophilic molecules within the cell interior [84,227]. Liver fatty acid-binding protein (LFABP, FABP1), the first member identified [122,164], is highly expressed in the liver and also found abundantly in the proximal intestine [228]. In contrast to other FABPs which bind a single molecule of ligand, LFABP binds two molecules of long-chain fatty acids (LCFAs) or two molecules of monoaglyceride (MG), in addition to a variety of other hydrophobic ligands including cholesterol, bile acids, lysophospholipids, and endocannabinoids (ECs) [170-173,202,203,229]. In addition to LFABP, intestinal fatty acid-binding protein (IFABP, FABP2) is also found in the small intestine (SI), its sole tissue of expression [216,228]. IFABP has a high affinity for both saturated and unsaturated LCFAs with a single ligand binding site [168,169,202], and has recently been shown to bind ECs as well [203]. While their precise functions are not entirely known, both of the enterocyte FABPs are considered to be important as reservoirs for cytoplasmic FAs, preventing lipotoxicity caused by elevated intracellular free fatty acid (FFA) levels, and to traffic FAs to enzymes involved in their synthetic incorporation into triglycerides (TGs) and phospholipids (PLs), or in their oxidation [84,230]. It is also suggested that FABPs may traffic their ligands to proteins involved in cellular signaling [157].

Although both IFABP and LFABP are expressed in the same cell type, the proximal intestinal enterocyte, and while both bind LCFAs, we have demonstrated that the two proteins are functionally distinct. In vitro studies revealed markedly different mechanisms of ligand transfer between IFABP or LFABP and membranes [84,175]. Further, it was found using mice null for either of these genes that LFABP is involved in directing intestinal MGs toward TG synthesis and FAs to oxidative pathways, while IFABP directs FAs toward

synthesis of TG [162,163]. In addition to these local cellular effects, many phenotypic and metabolic differences at the whole-body level have also been observed between the LFABP and IFABP null mice. Specifically, mice null for LFABP become heavier and fatter on a HFD than WT mice, with a lower respiratory exchange ratio (RER) indicative of increased fat oxidation [162,212,213], supporting a role of LFABP in regulating whole-body energy homeostasis. The increase in body weight of LFABP$^{-/-}$ mice was, in part, due to higher food intake which may be secondary to the increase in mucosal levels of the ECs, 2-arachidonoylglycerol (2-AG) and arachidonoylethanolamine (AEA) [162]. Despite their obese phenotype, LFABP$^{-/-}$ mice are normoinsulinemic, normoglycemic, normolipidemic, displayed higher levels of spontaneous activity than the WT control mice [162], and are protected against the HFD-induced decline in endurance exercise capacity [219]. Due to these aforementioned metabolic changes, mice null for LFABP are considered an example of a “metabolically healthy obese” (MHO) phenotype.

Conversely to LFABP$^{-/-}$, we found that ablation of IFABP results in less weight gain upon HFD feeding relative to WT, with IFABP$^{-/-}$ mice having a higher RER, indicative of greater carbohydrate oxidation, and a lower food intake than WT mice [162]. IFABP ablation did not result in higher fecal lipid concentration [162], however, we recently found that HFD fed IFABP$^{-/-}$ mice have blunt villi, a thinner muscularis layer, reduced goblet cell and Paneth cell densities, reduced transit time, increased fecal excretion, and increased intestinal permeability [222]. These findings are indicative of nutrient malabsorption, including lipid malabsorption, which likely contributes to the leaner phenotype observed in IFABP null mice [222]. The markedly different whole-body phenotypes in LFABP$^{-/-}$ vs. IFABP$^{-/-}$ mice support a growing understanding of gut lipid metabolism and transport as an important regulatory factor in whole-body energy homeostasis. Notably, the phenotypic changes were not due to compensatory changes in the expression of the other FABPs

located in the small intestine of IFABP$^{-/-}$ and LFABP$^{-/-}$ mice [162], further supporting the independent and distinct roles of the proximal SI FABPs, IFABP, and LFABP, in intestinal and whole-body homeostasis.

It is now well established that gut microbiota play an essential role in host health and can modulate many host metabolic processes including lipid metabolism [224] and energy homeostasis [223] through multiple direct and indirect biological mechanisms. These include production of a variety of metabolites such as short chain fatty acids (SCFAs), lipopolysaccharide (LPS), secondary bile acids and others [223,231]. The structure of the gut microbiota is dynamic and can be affected by the amount and composition of dietary carbohydrates and fats [232-235]. While most of the products of dietary lipid digestion are absorbed in the proximal small intestine, a minority will pass through the gastrointestinal tract and directly modulate the gut microbiota composition in the distal intestine, via modulation of bacterial growth and by influencing bacterial metabolism as substrates [231]. Additionally, host genetic factors can affect the gut microbiota composition. For example, using 113 different strains in the Hybrid Mouse Diversity Panel, Org et al. found that seven host loci were significantly associated with the gut microbiota composition [236]. The genes in the identified loci were involved in processes related to lipid metabolism, innate immune responses, and acute-phase immunological responses to LPS [236].

To gain insight into whether the observed dramatic whole-body phenotypic divergence between IFABP$^{-/-}$ and LFABP$^{-/-}$ mice was associated with gut microbiota, here we compared the microbiome of WT, IFABP$^{-/-}$ and LFABP$^{-/-}$ before and after an 11-week high saturated fat feeding period. Our findings indicate that alterations in bacterial communities as a function of genotype and secondary to HFD feeding are associated with the lean phenotype of the IFABP$^{-/-}$ mice, and with the MHO phenotype of the LFABP$^{-/-}$ mice.

Experimental Procedures

Animals and Diets

LFABP$^{-/-}$ mice on a C57BL/6N background were generously provided by Binas and coworkers [179]. The mice were additionally backcrossed with C57BL/6J mice from The Jackson Laboratory (Bar Harbor, ME) as described previously [163,219]. IFABP$^{-/-}$ mice used in the present studies are a substrain bred by intercrossing of the original IFABP$^{-/-}$ mice [216], and are also on a C57BL/6J background as described [162,163]. WT C57BL/6J mice from The Jackson Laboratory bred in our facility are used as controls. Mice were maintained on a 12-hour light/dark cycle and allowed *ad libitum* access to standard rodent chow (Purina Laboratory Rodent Diet 5015). At 2 months of age, male LFABP$^{-/-}$, IFABP$^{-/-}$, and WT mice were housed 2-3 per cage and fed a 45% Kcal fat HFD (D10080402; Research Diets, Inc., New Brunswick, NJ) for 11 weeks; the lipid sources were cocoa butter (43% kcal) and soybean oil (2% kcal) Table 2-1 and 2-2.

Table 2-1: Diet composition of high saturated fat diet [162].

	HFS	
	grams	**kcal**
Casein	200	800
L-Cystine	3	12
Corn starch 1.2/128	72.8	291
Maltodextrin	100	400
Sucrose	172.8	691
Cellulose	50	0
Soybean Oil	10	90
Cocoa Butter	192.5	1733
Mineral mix	45	0
Vitamin mix	10	40
Choline Bitartrate	2	0
Total	858.1	4057

Table 2-2: FA composition of high saturated fat diet [162].

	HFS grams/4057 kcal
C16	49.9
C16:1	0.4
C18	64.3
C18:1	65.2
C18:2	10.7
C18:3	1.0
%	
Saturated fatty acids	60.0
Monounsaturated fatty acids	33.9
Polyunsaturated fatty acids	6.1

Body Weight and Food Intake

At 2 months of age, mice were fed the HFD. The mice were maintained on this diet for 11 weeks, and body weights were measured each week. Food intake was assessed using the Oxymax system (Columbus Instruments, Columbus, OH) during week 10-11 of the feeding protocol. Mice were placed in chambers (1 mouse per chamber) with food for 48 hours. The first 24 hours were used as an acclimation period, while the second 24-hour period was used to measure food intake.

Intestinal Transit Time

Transit time measurements were performed between week 10 and 11 of the HFD period. Prior to the start of the experiment, mice were individually housed. After two hours of acclimation, mice were given 250µL of 6% carmine red and 0.5% methylcellulose (Sigma-Aldrich, St. Louis, MO) in PBS by oral gavage. After gavaging the mice, the cages were checked every 10 minutes and the time of appearance of the first red fecal pellet recorded [237,238].

Total Fecal Excretion

Mice were housed 2-3 per cage. Feces from each cage were collected every 3-4 days between weeks 10 and 11 of the HFD feeding period, dried overnight at 60ºC, and then weighed. The weight of the feces was divided by the number of mice in the cage, and by the number of days of collection. In order to control for differences in food intake, fecal excretion in grams was normalized by dividing it by the respective 24-hour food intake.

Gut microbiota analyses

Fresh fecal pellets were collected from 6 individual mice per genotype at baseline and again after 11 weeks of HFD feeding. Samples were snap frozen in liquid nitrogen and stored at -80°C until analysis. Genomic DNA was extracted using the QIAmp Power Fecal DNA kit (QIAGEN, Germantown, MD), as per manufacturer instructions. The hypervariable region V4 of the 16S rRNA gene was amplified using the 515F and 806R primers modified by Parada *et. al.* [239] and Apprill *et. al.* [240] and sequenced using the Ion GeneStudio S5 (ThermoFisher Scientific, Waltham, MA). Primers were trimmed from the raw reads using Cutadapt [241] in QIIME 2 [242]. Amplicon sequence variants (ASVs) [243] were obtained by denoising using the dada2 denoise-single command in QIIME 2 with parameters --p-trim-left 0 –p-trunc-len 215. Spurious ASVs were further removed by abundance filtering [244]. A phylogenetic tree of ASVs was built using the QIIME 2 commands alignment mafft, alignment mask, phylogeny fastree, and phylogeny midpoint-root to generate weighted UniFrac metrics. Taxonomy assignment was performed using the q2-feature-classifier plugin [245] in QIIME 2 based on the silva database (release 132) [246]. The data were rarified to 17,000 reads/sample for subsequent analyses.

Overall gut microbiota structure was evaluated using alpha diversity indices (Shannon index and observed ASVs) and beta diversity distance metric (weighted UniFrac).

Principal coordinates analysis (PCoA) was performed using the R "ape" package [247] to visualize differences in gut microbiota structure between treatment groups along principal coordinates that accounted for most of the variations. Random Forest analysis was performed and cross-validated using the R "randomForest" package [248] and the "rfcv" function respectively to test for correlations between gut microbiota composition and body weight. Figures were visualized by the R "ggplot2" package [249] and "pheatmap" package [250].

ASV shared by > 25% of the samples were considered prevalent and selected for the guild level analysis. Pairwise correlations among the ASVs were calculated using the method described by Bland and Altman [251]. The correlation values were converted to a correlation distance (1 – correlation value) and the ASVs were clustered using the Ward clustering algorithm. From the top of the clustering tree, permutational multivariate analysis of variance (PERMANOVA; 9999 permutations with a $P < 0.001$ cut-off) was used to sequentially determine whether the two clades were significantly different and accordingly clustered the prevalent ASVs into guilds [252].

GC/MS Analysis of SCFAs in fecal samples

SCFA species, including acetate, propionate, isobutyrate, butyrate, isovalerate, and valerate from fecal samples of WT, IFABP$^{-/-}$ and LFABP$^{-/-}$ mice were analyzed by GC/MS as described previously [253], at the core facility of the New Jersey Institute for Food, Nutrition, and Health of Rutgers University.

Results

Body weight gain differs in WT, IFABP$^{-/-}$ and LFABP$^{-/-}$ mice after chronic HF feeding

After 11 weeks of 45% Kcal HF feeding, IFABP$^{-/-}$ mice gained less weight and remained lean when compared to both WT and LFABP$^{-/-}$ mice, in agreement with previous results [162,222]. In addition, and also in keeping with our previous finding [162], LFABP$^{-/-}$ mice gained more weight than WT mice after 11 weeks on HFD (Fig. 2-1A).

Intestinal transit time and total fecal excretion are altered in mice lacking IFABP and LFABP

As we have reported previously [222], IFABP$^{-/-}$ mice displayed faster intestinal transit time on the HFD, and higher fecal output normalized for food intake, suggesting some malabsorption of lipid and other nutrients (Fig. 2-1B and C). Interestingly, the 45% Kcal HF fed LFABP$^{-/-}$ mice displayed significantly slower intestinal transit times than their WT controls (Fig. 2-1B), and a significant decrease in total fecal excretion normalized for total food intake (Fig. 2-1C). These changes may contribute, in part, to the increased body weight gain relative to the WT [162]. The observed changes in the intestinal transit time and fecal excretion in both IFABP$^{-/-}$ and LFABP$^{-/-}$ mice, relative to WT and to each other, imply that there might be an alteration in the gut microbiome composition as another study suggested [254].

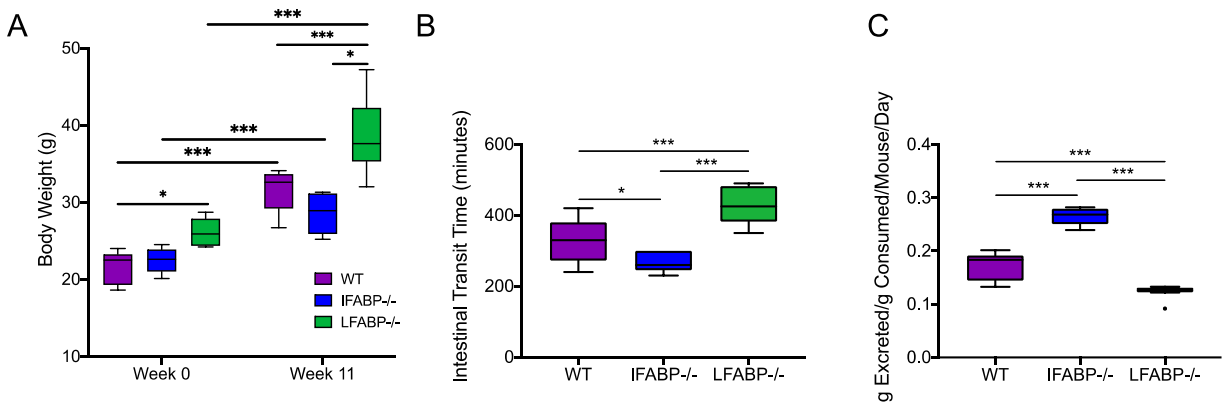

Figure 2-1: Alterations in body weight and intestinal motility in WT, IFABP and LFABP knockout mice after 11 week on HFD. A, body weight in week 0 and week 11; B, Intestinal transit time; C, Total fecal output. Repeated measures ANOVA with Tukey's post hoc was applied in (A). One-way ANOVA with Tukey's post hoc was applied in (B) and (C). * $P < 0.05$, *** $P < 0.001$. (B) and (C) were from a separate group of mice with the same genotypes and fed the same HFD.

The microbiota composition is altered by IFABP and LFABP ablation and shows different responses to HFD

To explore whether IFABP$^{-/-}$ and LFABP$^{-/-}$ mice displayed alterations in the gut microbiota, we collected fecal samples from WT, IFABP$^{-/-}$ and LFABP$^{-/-}$ mice (n = 6 per group) at both week 0 (8 weeks of age, prior to the HFD feeding period) and at week 11 of HF feeding, to profile gut microbiota composition via 16S rRNA gene v4 sequencing. In total, 785 bacterial amplicon sequence variants (ASVs) [243] were identified from the 36 samples. At week 0, LFABP$^{-/-}$ mice had a significantly higher Shannon index than WT (Fig. 2-2A). At week 11, the differences between LFABP$^{-/-}$ and WT mice remained and LFABP$^{-/-}$ mice also had significantly higher Shannon index than IFABP$^{-/-}$ mice. Within each genotype there was no change in Shannon index from week 0 to week 11. Both knockout groups had significantly more ASVs than WT mice at week 0 (Fig. 2-2B). At week 11, the ASV number showed the same differential pattern as the Shannon index among the 3 groups. Only in WT mice was there a significant increase in ASV number from week 0 to week 11. These results show that IFABP$^{-/-}$ mice have increased gut microbiota diversity relative to WT only under normal chow, while LFABP$^{-/-}$ mice have increased diversity relative to WT under both normal chow and following prolonged HF feeding, and to IFABP$^{-/-}$ mice under HFD only. In contrast to the WT mice, the HFD treatment had no effect on the alpha diversity of gut microbiota in either of the FABP knockout mice.

To compare the overall structure of the gut microbiota across groups, scatter plots of principal coordinate analysis based on weighted UniFrac distance were constructed (Fig. 2-2C). The HFD significantly changed the gut microbiota structure in all groups, with clear segregations observed between week 0 and week 11 within each genotype (PERMANOVA test P = 0.004 in each group). At week 0, both knockout groups were significantly different from WT (IFABP$^{-/-}$ vs. WT P = 0.009; LFABP$^{-/-}$ vs. WT P = 0.004),

while there was no significant difference between IFABP$^{-/-}$ and LFABP$^{-/-}$ mice (P = 0.072). The dissimilarity between LFABP$^{-/-}$ and WT was significantly greater than that between IFABP$^{-/-}$ and WT (Fig. 2-2D). After the 11-week HF feeding, the three genotypes were significantly different from each other (IFABP$^{-/-}$ vs. WT P = 0.041; LFABP$^{-/-}$ vs. WT P = 0.028; IFABP$^{-/-}$ vs LFABP$^{-/-}$ P = 0.004), and the dissimilarity between IFABP$^{-/-}$ and WT was similar to that between LFABP$^{-/-}$ and WT. These results show that compared with WT, both IFABP$^{-/-}$ and LFABP$^{-/-}$ significantly altered the overall gut microbiota structure under both normal chow and HFD treatment. The HFD altered the gut microbiome structure in the 3 genotypes, however, this effect was more profound in LFABP$^{-/-}$ mice.

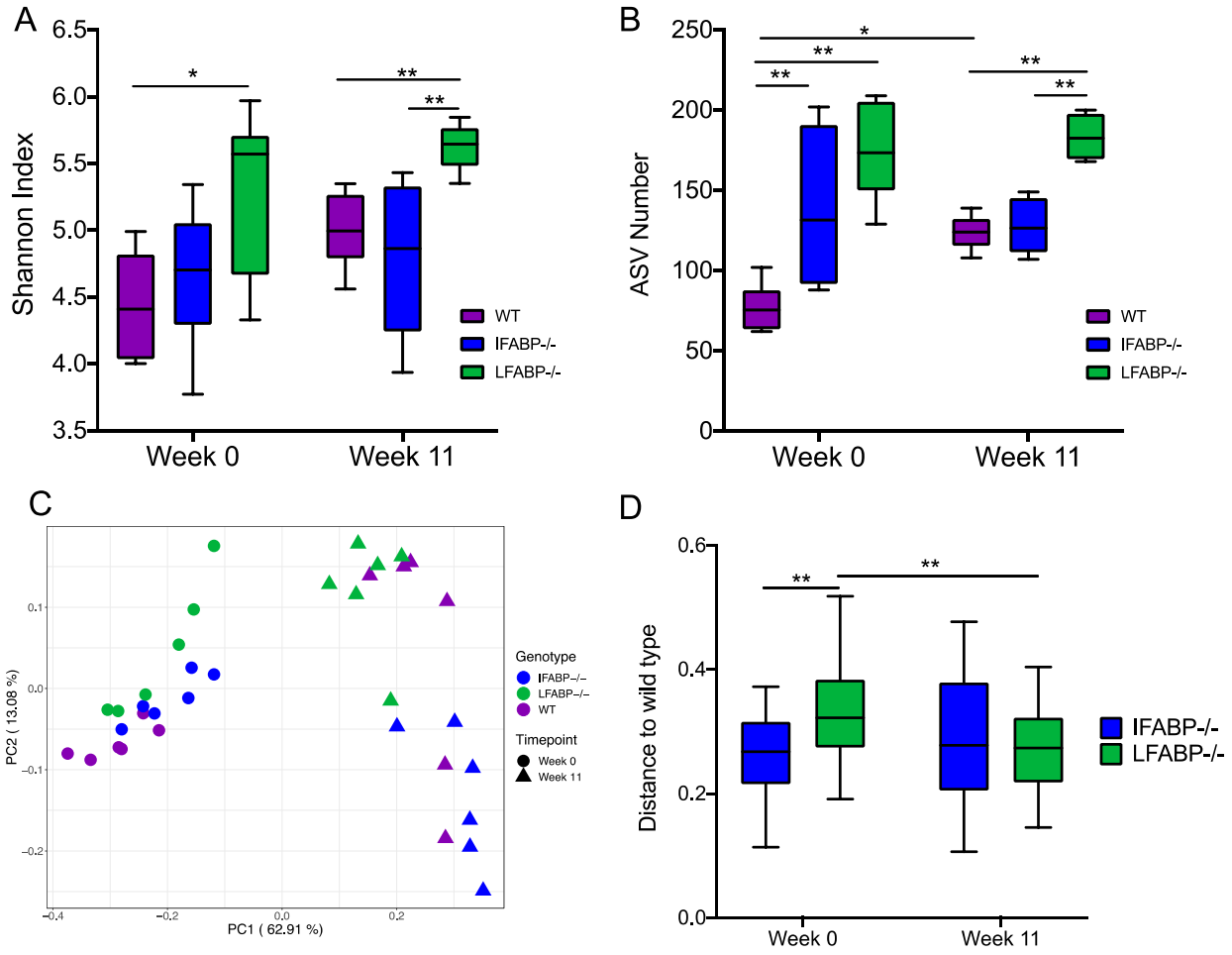

Figure 2-2: Effect of IFABP and LFABP knockout and a HF diet on the gut microbiota. A, Shannon Index; B, ASV number; C, Principal coordinate plot based on weighted UniFrac distance; D, Weighted UniFrac distance from IFABP$^{-/-}$ and LFABP$^{-/-}$ to WT at each time point. Data at different time points within the same genotype group were compared using the Wilcoxon matched-pairs signed-ranks test (two-tailed) and data at the same time point between the groups were compared using the Mann-Whitney test (two-tailed). * $P < 0.05$, ** $P < 0.01$. Boxes show the medians and the interquartile ranges (IQRs), and the whiskers denote the lowest and highest values within 1.5 times the IQR from the 1st and 3rd quartiles.

The abundance of bacteria is affected by genotypes and HF feeding

Bacteria in the gut ecosystem form complex interactions as functional groups rather than existing in isolation [255]. Members that exploit the same class of resources in a similar way can be considered as a guild [256], in which the guild members typically show co-abundance patterns. Thus, to identify potential guilds, we explored the co-abundance relationships among the 202 prevalent and dominant ASVs, which were shared in at least 25% of the samples and accounted for ~90% of the total abundance. The 202 ASVs were grouped into 24 different guilds (Table 2-3).

Table 2-3: 202 ASVs were grouped into 24 different guilds

ASV ID	Guild ID	ASV ID	Guild ID
Odoribacter.ASV_16	Guild 1	Oscillibacter.ASV_88	Guild 8
Ruminiclostridium.9.ASV_29	Guild 1	Lachnospiraceae.NK4A136.group.ASV_104	Guild 8
Turicibacter.ASV_44	Guild 1	Lachnospiraceae.UCG.004.ASV_133	Guild 8
Ruminococcaceae.UCG.010.ASV_155	Guild 1	Lachnospiraceae.ASV_163	Guild 8
Ruminococcaceae.UCG.004.ASV_212	Guild 1	Lachnospiraceae.ASV_11	Guild 9
Ruminiclostridium.5.ASV_215	Guild 1	Acetatifactor.ASV_38	Guild 9
Ruminococcaceae.ASV_258	Guild 1	Lachnospiraceae.NK4A136.group.ASV_58	Guild 9
Eubacterium.nodatum.group.ASV_289	Guild 1	Ruminiclostridium.ASV_59	Guild 9
Alistipes.ASV_47	Guild 2	Oscillibacter.ASV_64	Guild 9
Bacteroides.ASV_56	Guild 2	Ruminiclostridium.ASV_118	Guild 9
Odoribacter.ASV_84	Guild 2	Ruminiclostridium.5.ASV_132	Guild 9
Alistipes.ASV_86	Guild 2	Lachnospiraceae.ASV_191	Guild 9
Muribaculaceae.ASV_94	Guild 2	Desulfovibrionaceae.ASV_2	Guild 10
Muribaculaceae.ASV_105	Guild 2	Brachyspira.sp..NSH.25.ASV_100	Guild 10
Muribaculaceae.ASV_119	Guild 2	Desulfovibrionaceae.ASV_101	Guild 10
Muribaculaceae.ASV_161	Guild 2	Ruminococcaceae.ASV_157	Guild 10
Lachnospiraceae.ASV_206	Guild 2	Lachnospiraceae.ASV_203	Guild 10
Muribaculaceae.ASV_208	Guild 2	Desulfovibrio.ASV_286	Guild 10
Ruminococcaceae.ASV_292	Guild 2	Lachnospiraceae.ASV_331	Guild 10
Lachnospiraceae.bacterium.609.ASV_13	Guild 3	Muribaculaceae.ASV_12	Guild 11
Lachnoclostridium.ASV_23	Guild 3	Faecalibaculum.ASV_48	Guild 11
Odoribacter.ASV_36	Guild 3	Muribaculaceae.ASV_95	Guild 11
Rikenellaceae.RC9.gut.group.ASV_37	Guild 3	Rikenellaceae.RC9.gut.group.ASV_103	Guild 11
Lachnospiraceae.ASV_55	Guild 3	Parabacteroides.ASV_123	Guild 11
Rikenellaceae.RC9.gut.group.ASV_62	Guild 3	Roseburia.ASV_199	Guild 11
Lachnospiraceae.ASV_130	Guild 3	Clostridium.sp..Culture.Jar.19.ASV_274	Guild 11
Anaerovorax.ASV_174	Guild 3	Ileibacterium.ASV_3	Guild 12
Blautia.ASV_188	Guild 3	Lactobacillus.ASV_4	Guild 12
Mollicutes.RF39.ASV_340	Guild 3	Bifidobacterium.ASV_5	Guild 12
Oscillibacter.ASV_352	Guild 3	Lactobacillus.ASV_45	Guild 12
Ruminococcaceae.ASV_374	Guild 3	Lactococcus.ASV_46	Guild 12
Romboutsia.ASV_114	Guild 4	Dubosiella.newyorkensis.ASV_66	Guild 12
Mollicutes.RF39.ASV_116	Guild 4	Ruminococcaceae.ASV_76	Guild 12
Eubacterium.coprostanoligenes.group.ASV_171	Guild 4	Ruminococcaceae.UCG.003.ASV_168	Guild 12
Acetatifactor.ASV_173	Guild 4	Clostridium.scindens.ASV_177	Guild 12
Lachnospiraceae.ASV_238	Guild 4	Lachnospiraceae.ASV_195	Guild 12
Lachnospiraceae.ASV_246	Guild 4	Enterorhabdus.ASV_364	Guild 12
Lachnospiraceae.ASV_300	Guild 4	Streptococcus.ASV_432	Guild 12
Lachnospiraceae.ASV_303	Guild 4	Bacteroides.ASV_41	Guild 13

Ruminiclostridium.ASV_57	Guild 5	Bacteroides.ASV_61	Guild 13
Oscillibacter.ASV_99	Guild 5	Lachnoclostridium.ASV_107	Guild 13
Lachnospiraceae.ASV_108	Guild 5	Peptococcaceae.ASV_137	Guild 13
Intestinimonas.ASV_134	Guild 6	Erysipelatoclostridium.ASV_141	Guild 13
Clostridium.sp..Culture.54.ASV_181	Guild 6	Lachnospiraceae.ASV_164	Guild 13
Lachnospiraceae.UCG.006.ASV_183	Guild 6	Bilophila.ASV_175	Guild 13
Ruminococcaceae.ASV_235	Guild 6	Peptococcus.ASV_185	Guild 13
Lachnospiraceae.ASV_290	Guild 6	Coriobacteriaceae.UCG.002.ASV_293	Guild 13
Ruminiclostridium.9.ASV_7	Guild 7	Rikenellaceae.RC9.gut.group.ASV_51	Guild 14
Lachnospiraceae.NK4A136.group.ASV_8	Guild 7	Bacteroides.ASV_79	Guild 14
Ruminiclostridium.ASV_21	Guild 7	Muribaculaceae.ASV_83	Guild 14
Lachnospiraceae.ASV_54	Guild 7	Gastranaerophilales.ASV_126	Guild 14
Lachnospiraceae.ASV_65	Guild 7	Gastranaerophilales.ASV_152	Guild 14
Roseburia.ASV_110	Guild 7	Muribaculaceae.ASV_156	Guild 14
Blattella.germanica..German.cockroach..ASV_150	Guild 7	Akkermansia.ASV_10	Guild 15
Clostridium.sp..Culture.1.ASV_31	Guild 8	Parabacteroides.distasonis.ASV_18	Guild 15
Lachnospiraceae.ASV_33	Guild 8	Muribaculaceae.ASV_20	Guild 15
Lachnospiraceae.ASV_69	Guild 8	Muribaculaceae.ASV_75	Guild 15
Tyzzerella.ASV_71	Guild 8	Muribaculaceae.ASV_93	Guild 15
Muribaculaceae.ASV_129	Guild 15	Muribaculaceae.ASV_159	Guild 19
Muribaculaceae.ASV_136	Guild 15	Muribaculaceae.ASV_265	Guild 19
Lachnoclostridium.ASV_146	Guild 15	Helicobacter.ASV_15	Guild 20
Bacteroides.ASV_149	Guild 15	Mucispirillum.ASV_24	Guild 20
Alistipes.ASV_176	Guild 15	Muribaculaceae.ASV_28	Guild 20
Ureaplasma.ASV_317	Guild 15	Muribaculaceae.ASV_63	Guild 20
Muribaculaceae.ASV_39	Guild 16	Lachnospiraceae.ASV_70	Guild 20
Helicobacter.ASV_42	Guild 16	Tyzzerella.3.ASV_77	Guild 20
Mucispirillum.ASV_82	Guild 16	Muribaculaceae.ASV_201	Guild 20
Muribaculaceae.ASV_109	Guild 16	Lachnospiraceae.NK4A136.group.ASV_282	Guild 20
Lachnoclostridium.ASV_6	Guild 17	Ruminococcaceae.ASV_315	Guild 20
Muribaculaceae.ASV_9	Guild 17	Helicobacter.ASV_35	Guild 21
Muribaculaceae.ASV_14	Guild 17	Lachnospiraceae.NK4A136.group.ASV_72	Guild 21
Bacteroides.ASV_19	Guild 17	Ruminiclostridium.9.ASV_87	Guild 21
Muribaculaceae.ASV_26	Guild 17	Lachnospiraceae.ASV_131	Guild 21
Lactobacillus.ASV_49	Guild 17	Desulfovibrio.ASV_142	Guild 21
Parasutterella.ASV_73	Guild 17	Eubacterium.xylanophilum.group.ASV_151	Guild 21
Muribaculaceae.ASV_80	Guild 17	Lachnospiraceae.ASV_166	Guild 21
Parabacteroides.ASV_81	Guild 17	Lachnospiraceae.ASV_189	Guild 21
Muribaculaceae.ASV_90	Guild 17	Alistipes.ASV_106	Guild 22
Rhodospirillales.ASV_153	Guild 17	Peptococcaceae.ASV_167	Guild 22
Burkholderiales.bacterium.YL45.ASV_165	Guild 17	Lachnospiraceae.ASV_172	Guild 22
Clostridium.sp..K4410.MGS.306.ASV_209	Guild 17	Oscillibacter.ASV_180	Guild 22
Muribaculaceae.ASV_222	Guild 17	Lachnospiraceae.ASV_192	Guild 22
Alistipes.ASV_316	Guild 17	Prevotellaceae.UCG.001.ASV_22	Guild 23
Lactobacillus.ASV_50	Guild 18	Muribaculaceae.ASV_85	Guild 23
Muribaculaceae.ASV_74	Guild 18	Gastranaerophilales.ASV_139	Guild 23
Muribaculaceae.ASV_135	Guild 18	Muribaculaceae.ASV_211	Guild 23
Muribaculaceae.ASV_147	Guild 18	Rhodospirillales.ASV_255	Guild 23
Muribaculaceae.ASV_160	Guild 18	Ruminococcus.1.ASV_321	Guild 23
Alistipes.ASV_299	Guild 18	Muribaculaceae.ASV_325	Guild 23
Muribaculaceae.ASV_1	Guild 19	Gastranaerophilales.ASV_379	Guild 23
Muribaculaceae.ASV_17	Guild 19	Muribaculaceae.ASV_115	Guild 24
Muribaculaceae.ASV_25	Guild 19	Ruminiclostridium.9.ASV_121	Guild 24
Muribaculaceae.ASV_30	Guild 19	Ruminiclostridium.9.ASV_138	Guild 24
Muribaculum.ASV_32	Guild 19	Lachnospiraceae.ASV_154	Guild 24
Muribaculaceae.ASV_34	Guild 19	Lachnospiraceae.ASV_179	Guild 24
Muribaculaceae.ASV_40	Guild 19	Alistipes.ASV_198	Guild 24
Muribaculaceae.ASV_43	Guild 19	Ruminiclostridium.5.ASV_252	Guild 24
Muribaculaceae.ASV_52	Guild 19	Butyricicoccus.ASV_270	Guild 24
Muribaculaceae.ASV_98	Guild 19	Lachnospiraceae.ASV_338	Guild 24

As shown in Figure 2-3, at week 0, the abundance of 3 guilds (Guilds #19, 23 and 24) was significantly higher and that of 2 guilds (Guilds #14 and 15) was significantly lower in IFABP$^{-/-}$ mice compared with WT. A comparison of LFABP$^{-/-}$ and WT mice revealed even more significantly different guilds, i.e., 11 (Guilds #1, 3, 4, 7, 8, 11, 18, 19, 20, 22 and 24) were higher in abundance and 3 (Guilds #14, 15 and 17) were lower in the LFABP$^{-/-}$ mice. Among the 24 differentially regulated guilds, Guilds #19 and 24 increased, and Guilds #14 and 15 decreased in both knockout groups. These results show that, under a low fat chow diet, both FABP gene knockouts affected several functional guilds. IFABP$^{-/-}$ changed fewer guilds than LFABP$^{-/-}$, consistent with the aforementioned results that the dissimilarity between IFABP$^{-/-}$ and WT was smaller than that between LFABP$^{-/-}$ and WT.

Over the HFD feeding period from week 0 to week 11, 12 guilds (Guilds #1, 2, 3, 4, 5, 6, 7, 8, 10, 11, 12 and 13) increased and 5 (Guilds #14, 17, 19, 20 and 23) decreased significantly in LFABP$^{-/-}$ mice; 9 guilds (Guilds #1, 3, 4, 5, 7, 8, 9, 10 and 12) increased and 5 (Guild #15, 17, 19, 20 and 23) decreased significantly in IFABP$^{-/-}$ mice; 11 guilds (Guilds #1, 3, 4, 6, 7, 8, 9, 10, 11, 12 and 21) increased and 5 (Guild #14, 15, 17, 19 and 23) decreased significantly in WT mice (Fig. 2-3). Among these 20 HF-responding guilds, 10 (Guilds #1, 3, 4, 7, 8, 10 and 12 which increased; Guilds #17, 19, and 23 which decreased) displayed changes in the same direction in all the groups, while the other 10 changed in two or only one of the groups. These results indicate that while some of the HFD-induced changes were independent of genotype, the gut microbiota of WT, IFABP$^{-/-}$ and LFABP$^{-/-}$ mice also displayed differential responses to the HFD.

At week 11 of the HFD, only Guild #18 showed a significant difference between IFABP$^{-/-}$ and WT, being higher in IFABP$^{-/-}$. Compared with WT, the LFABP$^{-/-}$ had 5 guilds (Guilds #1, 2, 4, 18 and 20) that were significantly higher and 2 guilds (Guilds #7 and 14) that

were lower. Under both normal chow and HFD, no guilds showed consistent differences between WT and IFABP$^{-/-}$, however, Guilds #1, 4, 18 and 20 were consistently higher in LFABP$^{-/-}$ compared with WT mice. These results indicate that, at the guild level, the differences between the 2 knockout groups and WT remain but become smaller after HF feeding as the number of different guilds decreased. Notably, however, the differences in 4 guilds between LFABP$^{-/-}$ and WT mice are present regardless of the diet.

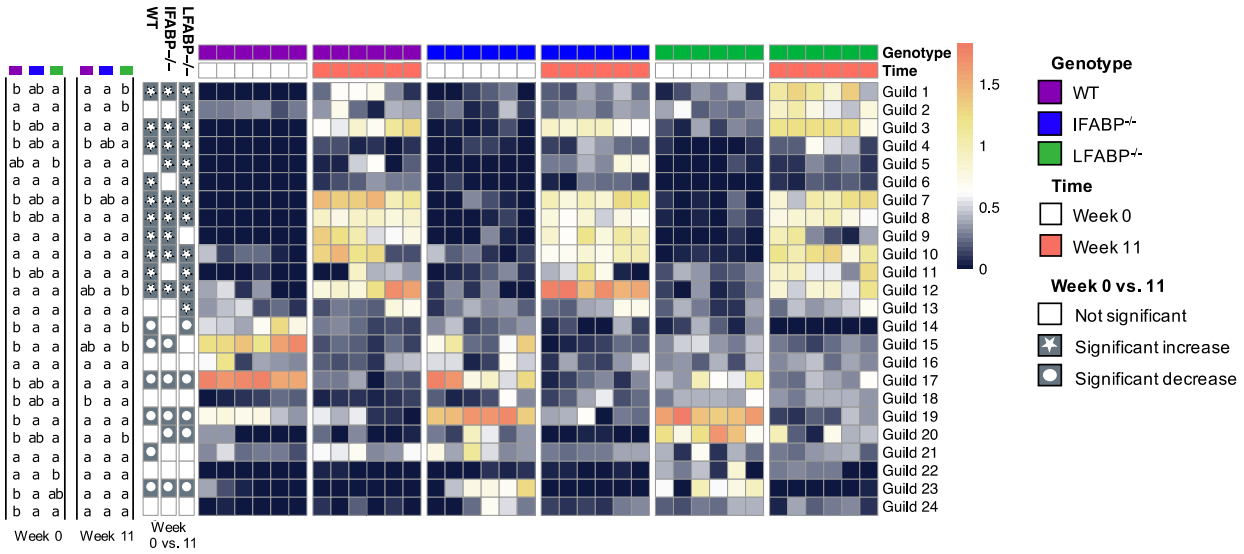

Figure 2-3: Differences and changes in the guilds of the 3 different genotypes. The heatmap shows the log10 transformed relative abundance of each guild. At each time point, guilds were compared among the groups using the Kruskal-Wallis test and post hoc Dunn's test. Values not sharing common letters are significantly different from one another ($P < 0.05$). Wilcoxon matched-pairs signed-ranks test (two-tailed) was used to test the same guild between week 0 and week 11 within each genotype, $P < 0.05$ was considered as significant.

Associations between gut microbiota and body weight

To explore the associations between gut microbiota and body weight, we applied a Random Forest regression model to correlate the 24 guilds and body weight. Using the data at week 0, based on the leave-one-out cross-validation and feature selection process, the best regression model with minimum mean square error for body weight contained 8 guilds (Fig. 2-4A and B), all of which showed differences between the 3 genotype groups. Each of the 8 guilds showed significant correlation with body weight. Particularly, among them, 3 guilds showed very large differences between the 3 genotype groups (Fig. 2-4C). Guild #17 accounted for 48.0% of the total abundance in WT, 22.1% in IFABP$^{-/-}$ and 5.3% in LFABP$^{-/-}$ mice. Similarly, Guild #15 was the most abundant in WT (27.2%) followed by IFABP$^{-/-}$ (6.8%) and LFABP$^{-/-}$ (1.6%). In contrast, the abundance of Guild #20 was the lowest in WT (0.4%) but higher in IFABP$^{-/-}$ (2.2%) and markedly higher in LFABP$^{-/-}$ (18.5%). The predicted body weights from cross-validation were significantly correlated with the measured values ($r = 0.721$, $p = 0.001$) (Fig. 2-4D). This result indicates that the genotype-related guilds associate with the host body weight under normal chow at 8 weeks of age.

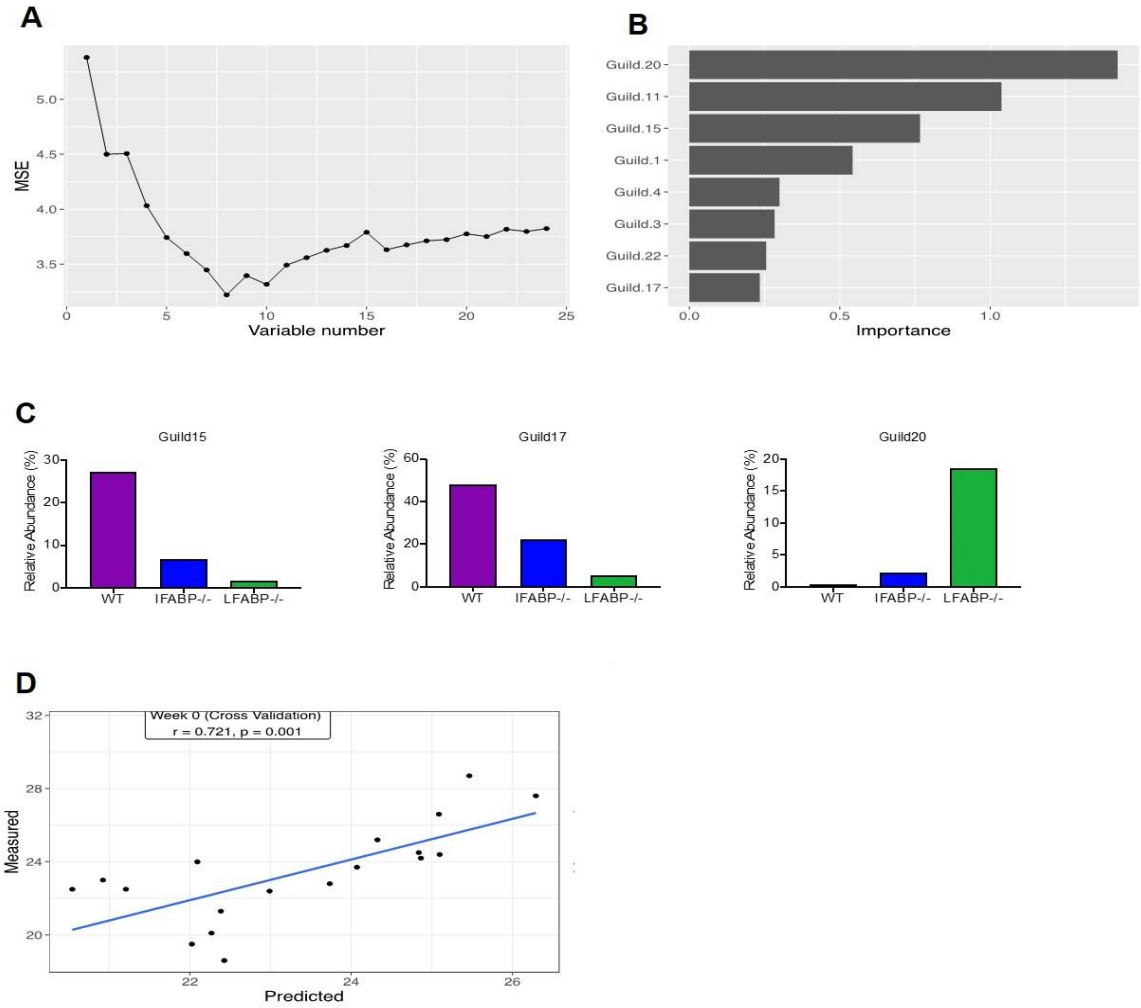

Figure 2-4: The association between gut microbiota and body weight at week 0, prior to HF feeding (chow fed from weaning until 8 weeks of age). Random Forest (RF) model regressing body weight on the guild abundance at week 0. A, shows the number of variables and mean squared error of the corresponding model; B, The RF assigns a mean error rate, or feature-importance score to each feature; this value indicates the extent to which each predictor contributes to the accuracy of the model; C, The average abundance of the guilds at week 0 prior to HF feeding initiation; D, Significantly positive correlation between the measured body weight and the predicted values from leave-one-out cross-validation based on RF model. Pearson correlation was applied.

To determine associations between guilds and body weight following the HFD period, we applied the Random Forest regression model to correlate the 24 guilds and body weight at week 11 (Fig. 2-5A and B). Ten guilds were included in the best model, having a minimum mean square error. Among these 10, 6 guilds had >5% differences between the 3 genotypes (Fig. 2-5C). Guild #12 was most dominant in the IFABP$^{-/-}$ mice (0.2% in WT, 43.8% in IFABP$^{-/-}$ and 6.23% in LFABP$^{-/-}$). In contrast, the abundance of Guild #10 was the lowest in IFABP$^{-/-}$ mice (13.7% in WT, 5.69% in IFABP$^{-/-}$ and 12.4% in LFABP$^{-/-}$). Guilds #1 and 3 were most abundant in LFABP$^{-/-}$ mice (Guild #1: 2.2% in WT, 1.0% in IFABP$^{-/-}$ and 11.6% in LFABP$^{-/-}$; Guild #3: 7.5% in WT, 6.0% in IFABP$^{-/-}$ and 13.4% in LFABP$^{-/-}$). Guild #9 had the lowest abundance in LFABP$^{-/-}$ mice (9.3% in WT, 8.3% in IFABP$^{-/-}$ and 3.8% in LFABP$^{-/-}$). As shown in Figure 2-5D, the predicted body weight from cross-validation were significantly correlated with the measured values ($r = 0.734$, $p = 0.001$). In addition, we found 4 common guilds (Guilds #1, 3, 4 and 22) in the two Random Forest regression models built on the data at week 0 and week 11. The predicted body weight values, which were based on the week 0 model and the week 11 guilds, were significantly correlated with the measured body weights at week 11 as well ($r= 0.519$, $p = 0.0207$) (Fig. 2-5E). These results indicate that the associations between guilds and body weight identified under normal chow are retained, in part, after HFD feeding. The contribution of some guilds to the body weight, by contrast, were manifested only after HFD feeding.

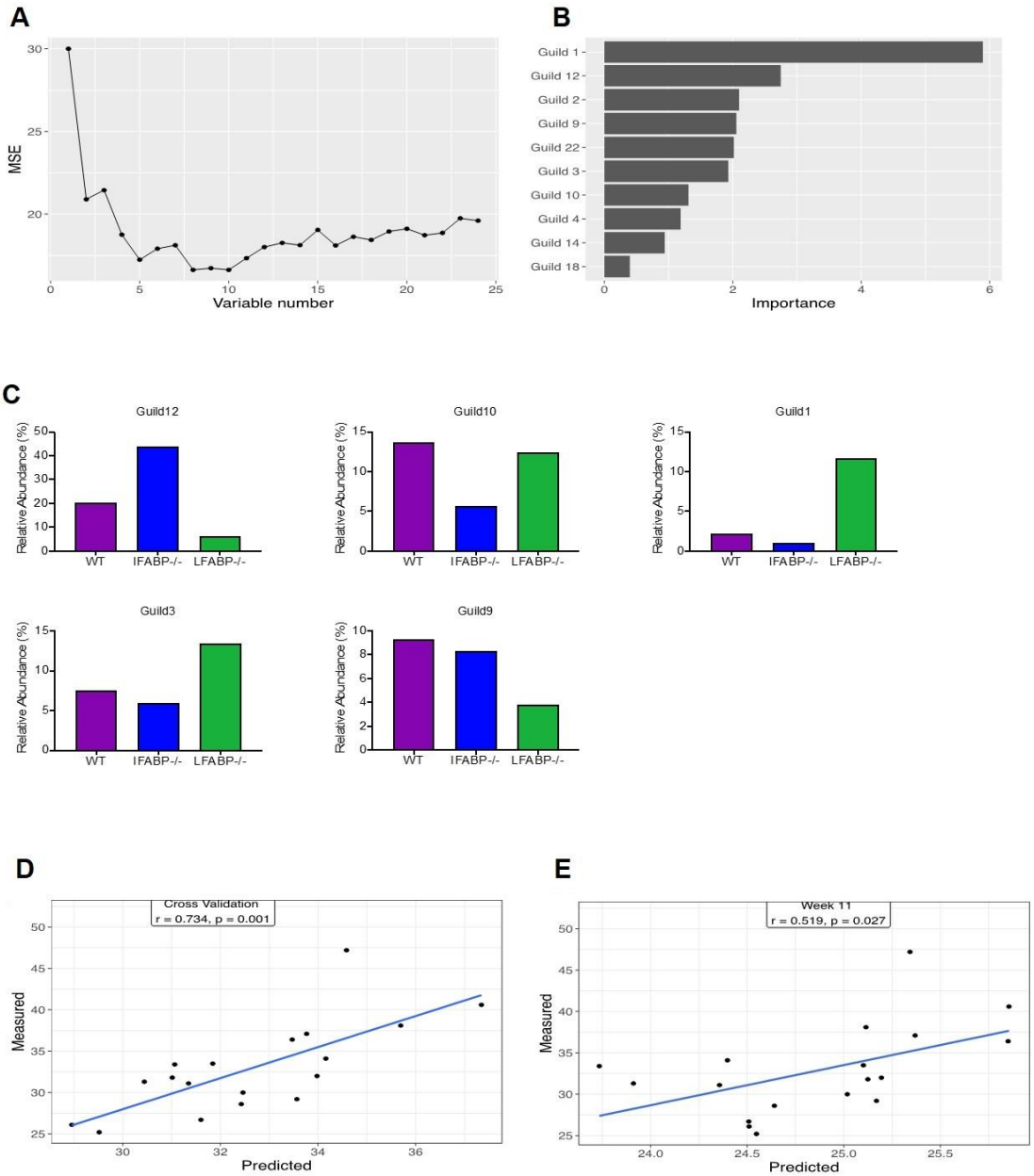

Figure 2-5: The association between gut microbiota and body weight following 11 weeks of the HF diet. Random Forest (RF) model regressing body weight on the guild abundance at week 11. A, shows the number of variables and mean squared error of the corresponding model; B, The RF assigns a mean error rate, or feature-importance score to each feature; this value indicates the extent to which each predictor contributes to the accuracy of the model; C, The average abundance of the guilds after 11 weeks of HF

feeding; D, Scatter plot of the measured body weight and the predicted values from leave-one-out cross-validation; E, Significantly positive correlation between the measured body weight and the predicted values from guild abundance at week 11 based on the week 0 model. Pearson correlation was applied.

IFABP and LFABP ablation and HF feeding alter fecal SCFA levels.

At week 0, prior to starting the HFD, the levels of all measured SCFAs, including acetate, propionate, isobutyrate, butyrate, isovalerate and valerate showed significant differences between the 3 genotypes (Fig. 2-6). Acetate, propionate, butyrate and valerate were significantly higher in both IFABP$^{-/-}$ and LFABP$^{-/-}$ mice compared to their control counterparts (Fig. 2-6A, B, D and F). Isobutyrate and isovalerate were significantly higher than the WT group only in the LFABP$^{-/-}$ mice (Fig. 2-6C and E).

After 11 weeks of HF feeding, the concentrations of SCFAs remained different between the 3 genotypes. In all 3 genotypes, acetate, propionate and butyrate levels were significantly decreased when compared to week 0 (Fig. 2-6A, B and D), while valerate was significantly increased after HF feeding (Fig. 2-6F). In keeping with what was observed at week 0, all of the SCFAs levels were significantly greater in both IFABP$^{-/-}$ and LFABP$^{-/-}$ mice when compared to the WT mice at week 11 of the HFD period. Both butyrate and valerate were higher in IFABP$^{-/-}$ mice when compared to LFABP$^{-/-}$ (Fig. 2-6D and F), while isovalerate was higher in LFABP$^{-/-}$ compared to IFABP$^{-/-}$ mice (Fig. 2-6E). These results indicate that differences in the levels of SCFAs are primarily due the genetic ablation of IFABP and LFABP, and persisted after chronic HF feeding.

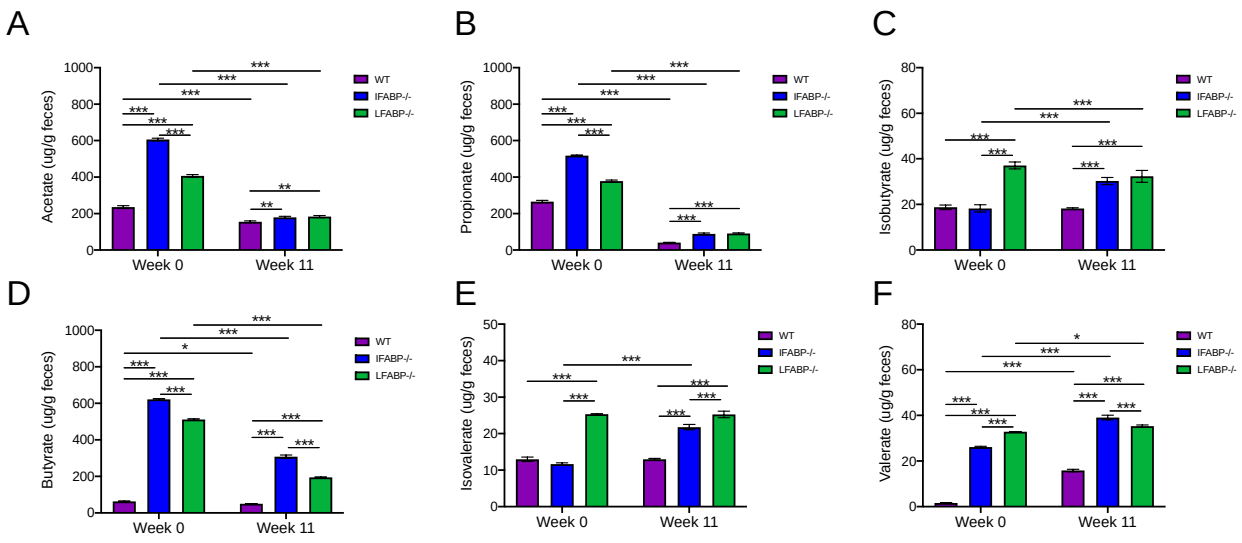

Figure 2-6: Analysis of SCFAs in WT, IFABP$^{-/-}$ and LFABP$^{-/-}$ mice at week 0 (chow diet from weaning until 8 weeks of age) and after 11 weeks of the HF diet. A, Acetate; B, Propionate; C, Isobutyrate; D, Butyrate; E, Isovalerate; F, Valerate. Feces were pooled from 6 mice in each genotype. Two-way ANOVA with Tukey's post-hoc was applied. * P < 0.05, **P <0.01, *** P < 0.001.

Discussion:

In the present study, we found divergent effects of IFABP vs. LFABP gene knockout on intestinal transit times and fecal output. The LFABP$^{-/-}$ mice had significantly slower transit, i.e. longer transit times, and lower fecal output per gram consumed. In agreement with our prior findings [222], the opposite was found in the IFABP$^{-/-}$ mice. Thus, the opposing body weight phenotypes of the IFABP and LFABP null mice are likely due, in part, to increased energy harvest in LFABP$^{-/-}$ and decreased energy harvest in IFABP$^{-/-}$ mice.

In recent years, it has been shown that FABPs, including both LFABP and IFABP, bind not only LCFAs, but also have high affinity binding for the ECs 2-AG and AEA [170,171,203,257]. ECs are involved in the regulation of food intake and intestinal motility through activation of the cannabinoid 1 receptor (CB1R) on vagal afferent neurons [258-260]. It has been shown that activation of the CB1R by receptor agonists like 2-AG inhibits peristalsis and can increase appetite [38-40]. Indeed, we previously showed that mucosal levels of 2-AG were lower in IFABP$^{-/-}$ mice whereas they were significantly higher in LFABP$^{-/-}$ mice, when compared to their WT counterparts [162]. Thus, the highly divergent phenotypes that have been observed in body weight, in the amount of fecal output, and in the intestinal motility of both IFABP$^{-/-}$ and LFABP$^{-/-}$ mice could, in part, be secondary to altered CB1R activation secondary to different mucosal ECs levels.

Compared with WT mice, both IFABP$^{-/-}$ and LFABP$^{-/-}$ had altered overall gut microbiota structure under a normal chow diet. Although shifting from normal chow to HFD changed the gut microbiota structure dramatically in all the three genotypes, the responses of the gut microbiota in each genotype were different. Such differences together with their different gut microbiota after HF feeding may be associated with the aforementioned variations in intestinal motility. Transit time is related to bacterial composition and

metabolism in the gut [254,261]. Interestingly, the LFABP$^{-/-}$ mice had the longest transit time and highest number of bacterial ASVs among the three genotypes, which is consistent with the finding that a long transit time associates with high microbial richness [254,261].

To assess the functional significance of the alterations in gut microbiota we applied guild analysis, which overcomes the pitfalls of commonly used taxonomy analysis and is a more ecologically sound approach for finding host phenotype-associated gut microbial members [252]. Under normal chow, among the 8 guilds that were associated with body weight, Guild #15, 17 and 20 showed remarkable and significant differences between the three genotypes. Guild #15 was negatively correlated with body weight and had one ASV from *Akkermansia*; the species *Akkermansia muciniphila* in this genus has been characterized as beneficial in whole-body energy metabolism [262]. Guild #17, which was negatively correlated with body weight, had ASVs from genera including *Lactobacillus* and *Lachnoclostridium*. Many members of *Lactobacillus* are considered as probiotics and are associated with host health [263], and members in *Lachnoclostridium* has been reported to be associated with an anti-obesity function [264]. Guild #20, which was positively correlated with body weight, contained one ASV from *Tyzzerella,* which have been reported as pro-inflammatory bacteria and to be related to obesity [265,266]. Compared with WT and IFABP$^{-/-}$, LFABP$^{-/-}$ mice not only had the lowest abundance of the potentially beneficial Guilds #15 and 17 but also highest abundance of the potentially obesogenic Guild #20.

After HF feeding, among the 10 guilds that were associated with body weight, Guild #12 was most dominant in the IFABP$^{-/-}$ mice and negatively correlated with body weight. This guild had 2 ASVs from *Lactobacillus*, 1 from *Bifidobacterium*, 1 from *Ileibacterium*, 1 from

Lactococcus, 1 from *Dubosiella newyorkensis*, 2 from *Lachnospiraceae*, 2 from *Ruminococcaceae,* 1 from *Enterorhabdus* and 1 from *Streptococcus*. Several members in *Lactobacillus*, *Bifidobacterium* and *Lactococcus,* have been reported to attenuate HFD induced obesity [267-269]. Guild #10, which had 3 ASVs from *Desulfovibrionaceae*, had the lowest abundance in the IFABP$^{-/-}$ mice and positively correlated with body weight. Members of *Desulfovibrionaceae*, which produce endotoxin and hydrogen sulfide, are considered pro-inflammatory and have been reported to be positively associated with obesity and inflammation [270,271]. Guilds #1 and 3, which had ASVs from *Odoribacter*, had the highest abundance in LFABP$^{-/-}$ mice and were positively correlated with body weight. *Odoribacter* has been reported to be positively correlated with body weight [272]. Indeed, under both diets, the LFABP$^{-/-}$ mice had the highest body weight among the three genotypes. Overall, the LFABP$^{-/-}$ mice had more potentially obesity-promoting guilds including bacteria such as those from *Tyzzerella*, *Desulfovibrionaceae and Odoribacter,* and fewer anti-obesity guilds including bacteria such as those from *Akkermansia, Lactobacillus, Lachnoclostridium and Bifidobacterium* [262-264,267-269]. The IFABP$^{-/-}$ mice, by contrast, had more anti-obesity and less obesity-promote guilds after HFD feeding, which appears associated with its lean phenotype relative to WT and LFABP$^{-/-}$ mice.

In addition to body weight, which was focused on here, our previous studies showed that LFABP$^{-/-}$ mice can be considered an example of “MHO” with higher levels of spontaneous activity [162] and a protection against the HFD-induced decline in endurance exercise capacity [219]. Recent human studies have highlighted that exercise can stimulate changes in gut microbiota associated with higher SCFA production [273,274]. Thus, in addition to the different transit time noted above, higher levels of endurance activity may be considered as another factor which potentially contributes to the significant differences

in gut microbiota between WT and LFABP$^{-/-}$ mice. Previously, we found that LFABP$^{-/-}$ mice had higher muscle glycogen levels and an increased FA oxidation rate when compared with WT mice [219]. Here, we found that SCFAs were significantly higher in LFABP$^{-/-}$ mice compared with WT mice. These findings are consistent with the recently proposed "gut-muscle axis" [225,275], in which SCFAs are considered as potential regulators, via increasing skeletal muscle glycogen and promoting FA uptake and oxidation [276]. Other studies have also shown that high levels of plasma and fecal acetate and propionate are associated with endurance exercise improvement [64,277]. Thus, gut microbiota may play an essential role in the "MHO" features of LFABP$^{-/-}$ mice.

In previous studies we showed that IFABP$^{-/-}$ mice remained lean (Fig 1A), a result that was also found in the present studies, and we also showed that the IFABP$^{-/-}$ mice had lower plasma glucose levels than their WT counterparts, and a normoinsulinimic phenotype after chronic HF feeding [162]. Here, we showed that IFABP$^{-/-}$ maintain a high level of fecal SCFAs. Many studies have indicated beneficial effects of SCFAs, specifically acetate, propionate and butyrate, on energy homeostasis and metabolism, and their crucial role in preventing HFD-induced obesity and improving insulin sensitivity [278-280]. Fecal SCFA levels can be modulated by several mechanisms including colonic absorption, colonic transit time, dietary intake and microbiota [281]. Though less SCFA-producing bacteria were identified in the LFABP$^{-/-}$ mice than in the IFABP$^{-/-}$ mice, their higher level of fecal SCFA may be related to their longer transit time, which increases the fermentation time [282]. The higher level of fecal SCFAs in the IFABP$^{-/-}$ mice may be related to increased SCFA production or reduced absorption. More SCFA-producing bacteria were identified in IFABP$^{-/-}$ mice, which suggests the possibility of increased SCFA production. However, as IFABP$^{-/-}$ mice have reduced transit time, this may result in reduced absorption of

SCFAs. In order to dissect the contributions of the observed SCFA changes to the IFABP$^{-/-}$ and LFABP$^{-/-}$ mice phenotypes, the measurement of SCFA absorption will be of interest.

In summary, our result show that gut microbiota is associated with the whole-body phenotypes of IFABP$^{-/-}$ and LFABP$^{-/-}$ mice. To determine whether the structure of the microbiota is an essential mediator of the effects of these gene knockouts on host phenotypes, future studies will assess the impact of transplanting the gut microbiota from the IFABP$^{-/-}$ and LFABP$^{-/}$ mice to germ-free or antibiotic-treated WT mice.

Chapter 3

Liver-Specific Ablation of Liver Fatty Acid-Binding Protein Regulates Whole-Body Energy Homeostasis and Hepatic Lipid Metabolism

Abstract

Liver fatty acid-binding protein (LFABP or FABP1) is a highly abundant intracellular lipid binding protein that is expressed in the liver, and the small intestine of mice, where it is thought to regulate fatty acids (FA) trafficking. Feeding whole-body LFABP knockout ($LFABP^{-/-}$) mice a high saturated fat diet resulted in increased body weight and fat mass (FM) relative to the wild-type (WT) controls, but also a metabolically healthy obese (MHO) phenotype; $LFABP^{-/-}$ mice displayed better exercise capacity and were protected against hepatic steatosis, when compared to the wild-type (WT) mice. However, it is uncertain whether these effects are due to the ablation of LFABP in the liver, in the intestine, or whether the simultaneous ablation in both tissues is necessary. Liver-specific LFABP null ($LFBAP^{liv-/-}$) mice were generated to assess the contribution of liver-LFABP to the MHO phenotype. The results show that female $LFABP^{liv-/-}$ mice were heavier and had increased FM, when compared to the control WT-LFABP floxed ($LFABP^{fl/fl}$) mice. The female $LFABP^{liv-/-}$ mice were also found to have better exercise capacity than their WT controls. In addition, ablation of liver-LFABP resulted in a reduction of hepatic FA uptake and a trend towards higher FA uptake by adipose tissues, suggesting a protection against Western-diet induced hepatic steatosis by shifting FAs to adipose storage. In the male $LFABP^{liv-/-}$ mice, some but not all aspects of the MHO phenotype were observed. Both female and male $LFABP^{liv-/-}$ mice displayed alterations in the expression of several hepatic lipid metabolism genes, when compared to their WT counterparts. Thus, in females, ablation of LFABP in the liver is sufficient to induce the MHO phenotype observed in the whole body knockout mouse. Males, however, may require the ablation of either intestine-LFABP or both liver- and intestine-LFABP. Overall, these findings show that deletion of LFABP in the liver alone is responsible for substantial protection against the high fat diet (HFD) induced a decline in exercise endurance and hepatic steatosis, despite the presence of marked obesity, particularly in female mice.

Introduction

Western-style diets, which are rich in saturated fats and associated with a sedentary life style, are the major causes of obesity, a chronic metabolic disorder that is considered a risk factor for many other metabolic comorbidities, like type II diabetes, cardiovascular diseases, cancer, autoimmune diseases, Alzheimer's disease, liver disease and many other diseases [283-285]. The prevalence of obesity around the world is increasing; it is estimated that by 2030, 38% of the global adult population will be overweight and 20% will be obese, while in the USA, it is expected that over 85% of adults will be overweight or obese [286]. Obesity is characterized by disturbances in food intake, fat storage, and energy utilization [284]. Given the contribution of calorie-dense lipids to the obesity epidemic in developed countries, it is necessary to understand how dietary lipids are digested, absorbed, metabolized, and processed by various body tissues.

The liver plays a major role in lipid metabolism, importing FA as well as synthesizing, storing, and exporting lipids [287,288]. There are several sources that constitute the hepatic pool of FA: *De novo* lipogenesis, chylomicron remnants directly taken up by the liver, TG stores, and plasma non-esterified FAs (NEFAs) released by adipose tissue. FA, whether they are from exogenous or endogenous sources, are either oxidized, stored as TG in lipid droplets, or recycled together with other hepatic lipids via assembly into new VLDL particles for export [98,100]. Plasma levels of NEFA are elevated during obesity and are positively correlated with body mass index, body fat percent, insulin resistance, and hepatic steatosis that is caused by the accumulation of TG-rich lipid droplets [289,290]. The hepatic content of TG is controlled by several intracellular molecules, which influence FA input and output through the regulation of hepatic FA uptake, synthesis, esterification, and oxidation, as well as hepatic TG export [291]. LFABP is a cytosolic, multi-ligand, lipid-binding protein that has a high affinity for long-chain FAs (LCFAs), monoglycerides (MGs),

prostaglandins, lysophospholipids, endocannabinoids (ECs), cholesterol, and other lipids [163,168,169,171-174]. It is highly expressed in hepatocytes, hepatic stellate cells (HSCs) [122,165,166], enterocytes [122] and in enteroendocrine cells (EECs) [36,292]. Many *in vitro* and *in vivo* studies have illustrated the functional significance of LFABP in the liver. Hepatic-LFABP can facilitate the uptake and delivery of diet-derived FA to the ER for the synthesis of TG, PLs, and CE [180,181,293]. LFABP can also direct FA towards mitochondrial or peroxisomal oxidation [178,213]. Moreover, LFABP bound FA can be directed to the nucleus where it facilitates FA binding to nuclear receptors, resulting in modulating the transcription of many genes involved in hepatic lipid metabolism, including LFABP itself [183-185].

A global body ablation of LFABP (LFABP$^{-/-}$) was generated by two laboratories on the C57BL/6 background [179,189]. The two lines showed a divergent body weight and lipid distribution; in response to HF feeding, LFABP$^{-/-}$ mice from Davidson group gained less weight [189] while mice from Schroeder and Binas group became obese [162,179]. Despite the difference in obesity, other observations were similar between these two lines, including reduced hepatic FA oxidation and uptake, and reduced hepatic steatosis [179,188,189,212].

The mice that are used in our lab were derived from Schroeder lab mice. Feeding our LFABP$^{-/-}$ mice a HFD resulted in increased body weight and FM, which were partly due to increased food intake relative to WT mice [162]. Despite their obese phenotype, however, LFABP$^{-/-}$ mice appear to be metabolically healthy, having fasting glucose, insulin, and lipids levels comparable to the WT mice, being protected against hepatic steatosis, and displaying a comparable intestinal TG secretion rates to their lean counterparts [162,213]. Furthermore, the LFABP$^{-/-}$ mice had higher spontaneous activity [162], and they were

protected against a HFD-induced decline in the exercise endurance [219]. Global LFABP$^{-/-}$ mice showed reduced FA β-oxidation in intestinal mucosa, which is thought to be due to impaired lipid transport rather than alteration in FA oxidative machinery [163]. Additionally, there was a shift in MG metabolism towards reduced TG synthesis in the enterocytes of LFABP$^{-/-}$ mice [162,163].

MHO or overweight is a newer term that has been proposed to describe a subgroup of people who are overweight or obese, but resistant to typically associated metabolic abnormalities [294,295]. Thus, whole-body LFABP$^{-/-}$ mice appear to be a model of the MHO phenotype. As mentioned previously, LFABP is expressed in both the liver and the intestine; it is unknown whether the observed MHO phenotype in the LFABP$^{-/-}$ mice is due to the ablation of LFABP in the intestine, in the liver, or if the simultaneous ablation in both the intestine and the liver is required. In order to unravel the underlying causes of the LFABP$^{-/-}$ phenotypes, LFABP conditional knockout (cKO) mice were generated in this study to assess the role of LFABP specifically within the liver, and to determine the contribution of liver-LFABP to the alterations in whole-body energy homeostasis and the MHO phenotype that were observed in the whole-body LFABP null mice.

Experimental Procedures

Generation of LFABP Floxed Mice

LFABP floxed mice were generated at the Rutgers Genome Editing Core Facility using clustered regulatory interspaced short palindromic repeats/CRISPR-associated Cas (CRISPR/Cas9) protein technology to introduce two loxP sites flanking exons 2 and 3 of the gene encoding LFABP. The type II bacterial CRISPR/Cas system can be used as an efficient gene-targeting technology [296,297]. First, two separate single guide RNAs (sgRNAs) were developed, with each formed to contain a targeting sequence (crRNA),

and a Cas9 nuclease-recruiting sequence (tracrRNA) [298]. The crRNA is a 20-nucleotide sequence that is homologous to sequences either upstream or downstream of exons 2 and 3 respectively of the lfabp gene. This sequence is adjacent to a sequence called a protospacer adjacent motif (PAM), which is required for Cas9 recognition, directing Cas9 nuclease activity specifically to the lfabp alleles. The Cas9 nuclease induces double-strand breaks (DSBs) at the sites of recognition (Fig 3-1A). To allow for a precise editing to occur, single stranded (ss) DNA donors were used to introduce two loxP sites within the host DNA via the homology directed repairmechanism. The ssDNA sequence is the same as for the WT lfabp gene, and contains the crRNA targeting sequence. Once the loxP site is successfully added, the crRNA sequence will be separated from the PAM sequence, and this will prevent further DSBs from occurring again. The ssDNA donor that is added upstream to exon 2 of lfabp contains also a PsiI restriction site, while the ssDNA donor that is added downstream to exon 3 contains an EcoRI restriction site (Fig 3-1B).

The ssDNA donors containing loxP, Cas9 protein, and the gRNA targeting downstream of the lfabp gene were microinjected into the oocytes of C57BL6/N mouse. After fertilization with sperm from C57BL6/J mice, the resultant mice contained only downstream loxP site. Then the oocytes from the resultant mice were microinjected again, but this time the gRNA targeted the upstream site of the lfabp gene. In this case, both exons 2 and 3 of the lfabp gene would be flanked by loxP sites. The resultant floxed mice ($LFABP^{fl/fl}$) mice on the mixed C57BL6/J and C57BL6/N background were backcrossed with WT C57BL6/J mice 4 additional times, yielding congenic $LFABP^{fl/fl}$ mice on the C57BL6/J background.

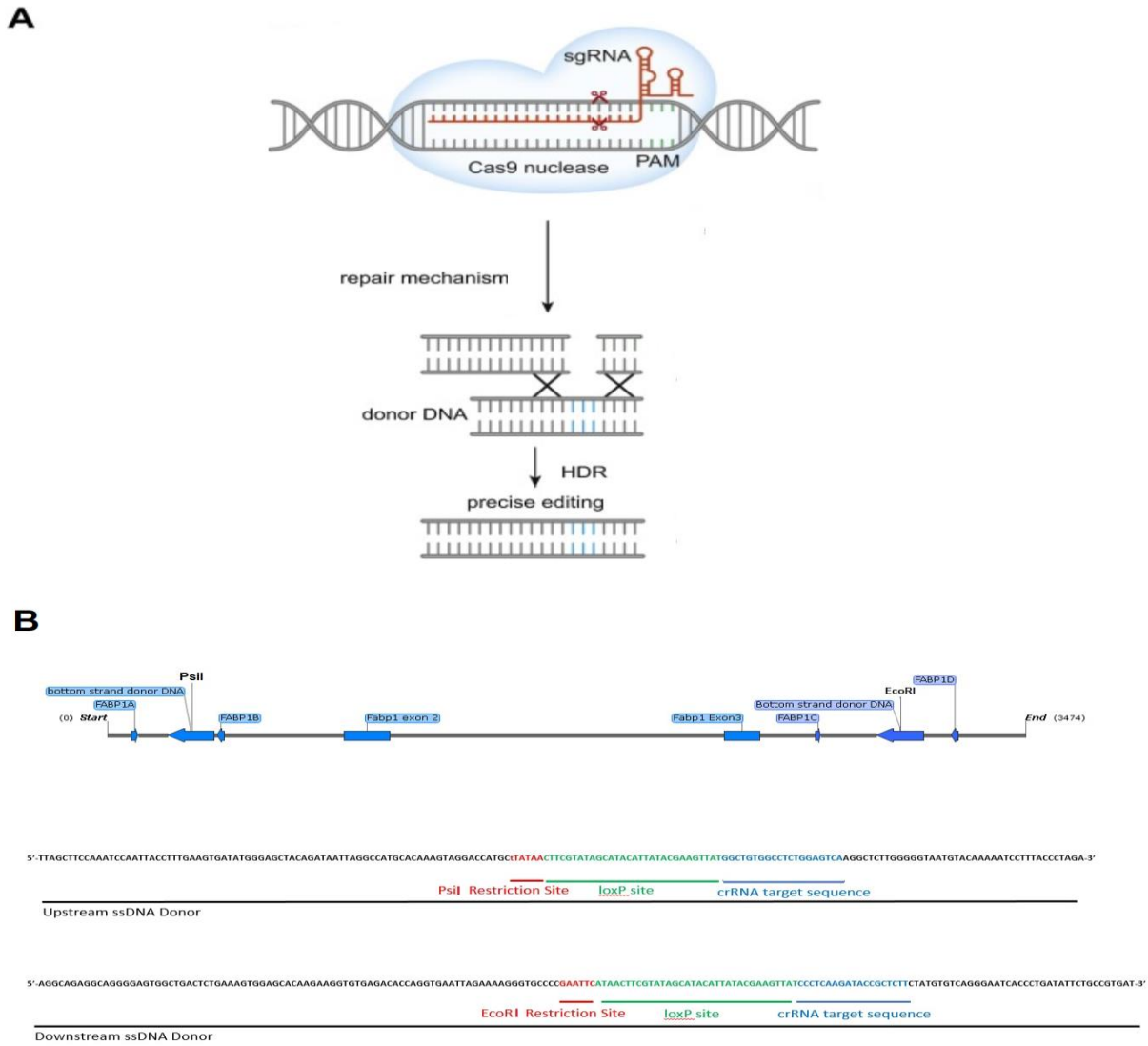

Figure 3-1: **The generation of Flox mice using the CRISPR/Cas9 system.** A, CRISPR guide sequences (gRNA) detect a specific DNA sequence in the gene of interest. The CRISPR associated Cas9 protein is able to recognize and induce a DSB in the DNA strands that are complementary to the CRISPR sequence. A ssDNA donor can be incorporated into the targeted sequence via homology driven DNA repair mechanisms, allowing for knock-in to occur. B, Sequences for the upstream and downstream ssDNA donors. The upstream ssDNA donor contains a PsiI restriction site, loxP sequences, and distinct crRNA targeting sequences, while the downstream ssDNA donor contains an EcoRI restriction site, loxP sequences, and distinct crRNA targeting sequences. PsiI and

EcoRI restriction sites are important for assessing the presence of both the upstream and downstream loxP sites. The illustration in (A) is adapted with edit from Zhan *et al*., 2019 [299]

Generation of Liver-Specific LFABP Null Mice

The resultant LFABP$^{fl/fl}$ mice were bred with mice that were homozygous for Cre recombinase, driven by the albumin promoter (A-cre), to generate double-mutants. These mice were then intercrossed to generate liver-specific LFABP KO (LFABP$^{liv-/-}$) and control WT (LFABP$^{fl/fl}$) mice (Fig 3-2). Mice were maintained on a 12-hour light/dark cycle, and a controlled temperature. They were allowed *ad libitum* access to standard rodent chow (Purina Laboratory Rodent Diet 5015) until the start of the study at two months of age.

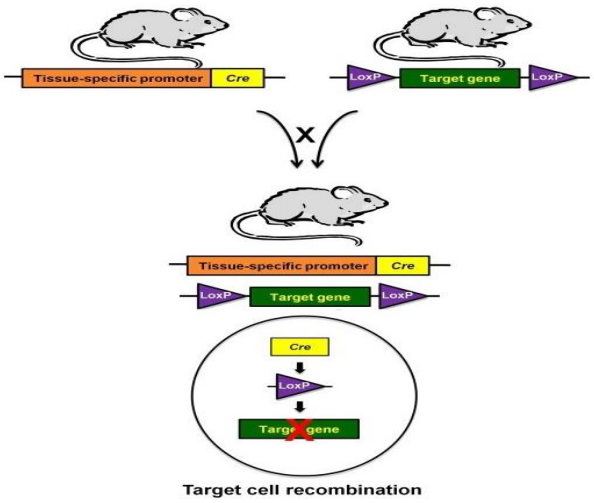

Figure 3-2: **Breeding scheme for the generation of tissue-specific KO mice using Cre/lox approach.**

Mating a homozygous floxed mouse of interest, in this case LFABP$^{fl/fl}$, to a cre transgenic mouse strain with an A-cre promoter will result in approximately 50% of the offspring heterozygous for the loxP allele and heterozygous for the cre transgene in the first generation. Backcrossing these mice with LFABP$^{fl/fl}$ mice will result in about 25% of the

offspring being the tissue-specific KO mice, which are homozygous for the loxP allele and hemizygous for the cre transgene. Also, about 25% of the offspring will be LFABP$^{fl/fl}$ mice which are used as the WT control mice. The illustration is adapted with permission from ref. [300]. Copyright 2013, Elsevier Inc.

DNA Extraction for Genotyping

DNA extraction was performed as described previously [163]. In brief, a 0.5 cm tail biopsy is incubated overnight at 37°C in lysis buffer (0.3M sodium acetate, 10mM Tris-HCL pH7.9, 1mM EDTA, 1% SDS, 0.2mg/mL proteinase K). The following morning, the lysate is cooled on ice, and the precipitate is pelleted. The supernatant is placed into a new 1.5 ml eppendrof tube, and ethanol precipitation is used for DNA isolation.

For the genotyping of the LFABP$^{fl/fl}$ mice, four primers were developed and used to assess the upstream and downstream loxP sites in two separate PCR reactions (Table 3-1, 3-2). The primer sequences for the LFABP$^{fl/fl}$ protocols are as follows:

1-Primers used for the upstream loxP:

FABP1A: AGACAAGTCAAAGATCATGAATGTGAG

FABP1B: TGGCTCTTAGAGTGGGAACACTTC

2-Primers used for the downstream loxP:

FABP1C: CGGAGTTGATAGATATCAGATC

FABP1D: GAAACAGGGCAAGGCCAGCTATG

After the reactions were done the PCR products for the upstream loxP reaction were digested with PsiI, while the PCR products for the downstream loxP site were digested with EcoRI. Then, electrophoresis was performed on a 2% agarose gel. WT mice that do not have the inserted loxP sites will only have one band for both the upstream (320BP)

and downstream (506BP) reactions. However, LFABP$^{fl/fl}$ mice will have two smaller bands for both the upstream (231BP and 119BP) and downstream (325BP and 215BP) reactions.

Table 3-1: PCR thermocycle for the upstream loxP site

Step #	Temp °C	Time min	Note
1	94	2:00	
2	94	0:15	
3	68	1:30	
4			repeat steps 2-3 for 34 cycles
5	72	7:00	
6	4		Hold
Put **12 ul** of the reaction mixture in each tube and run the PCR machine.			

Table 3-2: PCR thermocycle for the downstream loxP site

Step #	Temp °C	Time min	Note
1	94	2:00	
2	94	0:15	
3	64	0:30	
4	72	1:30	
5			repeat steps 2-4 for 34 cycles
6	72	7:00	
7	4		Hold
Put **23 ul** of the reaction mixture in each tube and run the PCR machine.			

The genotyping protocol for the A-cre mice uses 3 primers for one PCR reaction (Table 3-3). One primer, A-cre common, is shared with both WT and Mutant primers. The A-cre WT primer is used to detect a band that can be found in WT mice (~351 BP), while the A-cre mutant primer is used to detect a band that should only be observed in A-cre mice (~390 BP). The A-cre mice could be hemizygotes or homozygotes. The primer sequences used for the A-cre genotyping protocol are as follows:

A-cre reaction (WT and Mutant bands):

A-cre Common: 5’-TTG GCC CCT TAC CAT AAC TG-3’

A-cre WT: 5'-TGC AAA CAT CAC ATG CAC AC-3'

A-cre Mutant: 5'-GAA GCA GAA GCT TAG GAA GAT GG-3'

Table 3-3: PCR thermocycle for A-cre genotyping

Step #	Temp °C	Time min	Note
1	94	2:00	
2	94	0:20	
3	61	0:15	-0.5 C per cycle decrease
4	68	1:00	
5			repeat steps 2-4 for 10 cycles (Touchdown)
6	94	0:15	
7	60	0:15	
8	72	1:00	
9			repeat steps 6-8 for 28 cycles
10	72	2:00	
11	10		Hold
Put **20 ul** of the reaction mixture in each tube and run the PCR machine.			

Diet

Two months old male and female LFABP$^{liv-/-}$ mice and LFABP$^{fl/fl}$ control mice were fed a 45% Kcal fat semipurified HFD (D10080402, Research Diets, New Brunswick, NJ) (Table 3-4 and 3-5) for 12 weeks.

Table 3-4: Diet composition of high saturated fat diet [162]

	HFS	
	grams	**kcal**
Casein	200	800
L-Cystine	3	12
Corn starch 1.2/128	72.8	291
Maltodextrin	100	400
Sucrose	172.8	691
Cellulose	50	0
Soybean Oil	10	90
Cocoa Butter	192.5	1733
Mineral mix	45	0
Vitamin mix	10	40
Choline Bitartrate	2	0

Total	858.1	4057

Table 3-5: FA composition of high saturated fat diet [162]

	HFS grams/4057 kcal
C16	49.9
C16:1	0.4
C18	64.3
C18:1	65.2
C18:2	10.7
C18:3	1.0
%	
Saturated fatty acids	60.0
Monounsaturated fatty acids	33.9
Polyunsaturated fatty acids	6.1

Body Weight and Body Composition

During the HFD feeding period, the body weight was measured each week. FM and fat-free mass measurements were taken by MRI (Echo Medical Systems, LLC., Houston, TX) 1-2 days before starting the feeding protocol, and 1-2 days before sacrificing the mice. The instrument was calibrated each time according to the manufacturer's instructions. At each time point, two measurements were taken for each mouse and averaged.

Indirect Calorimetry, Activity, and Food Intake

Respiratory exchange ratio (RER), activity and food intake were assessed using the Oxymax system (Columbus Instruments, Columbus, OH) during week 10-11 of the feeding protocol. Mice were placed in an indirect calorimetry chamber (1 mouse per chamber) with food for 48 hours. The first 24 hours was used as an acclimation period, while the second 24 hours period was used for recording RER (VCO2/VO2), activity and food intake. Energy expenditure (EE) was measured by using the gas exchange measurements as follows: $(3.815 + 1.232 \times RER) \times VO2$ [301].

Intestinal Transit Time

Transit time measurements were performed between week 11 and 12 on HFD feeding period. Prior to the start of the experiment, mice were individually caged. After two hours of acclimation, mice were given 250μL of 6% carmine red and 0.5% methylcellulose (Sigma-Aldrich, St. Louis, MO) in PBS by oral gavage. After gavaging the mice, the cages were then checked every 10 minutes and the time of appearance of the first red fecal pellet was recorded [238,302].

Total Fecal Excretion

Mice were housed 2-3 per cage. Feces from each cage were collected for 3-4 days between weeks 11 and 12 of the HFD feeding period, dried overnight at 60◦C, and then weighed. The weight of the feces was converted into kcal energy excreted and divided by the number of mice in the cage, and by the number of days of collection. In order to control for differences in food intake (energy intake), the averaged energy intake was measured for the mice in the same cage from where the feces were collected. Then the results of the averaged feces excreted were normalized to their respective averaged 24 hour energy intakes, to generate values of kcal energy absorbed per mouse per day.

Treadmill Exercise Protocol

Exercise endurance testing was done after 12 weeks of HF feeding using a treadmill inclined at 25°. One day prior to the test mice were acclimated by walking at 5 m/min for 5 minutes. For the test, the speed began at 6 m/min for 5 minutes, and then was increased by 3 m/min every 2 minutes. The treadmill has a shock grid at the base, which was kept at a low intensity. When the mice fail to keep up with the treadmill belt, they come in contact with the shock grid. When the mice remained on the shock grid for 5 seconds,

they were considered to be exhausted and have fatigue; at this time the mice were removed from the apparatus, and the time to fatigue and total distance traveled were recorded [303,304].

Oral Glucose Tolerance Tests (OGTT)

Prior to the OGTT experiments, mice were fasted for 6 hours during week 11 of the HF feeding protocol. Blood was drawn from the tail vein, and glucose was measured using an Accu-Check monitor. Then an oral gavage of 2g glucose/Kg body weight was administered, and blood was sampled at time points of 30, 60, 90, and 120 minutes.

Tissue Preparation

At the end of the HF feeding period, mice were fasted for 16 hours prior to sacrifice. Before the surgery mice were anesthetized with ketamine-xylazine-acepromazine (80, 100, 150 mg/kg intraperitoneally, respectively). Epididymal fat pads and livers were removed, weighed, immediately placed on dry ice, and stored at -80°C for further analysis. The small intestine from stomach to cecum was removed, measured lengthwise, rinsed with 60 mL of ice-cold 0.1M NaCl, and opened longitudinally. Intestinal mucosa was scraped with a glass microscope slide into tared tubes on dry ice to be further used for mRNA extraction, protein extraction, or lipid extraction.

Blood Preparation and Analysis

At time of sacrifice, whole blood was used to measure glucose (Accu-Check, Roche Diagnostics). Plasma was isolated after centrifugation for 6 minutes at 4000 rpm, and stored at -80°C for further analysis. ELISA kits were used to measure plasma insulin and leptin (Millipore). Adiponectin was measured using a Sigma-Aldrich ELISA kit. Plasma cholesterol and FFA were measured colorimetrically using Cell Biolabs kits, and TG was

measured colorimetrically using a Cayman kit. Adiponectin and leptin indices were calculated by dividing adiponectin or leptin levels by the total FM determined by MRI.

RNA Extraction and Real-Time PCR

Total mRNA was extracted from small intestinal mucosa and liver, and analyzed as previously described [162,170]. Primer sequences (Table 3-6) were obtained from Primer Bank (Harvard Medical School QPCR Primer Database). The efficiency of PCR amplifications was checked for all primers to confirm similar amplification efficiency. Real time PCR reactions were performed in triplicate using an Applied Biosystems StepOne Plus instrument. Each reaction contained a suitable amount of cDNA, 250nM of each primer, and 12.5μL of SYBR Green Master Mix (Applied Biosystems, Foster City, CA) in a total volume of 25μL. Relative quantification of mRNA expression was calculated using the comparative Ct method, normalized to endogenous TATA-binding protein (TBP).

Table 3-6: Primers sequences for qPCR analysis of hepatic lipid metabolism

Genes		Sequences (5'→3')
Tpb	Forward	AGAACAATCCAGACTAGCAGCA
	Reverse	GGGAACTTCACATCACAGCTC
Fatp2	Forward	TCCTCCAAGATGTGCGGTACT
	Reverse	TAGGTGAGCGTCTCGTCTCG
Fapt5	Forward	TCTATGGCCTAAAGTTCAGGCG
	Reverse	CTTGCCGCTCTAAAGCATCC
Got1	Forward	GCGCCTCCATCAGTCTTTG
	Reverse	ATTCATCTGTGCGGTACGCTC
CD36	Forward	ATGGGCTGTGATCGGAACTG
	Reverse	GTCTTCCCAATAAGCATGTCTCC
Ldlr	Forward	TGACTCAGACGAACAAGGCTG
	Reverse	ATCTAGGCAATCTCGGTCTCC
Lfabp	Forward	ATGAACTTCTCCGGCAAGTACC
	Reverse	CTGACACCCCCTTGATGTCC
Scp2	Forward	CCTTCTGTCGCTTTGAAATCTCC
	Reverse	GCTTCCTTTGCCATATCAGGAT
Acbp	Forward	GAATTTGACAAAGCCGCTGAG
	Reverse	CCCACAGTAGCTTGTTTGAAGTG
Acc1	Forward	ATGGGCGGAATGGTCTCTTTC

	Reverse	TGGGGACCTTGTCTTCATCAT
Fasn	Forward	GGAGGTGGTGATAGCCGGTAT
	Reverse	TGGGTAATCCATAGAGCCCAG
Elovl6	Forward	GCACCCGAACTAGGTGACAC
	Reverse	CCCCAGCGACCATGTCTTT
Scd1	Forward	TTCTTGCGATACACTCTGGTGC
	Reverse	CGGGATTGAATGTTCTTGTCGT
Acsl1	Forward	TGCCAGAGCTGATTGACATTC
	Reverse	GGCATACCAGAAGGTGGTGAG
Acsl5	Forward	TCCTGACGTTTGGAACGGC
	Reverse	CTCCCTCAATCCCCACAGAC
Cpt1α	Forward	CTCCGCCTGAGCCATGAAG
	Reverse	CACCAGTGATGATGCCATTCT
Cpt2	Forward	CAGCACAGCATCGTACCCA
	Reverse	TCCCAATGCCGTTCTCAAAAT
Acadl	Forward	GAGAAGTGAGTAGAGAGGTCTGG
	Reverse	AACTGCTGTTGAGAGCAAGTC
Hmgcs2	Forward	AGAGAGCGATGCAGGAAACTT
	Reverse	AAGGATGCCCACATCTTTTGG
Acox1	Forward	TAACTTCCTCACTCGAAGCCA
	Reverse	AGTTCCATGACCCATCTCTGTC
Acaa1b	Forward	TGCAGTCAAGCACAAGCCT
	Reverse	CAGGGAGTTCAGGGTGCTAC
Pparα	Forward	AGAGCCCCATCTGTCCTCTC
	Reverse	ACTGGTAGTCTGCAAAACCAAA
Gpat1	Forward	CTTGGCCGATGTAAACACACC
	Reverse	CTTCCGGCTCATAAGGCTCTC
Mgll	Forward	ACCATGCTGTGATGCTCTCTG
	Reverse	CAAACGCCTCGGGGATAACC
Lipc	Forward	ATGGGAAATCCCCTCCAAATCT
	Reverse	GTGCTGAGGTCTGAGACGA
Hnf1α	Forward	GACCTGACCGAGTTGCCTAAT
	Reverse	CCGGCTCTTTCAGAATGGGT
Hnf4α	Forward	CACGCGGAGGTCAAGCTAC
	Reverse	CCCAGAGATGGGAGAGGTGAT
Fgf21	Forward	AGATCAGGGAGGATGGAACA
	Reverse	TCAAAGTGAGGCGATCCATA

Western Blotting

Small intestinal mucosa and liver were harvested as described above, and homogenized in 10x volume of PBS pH 7.4 with 0.5% (vol/vol) protease inhibitors (Sigma 8340) on ice with a Potter Elvejhem homogenizer for 10 strokes. Total cytosolic fractions were obtained by ultracentrifugation (100,000 x g, 1 hour at 4°C) and protein concentration was determined by the Bradford assay [305]. Thirty micrograms of cytosolic protein were mixed with an Instant-Bands pre-staining protein sample loading buffer in a 2:1 (v/v) ratio (EZBiolab, Carmel, IN) for visualization of total sample protein. Samples then were loaded onto 15% polyacrylamide gels and separated by SDS-PAGE. The proteins were then transferred onto 0.45μm nitrocellulose membranes using a semidry transfer system (Bio-Rad) at 100 V constant voltage for 1.5 to 2 h. Membranes were blocked by incubating in 5% non-fat dry milk overnight at 4°C, and were incubated with an α-LFABP primary antibody (1:2000 for 1 hour at room temperature) [163]. After thorough washing, blots were incubated in α-rabbit IgG-horseradish peroxidase conjugate (1:20,000) for 1 hour, and developed by chemiluminescence (WesternBright Quantum, Advansta, Menlo Park, CA). Protein expression was quantified by densitometric analysis with LI-COR Image Studio (Lite version 5.2). Target protein content was normalized to total protein content within a sample.

Lipid Extraction and Metabolites Analysis

Mucosa and liver samples collected as above were subsequently diluted with 10x volume of PBS, pH 7.4 per gram wet weight, and homogenized using 20 strokes with a Potter-Elvejhem homogenizer on ice. Protein concentration was determined by the Bradford assay [305], and lipid extraction was performed on samples containing 1 mg protein/ml using the Folch procedure [306]. Liver and intestinal lipid contents were normalized to the total protein. Lipids were extracted twice with 10 ml chloroform/methanol (2:1) and the

aqueous phase non-lipid fractions discarded. The organic lipid layer was dried under a nitrogen stream and resuspended in chloroform/methanol (1:1) and spotted onto Silica gel-G TLC plates along with authentic standards of known mass. The TLC plate was developed in a nonpolar solvent system consisting of hexanes: diethyl ether: and acetic acid (70:30:1 v/v/v). Another solvent system was used to separate cholesterol; hexane: diethyl ether: glacial acetic acid, 100:8:2, (v/v/v). The lipid spots were visualized by spraying the plates with solution contains 3% cupric acid in 8% phosphoric acid. Then, after evaporation in a 140 °C oven, the plate was scanned with a Hewlett-Packard scanner. Absolute values for lipid masses were obtained by densitometric analysis with ImageJ software based on the standard curves using authentic standards.

Histological Analysis

Livers were harvested as described above and fixed in 10% neutral buffered formalin. The optimum formalin: liver volume ratio used was 15:1, with15 ml of formalin used per 1cm^3 of tissue. These conditions allow liver tissues to become adequately fixed within 24 hours at room temperature. Tissues were then embedded in paraffin. For initial histological analysis, around 6μm liver tissue sections were stained with hematoxylin and eosin (H&E) (Rutgers Pathology Services, Piscataway, NJ). After that tissue sections were photographed using the Vs120-S5 System (Olympus, Center Valley, PA).

VLDL-TG Secretion Measurement

After 12 weeks of HF feeding, mice were fasted for 6 hrs. Then an intraperitoneal injection of Tyloxapol (500 mg/kg BW) was administered to block lipolysis of TG via inhibition of lipoprotein lipase. At time 60, 90, 120, 150 and 180 minutes after injection, 15 μl of blood was collected from conscious mice via the tail vein. Blood TG levels were measured using a Cardiochek instrument (Polymer Technology Systems, Inc. Zionsville, IN).

Oral Fat Tolerance Test (OFTT)

OFTT was performed as described previously [162]. After 12 weeks of HF feeding, mice were fasted for 6 h. Time 0 blood was taken from conscious mice via the tail vein and then an intraperitoneal injection of Tyloxapol (500 mg/kg BW) was administered to prevent lipolysis via inhibition of lipoprotein lipase. After 30 min, an orogastric gavage of 300 µL of olive oil was given. Blood was taken at t = 1, 2, 3, and 4 hours. Blood TG levels were measured using 15 µl of whole blood from the tail vein using a Cardiochek instrument (Polymer Technology Systems, Inc. Zionsville, IN).

FA Oxidation Measurements

FA oxidation rates in liver homogenates were measured as detailed by Huynh and co-workers [307]. Briefly, upon sacrifice, livers (200 mg) were gently homogenized with a Potter–Elvehjem homogenizer for 5 strokes on ice, using 5x the weight of the samples (wet weight) of sucrose–Tris–EDTA, and the homogenates were centrifuged at 420 x g for 10 min at 4°C, and then the supernatants were incubated for 30 min at 37°C with 370 µl of reaction mixture containing 1.6 µCi of ^{14}C oleate solubilized in 0.7% bovine serum albumin (BSA), and 500 µM palmitate. $^{14}CO_2$ generated from the reaction was released by adding 200 µl of 1 M perchloric acid and absorbed onto a piece of filter paper in the tube cap soaked with 10 µl of 1 M Sodium hydroxide. The filter paper and ^{14}C-labeled acid soluble metabolites (ASMs) in the reaction mixture were assessed for radioactivity by scintillation counting.

FA Uptake Assay

FA uptake into different tissues were measured according to [308-310] with minor modification. Overnight-fasted mice received an orogastric gavage of ^{14}C Oleic acid (2.5

μCi) in 200 μL olive oil. Four hours after the oral lipid load, mice were anesthetized with ketamine-xylazine-acepromazine (80, 100, 150 mg/kg ip, respectively). Blood samples were drawn from anesthetized mice, and plasma was extracted by adding 9% of perchloric acid and then centrifuged for 1 min at 16,000 x g. Liver, gastrocnemius muscle, and epidedmal white adipose tissue (eWAT) were removed, rinsed with NaCl and blotted dry. Tissues were weighed and EcoLume cocktail Counting Scintillant was added. Total radioactivity was measured using scintillation counting. Small intestines were also extracted, washed with 10 ml 0.8% NaCl and divided into two parts, the proximal intestine (PI) and distal intestine (DI). EcoLume cocktail Counting Scintillant was added and both the intestinal tissues and the non-absorbed luminal content (in NaCl) were examined for ^{14}C activity to determine the amount of absorbed versus non-absorbed FA present in the intestinal tract.

Statistical Analysis

The results were analyzed using Prism 8 version 2. Data are expressed as the mean ± standard error of the mean (S.E.M). Statistical comparisons were determined between genotypes on the same diet using a two-sided Student's t-test. Differences were considered significant at $P<0.05$, with symbols *<0.05, **<0.01 and ***<0.001.

Results:

<u>The ablation of LFABP was specific to the liver</u>

LFABP$^{fl/fl}$ mice were crossed with A-cre homozygous mice to generate double mutant mice with one floxed LFABP gene allele and one allele that contains A-cre (LFABP$^{fl/+;Acre/+}$). These double mutant mice were subsequently crossed with LFABP$^{fl/fl}$ mice to generate the liver-specific LFABP$^{-/-}$ mice (LFABP$^{fl/fl;Acre/+}$, known as LFABP$^{liv-/-}$), and littermate LFABP$^{fl/fl}$ mice that were used as WT controls (Fig 3-3A, B and C). Ablation of LFABP in the liver, but not the intestine of LFABP$^{liv-/-}$ mice, was confirmed by qPCR and Western blotting (Fig 3-3D and E). Control LFABP$^{fl/fl}$ mice were phenotypically similar to WT mice, expressing LFABP in both the liver and the intestine (Fig 3-3D and E).

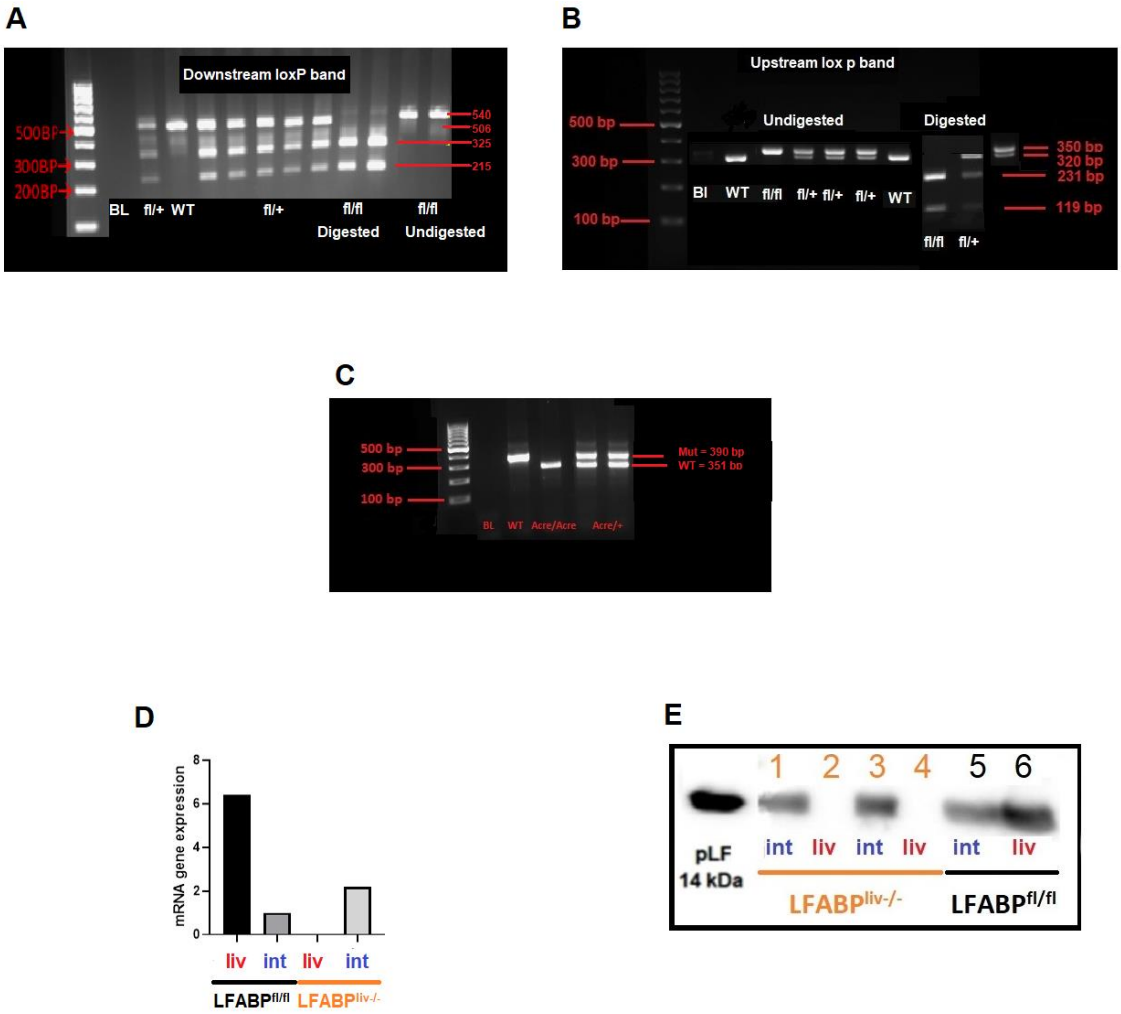

Figure 3-3: Generating LFABP$^{fl/fl}$ and LFABP$^{liv-/-}$ mice. A and B, DNA gels showing PCR reactions for loxP sites flanking the lfabp gene. A, For the downstream loxP site, 506 BP indicates a WT allele, while 540 BP indicates an allele with the loxP site (325BP and 215BP after digestion with EcoRI). B, For the upstream loxP site the band at 320 BP is indicative of an uncut WT band, while the 231BP and 119BP fragments indicate an allele that contains the loxP site after digestion with PsiI; C, DNA gel showing PCR reactions for A-cre genotyping; D and E, qPCR and Western blotting confirm the liver-specific ablation of LFABP in LFABP$^{liv-/-}$ mice. Purified LFABP protein (pLF) was used as a positive control.

Female LFABP$^{liv-/-}$ mice have greater body weight and FM compared to the control floxed mice

At two months of age, LFABP$^{fl/fl}$ and LFABP$^{liv-/-}$ mice were challenged with a 45% Kcal fat HFD. The body weight of female LFABP$^{liv-/-}$ mice was significantly higher than that of their LFABP$^{fl/fl}$ counterparts starting at week 7 of their HF challenge (Fig 3-4A), with higher body weight gain (Fig 3-4B). Female LFABP$^{liv-/-}$ mice also had greater FM % than female LFABP$^{fl/fl}$ mice (Fig 3-4C). For males, the average body weight gain did not change and FM % was slightly higher for LFABP$^{liv-/-}$, but did not reach statistical significance (Fig 3-4D, E and F).

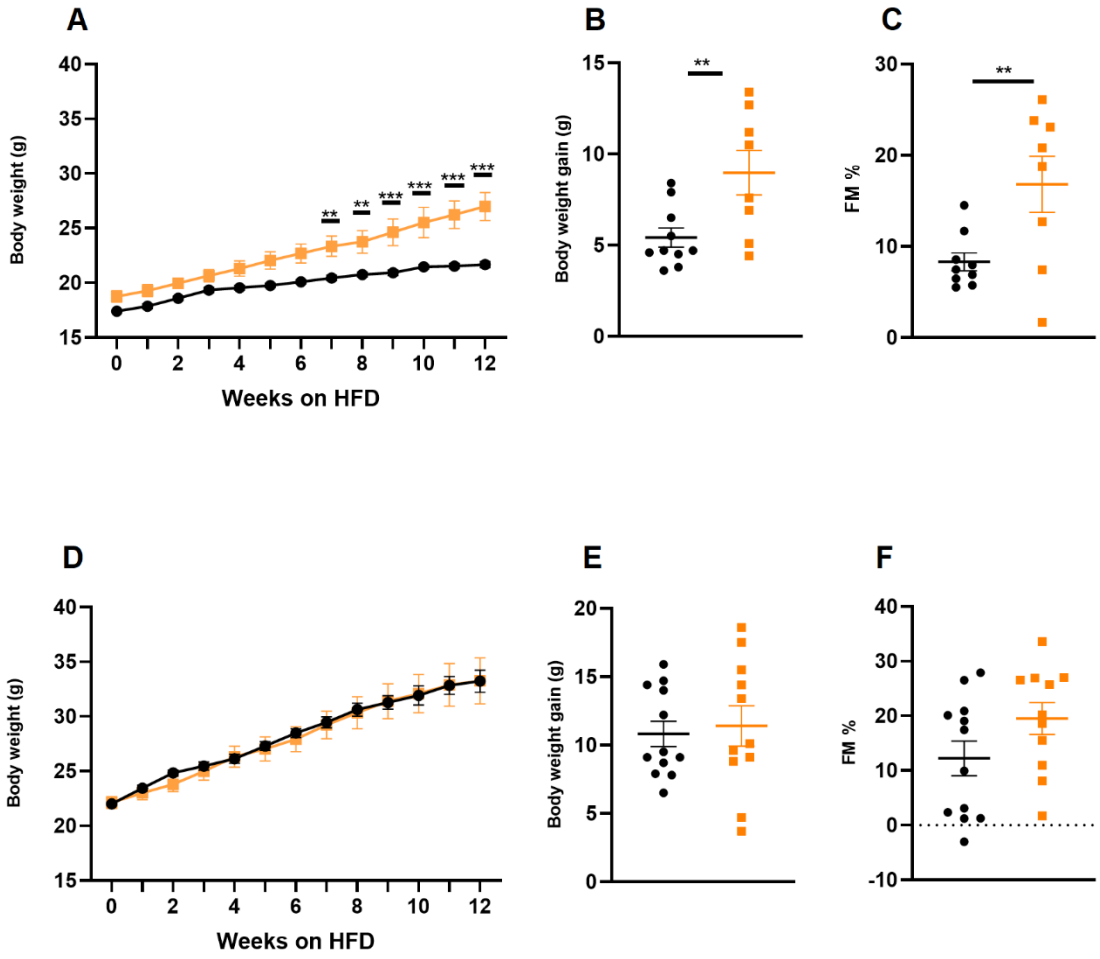

Figure 3-4: Body weight, body weight gain, FM % for LFABP$^{fl/fl}$ (●) and LFABP$^{liv-/-}$ (■) mice after 12 weeks of 45% Kcal HF feeding. A, Female mice body weights (n=8-10); B, Female mice body weight gain (n=8-10); C, Female mice FM percentage (n=8-9). D, Male mice body weights (n=11-12); E, Male mice body weight gain (n=11-12); F, Male mice FM percentage (n=11-12). Data are given as mean±S.E.M., analyzed using Student's t-test. **, $p < 0.01$ for LFABP$^{liv-/-}$ versus LFABP$^{fl/fl}$.

Mice lacking LFABP specifically from the liver have no difference in overall energy absorbed, feeding efficiency, or intestinal transit times

Mice were placed into the Oxymax system to assess food intake. Feces were collected to measure fecal mass excreted over 24 hours. Despite the observed differences in body weight and body composition between LFABP$^{fl/fl}$ and LFABP$^{liv-/-}$ female mice, there were no alterations in the calories consumed and energy absorbed (Fig 3-5A). While there was a trend towards higher feeding efficiency (g of body weight gained per kcal absorbed), it did not reach significance (Fig 3-5B). Additionally, there was no difference in the intestinal transit time between the female cKO mice and control mice (Fig 3-5C).

Male LFABP$^{liv-/-}$ mice ingested fewer calories per day, but also excreted fewer calories per day in their feces, resulting in no net differences in the amount of energy absorbed from the diet, when compared to LFABP$^{fl/fl}$ controls (Fig 3-5D). Similar to female cKO mice there was a trend towards higher feeding efficiency in male LFABP$^{liv-/-}$ mice compared to the control mice during HFD feeding but it did not reach significance (Fig 3-5E). Additionally, there were no significant differences in the intestinal transit time of male LFABP$^{liv-/-}$ mice when compared to their control mice (Fig 3-5F).

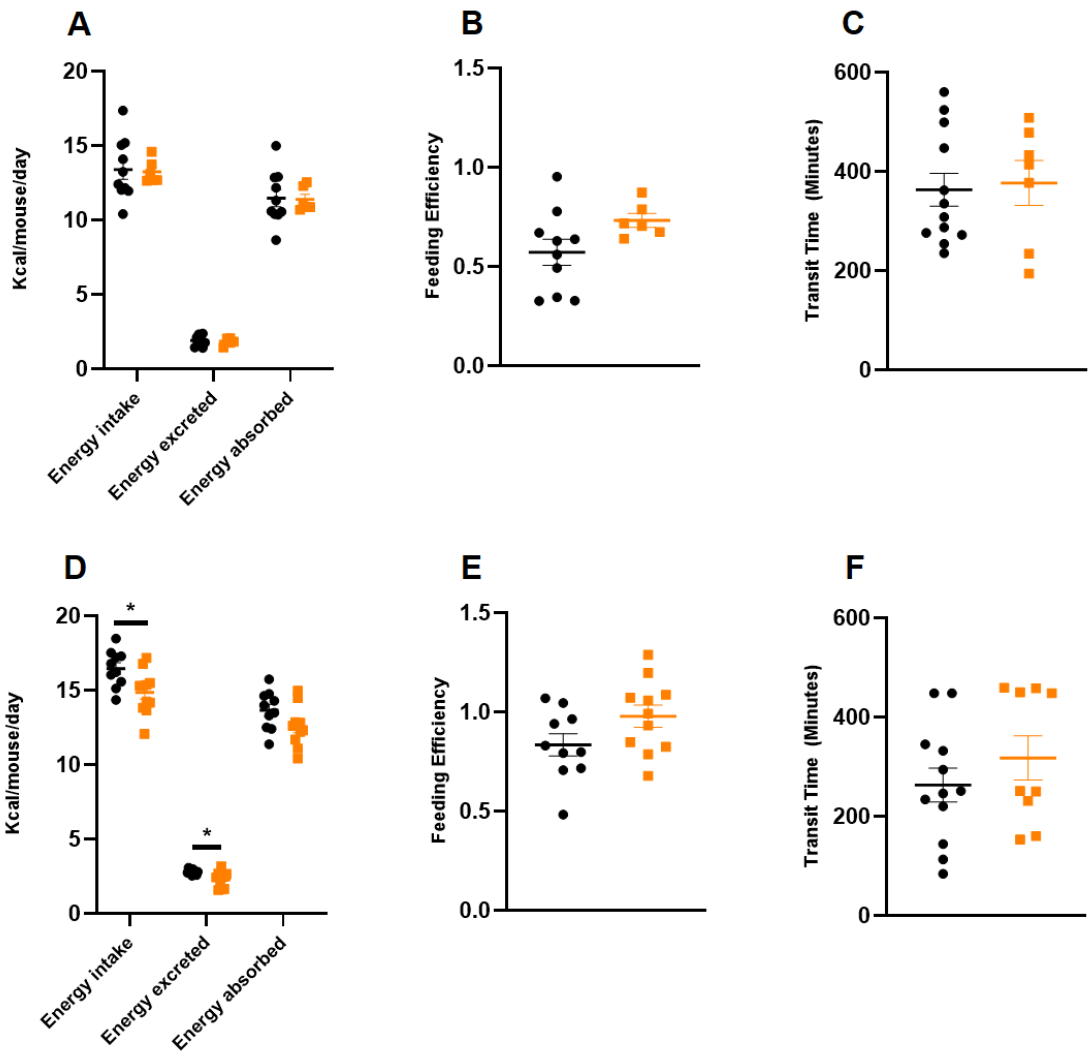

Figure 3-5: Food intake, feeding efficiency, and intestinal transit times in LFABP$^{fl/fl}$ (●) and LFABP$^{liv-/-}$ (■) mice after 12 weeks of 45% Kcal HF feeding. A, Female mice 24-hour energy intake, feces excreted and energy absorbed (n=6-10); B, Female mice feeding efficiency (n=6-10); C, Female mice intestinal transit time (n=7-12) ; D, Male mice 24-hour energy intake, feces excreted and energy absorbed (n=10-11); E, Male mice feeding efficiency (n=10-11); F, Male mice intestinal transit time (n=9-12). Data are given as mean±S.E.M., analyzed using Student's t-test. *, $p < 0.05$ for LFABP$^{liv-/-}$ versus LFABP$^{fl/fl}$.

<u>The liver-specific ablation of LFABP does not result in altered energy homeostasis</u>

Mice were placed into the Oxymax instrument to assess RER and EE. Despite the differences in body weight and body composition that were observed between female LFABP$^{fl/fl}$ and LFABP$^{liv-/-}$ mice, there were no differences in 24-hour RER or EE (Fig 3-6A and B). In male LFABP$^{liv-/-}$ mice, there were also no differences in the average 24-hour RER or EE relative to LFABP$^{fl/fl}$ mice (Fig 3-6C and D).

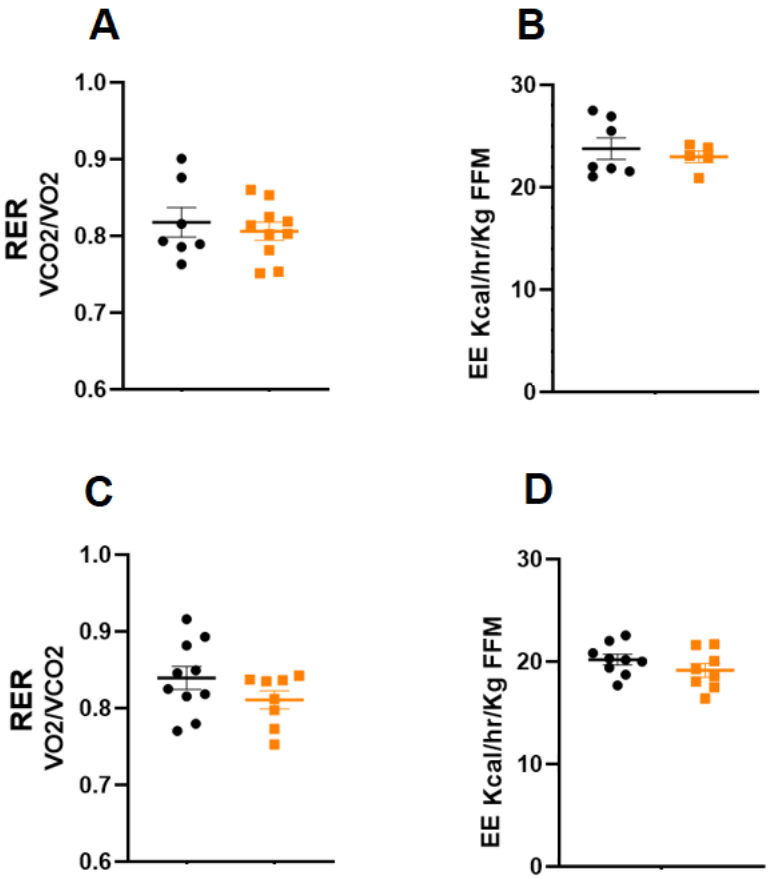

Figure 3-6: RER and EE for LFABP$^{fl/fl}$ (●) and LFABP$^{liv-/-}$ (■) mice after 12 weeks of 45% Kcal HF feeding. A, Female mice 24-hour RER (n=7-10); B, Female mice EE (n=5-7); C, Male mice 24-hour RER (n=8-10); D, Male mice EE (n=8-9). Data are given as mean±S.E.M., analyzed using Student's t-test.

LFABP$^{liv-/-}$ mice retain their exercise capacity relative to LFABP$^{fl/fl}$ controls following chronic HF feeding

Both spontaneous and induced physical activity parameters were assessed in the female and male LFABP liver-cKO mice. Female LFABP$^{liv-/-}$ mice did not have alterations in spontaneous activity (Fig 3-7A). However, female LFABP$^{liv-/-}$ mice display a higher exercise endurance capacity relative to their LFABP$^{fl/fl}$ controls (Fig 3-7B). Unlike their female counterparts, the male LFABP$^{liv-/-}$ mice had higher 24-hour spontaneous activity when compared to control LFABP$^{fl/fl}$ mice (Fig 3-7C). Furthermore, male LFABP$^{liv-/-}$ mice had higher exercise endurance capacity when compared to the LFABP$^{fl/fl}$ control mice, being able to run on the treadmill for a longer time and distance (Fig 3-7D).

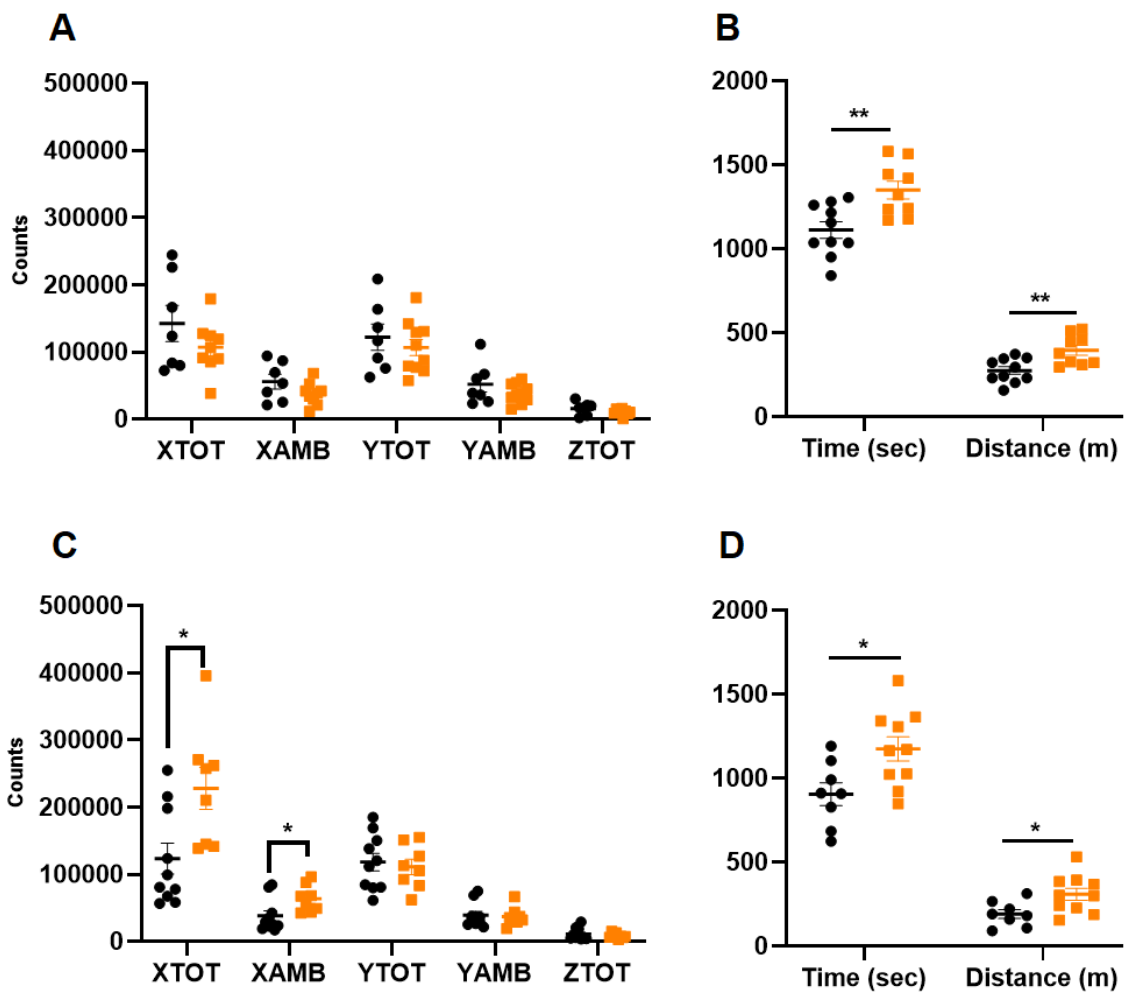

Figure 3-7: Analyses of spontaneous activity and endurance capacity for LFABP$^{fl/fl}$ (●) and LFABP$^{liv-/-}$ (■) mice after 12 weeks of 45% Kcal HF feeding. A, Female mice 24-hour spontaneous activity (n=7-10); B, Female mice exercise endurance running time and distance (n=9-10). C; Male mice 24-hour spontaneous activity (n=8-10); D, Male mice exercise endurance running time and distance (n=8-10). Data are given as mean±S.E.M., analyzed using Student's t-test. *, $p < 0.05$ and **, $p < 0.01$ for LFABP$^{liv-/-}$ versus LFABP$^{fl/fl}$.

LFABP$^{liv-/-}$ mice do not display alterations in plasma markers of energy balance

To assess glucose handling in the LFABP-cKO mice, OGT and fasting plasma insulin were measured. Female LFABP$^{liv-/-}$ mice showed no differences in blood glucose concentrations at any time point and no differences in fasting plasma insulin, when compared to LFABP$^{fl/fl}$ mice (Fig 3-8A, B and C). Fasting plasma leptin was found to be higher in female LFABP$^{liv-/-}$ mice relative to female LFABP$^{fl/fl}$ mice (Fig 3-8D), but a calculation of leptin index factoring in FM revealed no significant difference between these two groups (Fig 3-8E). Adiponectin level and index in female mice showed no difference between the two groups (Fig 3-8F and G). Also, in female LFABP$^{liv-/-}$ mice, there were no significant changes in the levels of NEFA, TG and cholesterol compared to their respective control mice (Figures 3-8H, I and J).

Male LFABP-cKO mice displayed similar glucose handling patterns, with LFABP$^{liv-/-}$ mice having no differences in glucose tolerance or fasting plasma insulin, when compared to LFABP$^{fl/fl}$ mice (Fig 3-8K, L and M). Additionally, fasting plasma levels of leptin (Fig 3-8N and O) and adiponectin (Fig 3-8P and Q) also did not differ between the two groups. Plasma levels of NEFA, TG and cholesterol in male LFABP$^{liv-/-}$ mice, were not different from the control LFABP$^{fl/fl}$ mice (Fig 3-8R, S and T).

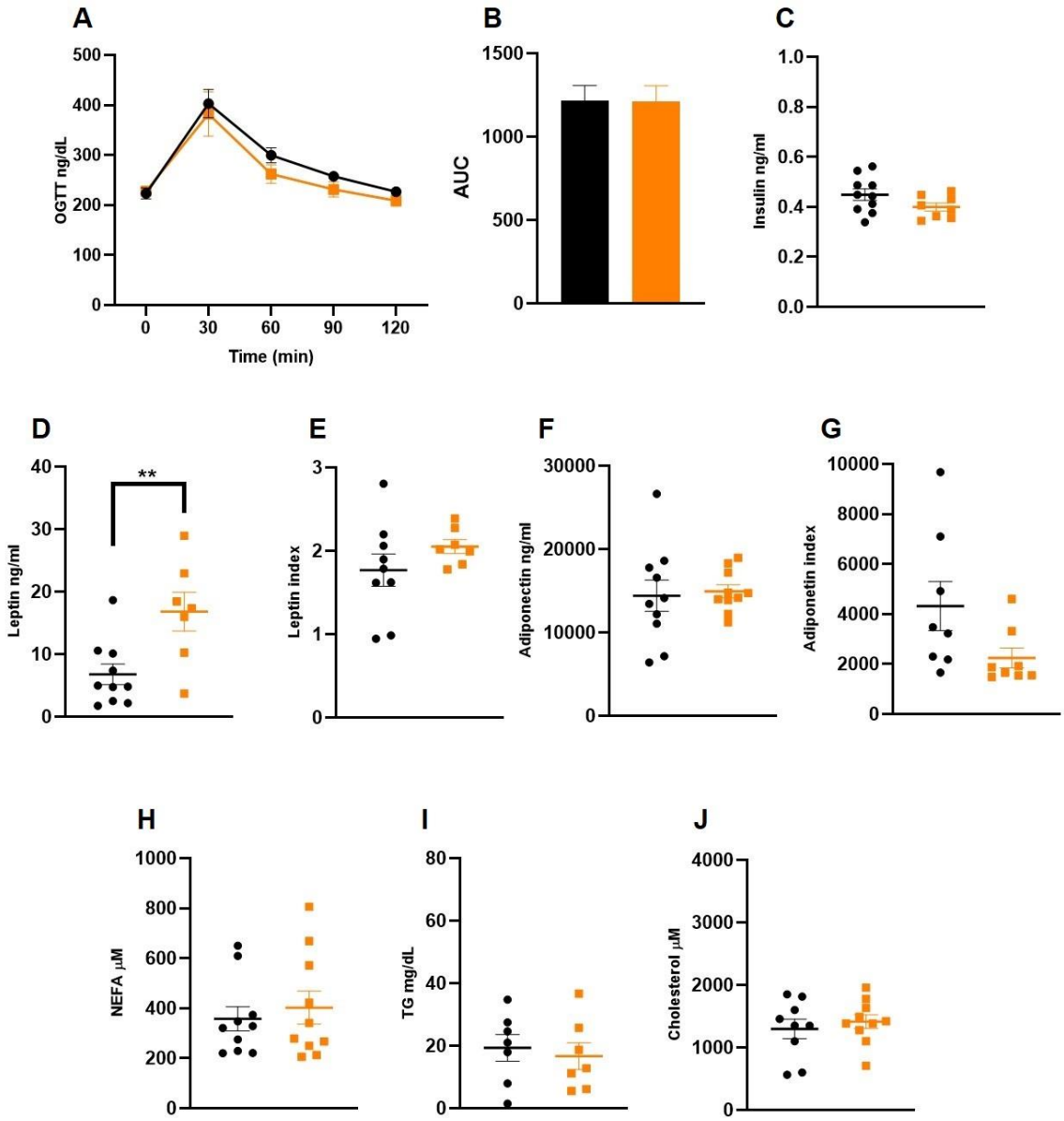
A
OGTT ng/dL
Time (min)
B
AUC
C
Insulin ng/ml
D
Leptin ng/ml
**
E
Leptin index
F
Adiponectin ng/ml
G
Adiponetin index
H
NEFA µM
I
TG mg/dL
J
Cholesterol µM

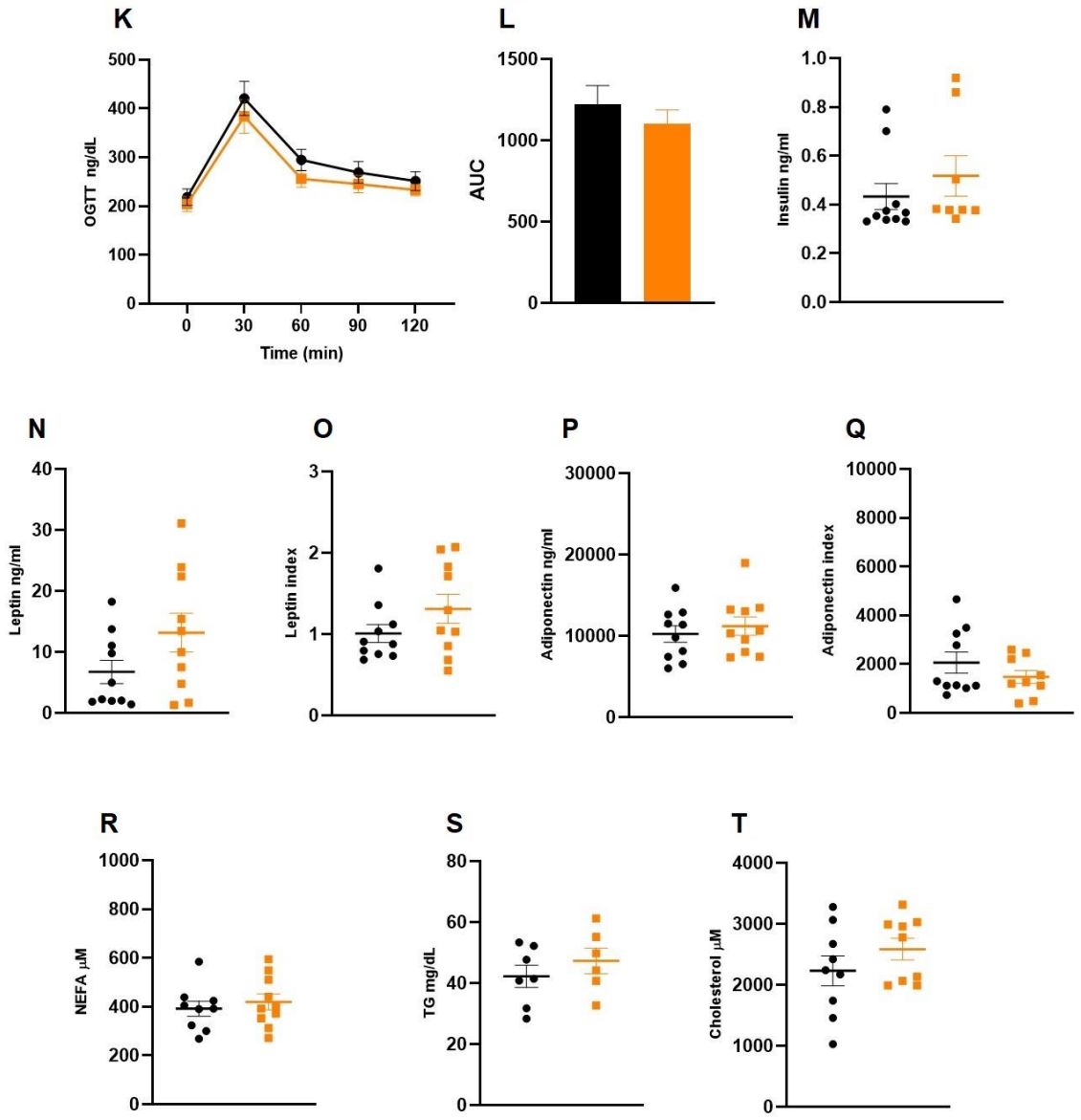

Figure 3-8: Blood analyses for fasted LFABP$^{fl/fl}$ (●) and LFABP$^{liv-/-}$ (■) mice after 12 weeks of 45% Kcal HF feeding. A, Female mice glucose tolerance test (n=9-13); B, Female mice glucose tolerance area under the curve (n=9-13); C, Female mice fasting plasma insulin (n=8-10); D, Female mice fasting plasma leptin (n=7-10); E, Female mice leptin index (n=7-10); F, Female mice fasting plasma adiponectin (n=10); G, Female mice adiponectin index (n=8); H, Female mice fasting plasma NEFA (n=10); I, Female mice fasting plasma TG (n=7); J, Female mice fasting plasma cholesterol (n=9-10); K, Male

mice glucose tolerance test (n=7-11); L, Male mice glucose tolerance area under the curve (n=7-11); M, Male mice fasting plasma insulin (n=8-10); N, Male mice fasting plasma leptin (n=10); O, Male mice leptin index (n=10); P, Male mice fasting plasma adiponectin (n=10); Q, Male mice adiponectin index (n=9-10); R, Male mice fasting plasma NEFA (n=9-10); S, Male mice fasting plasma TG (n=6-7); T, Male mice fasting plasma cholesterol (n=9). Data are given as mean±S.E.M., analyzed using Student's t-test. **, $p < 0.01$ for $LFABP^{liv-/-}$ versus $LFABP^{fl/fl}$.

Despite obesity, liver weight/body weight ratio in female LFABP$^{liv-/-}$ mice implies that there might be a protection against hepatic steatosis

Since mice challenged with chronic HF feeding progressively develop not only obesity but also fatty liver, we investigated the long-term effects of HFD combined with liver-LFABP ablation on the liver phenotype. While the liver weight was significantly higher in female LFABP$^{liv-/-}$ mice, the ratio of liver weight/body weight was significantly lower relative to LFABP$^{fl/fl}$ control mice, implying that there might be protection against hepatic steatosis. (Fig 3-9A and B). HF feeding did not affect liver weights or the liver weight to body weight ratio in male LFABP$^{liv-/-}$ mice (Fig 3-9C and D).

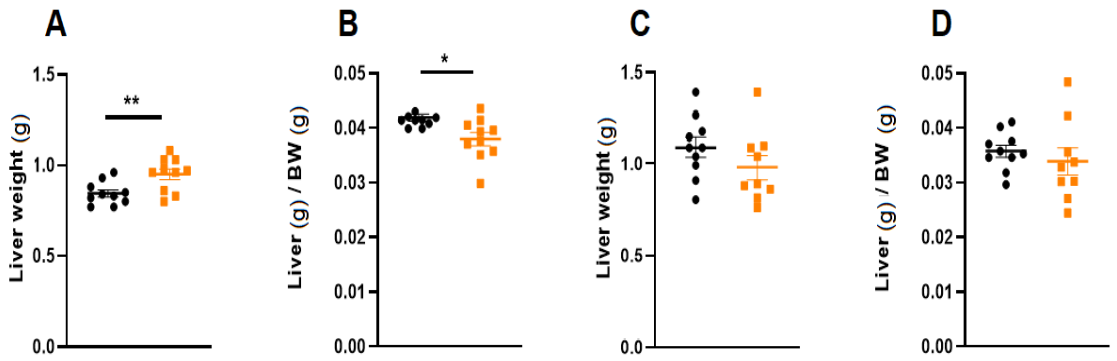

Figure 3-9: Liver weight and liver weight/body weight in fasted LFABP$^{fl/fl}$ (●) and LFABP$^{liv-/-}$ (■) mice after 12 weeks of 45% Kcal HF feeding. A, Female mice liver weight (n=10); B, Female mice liver weight/body weight (n=9-10); C, Male mice liver weight (n=9-10); D, Male mice liver weight/body weight (n=9-10). Data are given as mean±S.E.M., analyzed using Student's t-test. *, $p < 0.05$ and **, $p < 0.01$ for LFABP$^{liv-/-}$ versus LFABP$^{fl/fl}$.

Obese female LFABP$^{liv-/-}$ mice have no accumulation of hepatic neutral lipids or their precursor FA compared to the control mice

Hepatic TG, CE and FFA levels were analyzed in overnight fasted female and male mice. Although female LFABP$^{liv-/-}$ mice had higher body weight gain and increased FM compared to their controls, their hepatic TG and CE were comparable to their WT control counterparts (Fig 3-10A). FA, a precursor that can be used for TG and CE synthesis, was also similar in the liver of female LFABP$^{liv-/-}$ mice relative to their controls (Fig 3-10A). In male LFABP$^{liv-/-}$ mice, hepatic TG, CE and FA levels were not different from their control mice (Fig 3-10B). This was consistent with the results of liver weight/body weight. These findings were further confirmed by liver histology cross sections in female (Fig 3-10C) and male (Fig 3-10D) LFABP$^{liv-/-}$ mice, where no more accumulation of hepatic lipid droplets than the control mice was found.

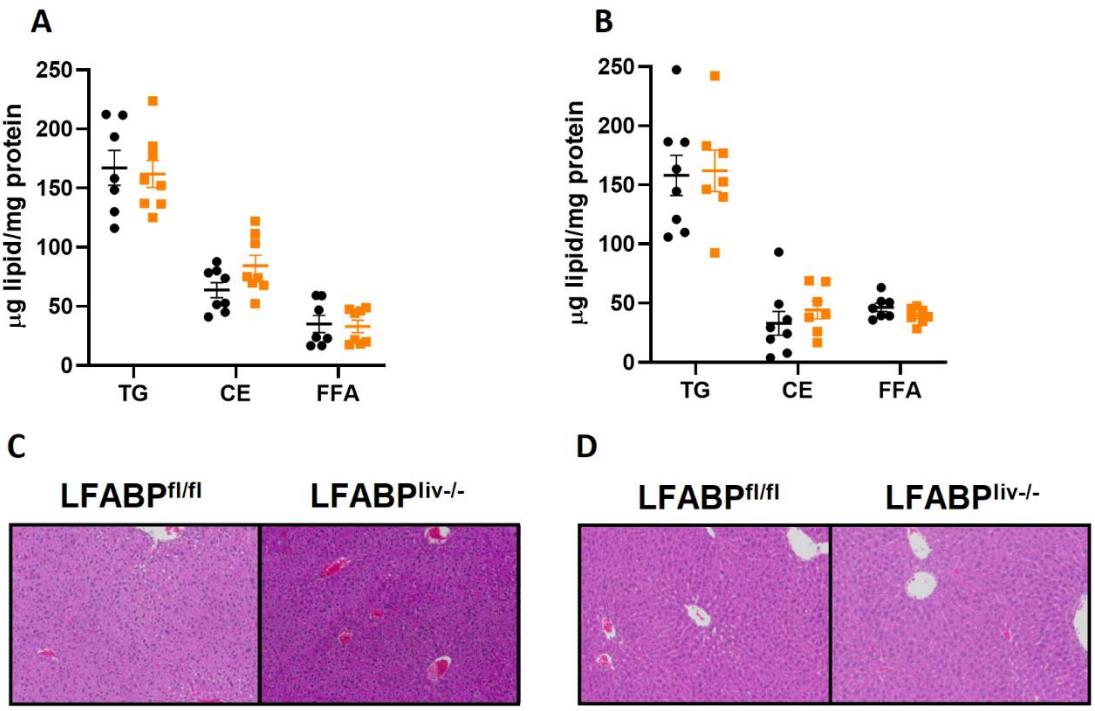

Figure 3-10: Hepatic neutral lipids levels in LFABP$^{fl/fl}$ (●) and LFABP$^{liv-/-}$ (■) mice after 12 weeks of 45% Kcal HF feeding. A, Female mice hepatic TG, CE and FFA levels (n=7-8); B, Male mice hepatic TG, CE and FFA levels (n=6-7); C, Female mice H & E stained liver tissue; D, Male mice H & E stained liver tissue. Data are given as mean±S.E.M., analyzed using Student's t-test.

Plasma VLDL-TG concentrations in LFABP$^{liv-/-}$ mice are comparable to their WT littermates

In order to investigate the mechanisms underlying the reduced hepatic lipid accumulation in the obese female LFABP$^{liv-/-}$ mice, plasma levels of TG-rich VLDL were assessed. There is a possibility that TG is preferentially incorporated into VLDL particles for secreting it into the blood rather than storing. The results showed that female LFABP$^{liv-/-}$ mice were found to have a trend toward higher VLDL-TG secretion at 150 and 180 minutes, however, it did not reach statistical significance (Fig 3-11A). VLDL-TG secretion in male LFABP$^{liv-/-}$ mice was not different from their control at all-time points. (Fig 3-11B).

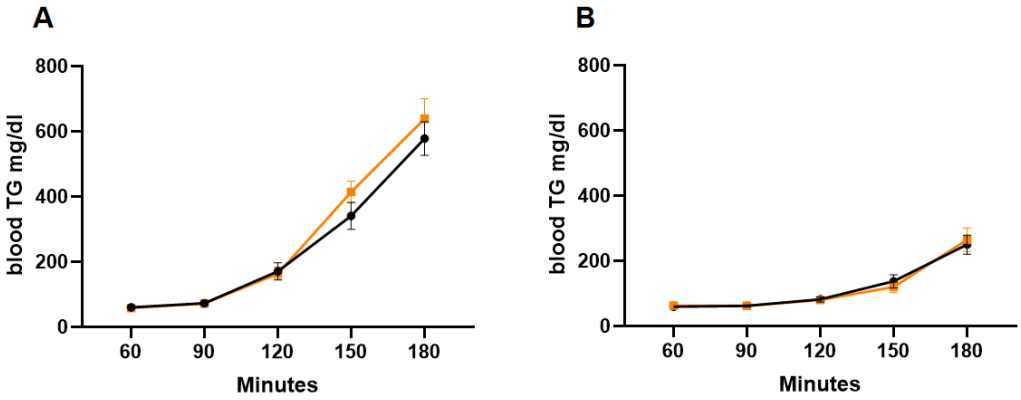

Figure 3-11: VLDL secretion in LFABP$^{fl/fl}$ (●) and LFABP$^{liv-/-}$ (■) mice after 12 weeks of 45% Kcal HF feeding. A, Female mice blood VLDL-TG level (n=11-14); B, Male mice blood VLDL-TG level (n=10-12). Data are given as mean±S.E.M., analyzed using Student's t-test.

<u>The concentrations of other lipid species show no differences in the livers of LFABP$^{liv-/-}$ mice compared to control mice</u>

Another mechanism that might contribute to the reduced hepatic lipid accumulation in female cKO mice is a change in the pattern of hepatic FA distribution into other lipids such as PL rather than TG. However, the ablation of liver-LFABP did not result in altered hepatic lipid distribution; both female and male LFABP$^{liv-/-}$ mice displayed no differences in PL, cholesterol, or other glyceride species, such as DG and MG, when compared to their LFABP$^{fl/fl}$ counterparts (Fig 3-12A and B).

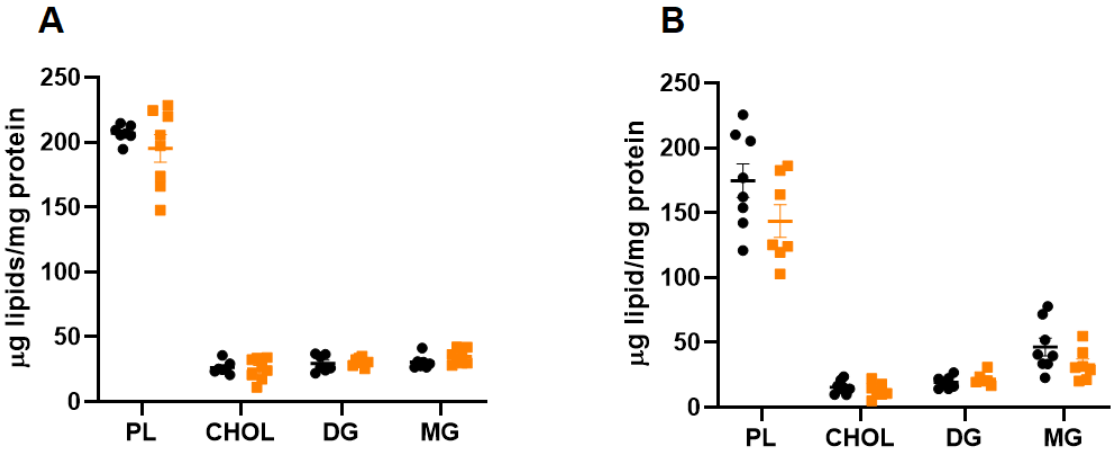

Figure 3-12: Hepatic lipids in LFABP$^{fl/fl}$ (●) and LFABP$^{liv-/-}$ (■) mice after 12 weeks of 45% Kcal HF feeding. A, Female mice hepatic lipid species (n=6-8); B, Male mice hepatic lipid species (n=6-8). CHOL, cholesterol; DG, diacylglycerol; MG, monoacylglycerol; PL, phospholipid. Data are given as mean±S.E.M., analyzed using Student's t-test.

Liver-specific ablation of LFABP in the female mice causes alteration in intestinal lipids composition

In LFABP$^{liv-/-}$ mice, LFABP is still expressed in the intestine. Therefore, we wanted to know whether LFABP ablation specifically from the liver would affect the intestine. The ratio of intestinal length to body weight was not different for both female and male LFABP$^{liv-/-}$ mice relative to their controls (Fig 3-13A and C). However, the intestine of female LFABP$^{liv-/-}$ mice displayed a significant accumulation of TG and a reduction of PL (Fig 3-13B) suggesting a redistribution of FA towards more TG synthesis at the expense of PL synthesis. The lipid composition of the proximal and distal intestinal mucosa revealed no difference for all of the lipid species in male LFABP$^{liv-/-}$ mice when compared to the control mice (Fig 3-13D).

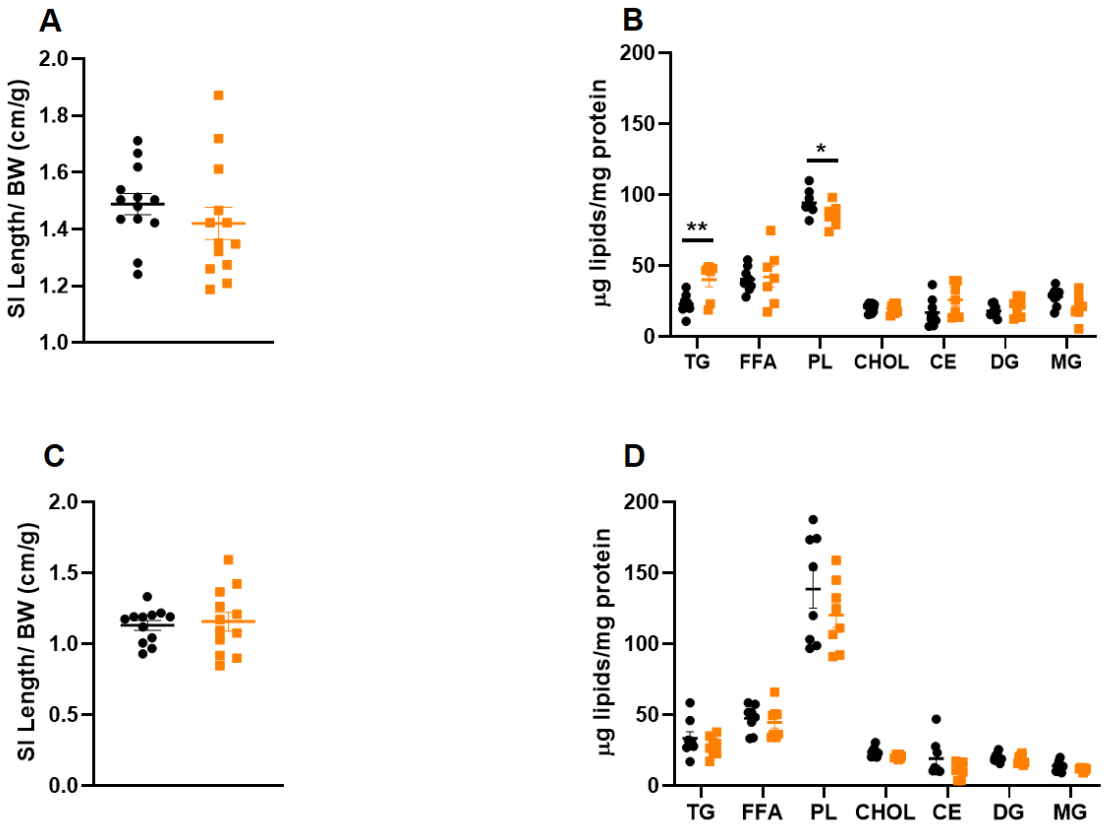

Figure 3-13: Intestinal length and lipid composition in LFABP$^{fl/fl}$ (●) and LFABP$^{liv-/-}$ (■) mice after 12 weeks of 45% Kcal HF feeding. A, Female mice intestine length/body weight ratio (n=13); B, Female mice lipid species concentrations (n=6-9); C, Male mice intestine length/body weight ratio (n=12-13); D, Male mice lipid species concentrations (n=8). CHOL, cholesterol; CE, cholesteryl ester; DG, diacylglycerol; FFA, free fatty acid; MG, monoacylglycerol; PL, phospholipid; TG, triglyceride. Data are given as mean±S.E.M., analyzed using Student's t-test. *, $p < 0.05$ and **, $p < 0.01$ for LFABP$^{liv-/-}$ versus LFABP$^{fl/fl}$.

Chylomicron secretion rates show no differences in female and male cKO LFABP mice relative to the control mice

The redistribution of intestinal lipids could result from changes in TG-rich chylomicron secretion. Therefore, OFTTs were performed to assess whether the secretion of TG-rich chylomicrons was affected by the ablation of LFABP specifically from the liver. No significant differences in chylomicron secretion were found in female $LFABP^{liv-/-}$ mice relative to their floxed control mice (Fig 3-14A). In male $LFABP^{liv-/-}$ mice, TG levels were slightly but significantly higher at baseline and 1 hour post oil gavage ($p< 0.001$, $p< 0.01$ respectively) than what was found in their control mice (Fig 3-14C). Overall, the area under the curve (AUC) showed a non-significant trend towards lower chylomicron secretion rates in both female and male $LFABP^{liv-/-}$ mice (Fig 3-14B and D).

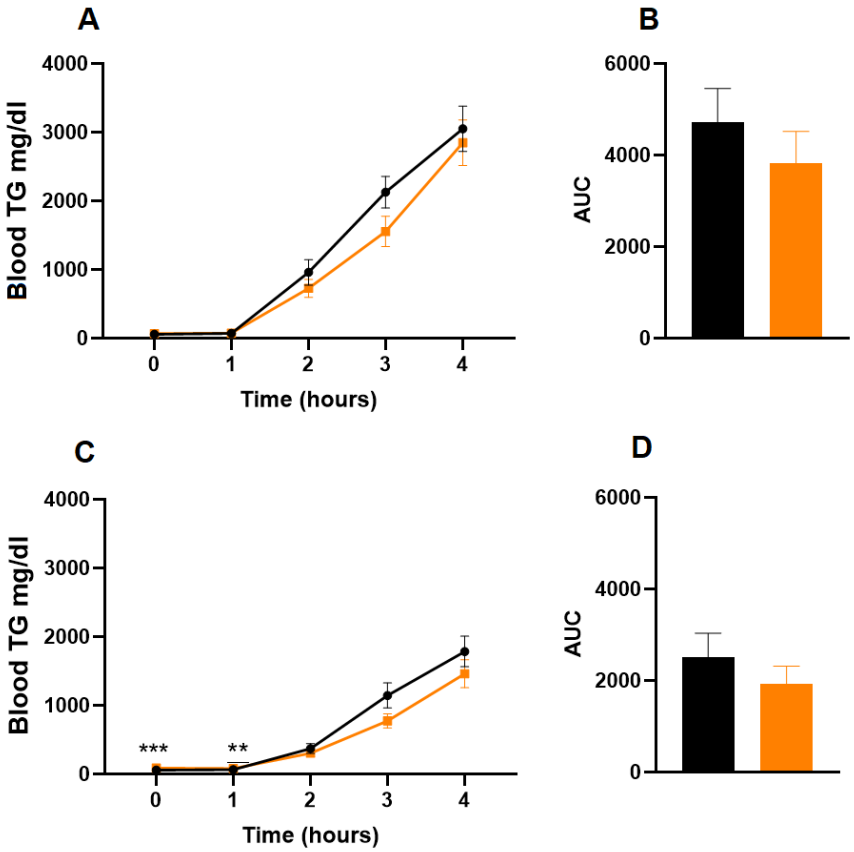

Figure 3-14: Intestinal chylomicron secretion rates in LFABP$^{fl/fl}$ (●) and LFABP$^{liv-/-}$ (■) mice after 12 weeks of 45% Kcal HF feeding. A, Female mice blood TG levels (n=6-8); B, Female mice fat tolerance AUC (n=6-8); C, Male mice blood TG levels (n=7-9); D, Male mice fat tolerance AUC (n=7-9). Data are given as mean±S.E.M., analyzed using Student's t-test. **, $p < 0.01$ and ***, $p < 0.001$ for LFABP$^{liv-/-}$ versus LFABP$^{fl/fl}$.

Hepatic FA oxidation in female and male LFABP$^{liv-/-}$ mice.

FA oxidation rates were measured by quantifying the appearance of $^{14}CO_2$ and ^{14}C-labeled ASMs after adding ^{14}C-oleate to the liver homogenates of 16 hour fasted mice. Female (Fig 3-15A and B) and male LFABP$^{liv-/-}$ mice (Fig 3-15C and D) showed a slight trend toward reduction in hepatic FA oxidation rate manifested by reduction in the amount of $^{14}CO_2$ and ^{14}C-labeled ASMs, when compared to their floxed control mice. However, these reductions did not reach statistical significance, suggesting that ablation of LFABP specifically from the liver did not exert its influence on FA oxidation capacity to a large extent.

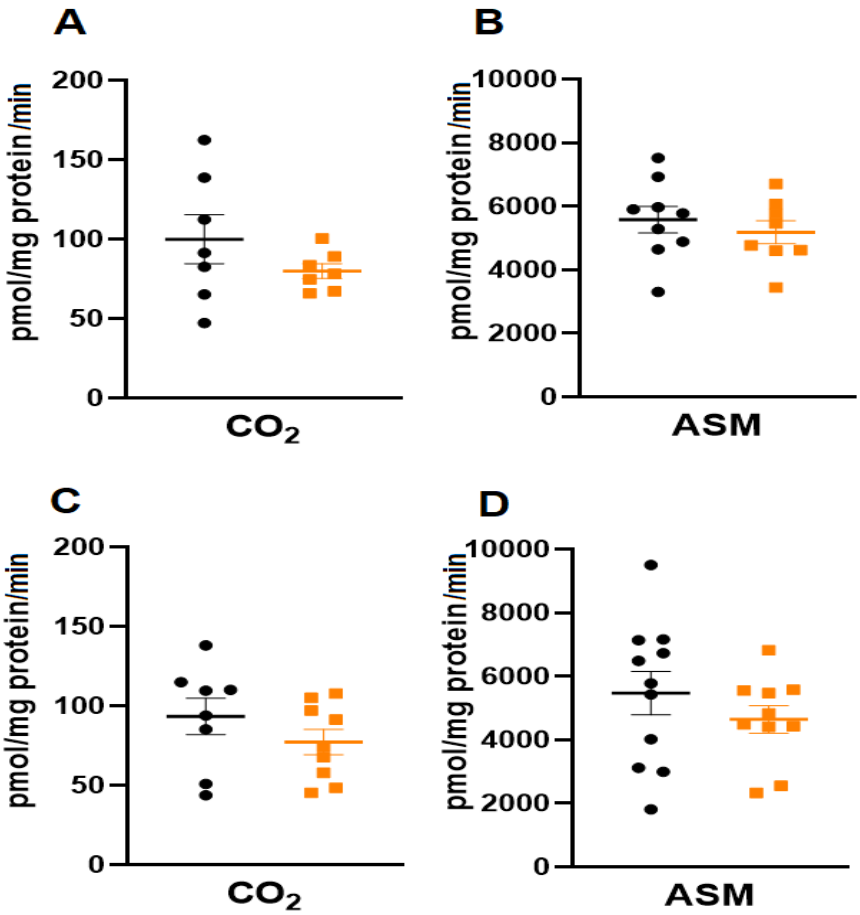

Figure 3-15: FA oxidation rate after ^{14}C-oleic acid administration to the liver homogenates of LFABP$^{fl/fl}$ (●) and LFABP$^{liv-/-}$ (■) mice under overnight fasting condition. A, Female mice $^{14}CO_2$ production (n=8-9); B, Female mice ^{14}C-labeled ASMs (n=10-11); C, Male mice $^{14}CO_2$ production (n=7); D, Male mice ^{14}C-labeled ASMs (n=8-9). Data are given as mean±S.E.M, analyzed using Student's t-test.

FA uptake is significantly reduced in the liver and the intestine of female LFABP$^{liv-/-}$ mice

As mentioned previously, LFABP is thought to control FA uptake via generating a concentration gradient cross the plasma membrane [311]. In order to determine impact of liver-LFABP ablation on FA uptake, LFABP-cKO mice were fasted overnight and gavaged with ^{14}C-oleic acid. In female LFABP$^{liv-/-}$ mice, FA uptake was significantly reduced in the liver and proximal intestine, and trended towards a lower uptake in the distal intestine, relative to the WT control mice (Fig 3-16A). Furthermore, the results showed a trend towards a higher FA uptake in the adipose tissue (Fig 3-16A). The radioactivity of other tissues, feces and blood was not different from the control mice (Fig 14A and B). On the other hand, the ablation of liver-LFABP in male mice did not influence FA uptake in the assessed tissues, when compared to male WT control mice (Fig 3-16C and D).

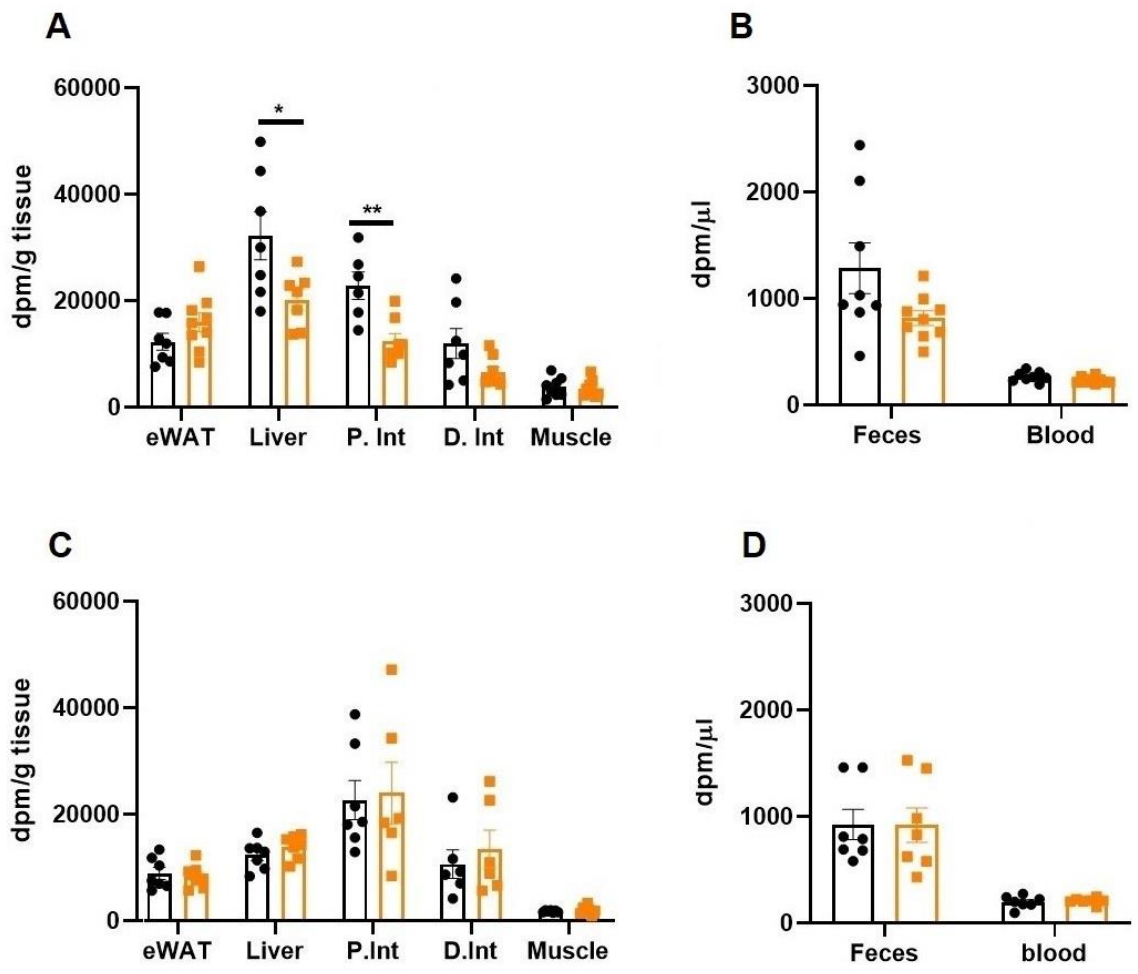

Figure 3-16: Tissues FA uptake after oral administration of ^{14}C-oleic acid into LFABP$^{fl/fl}$ (●) and LFABP$^{liv-/-}$ (■) mice under overnight fasting condition. A, Female mice FA uptake into eWAT, liver, P. Int, D. Int and gastrocnemius muscle (n=6-7); B, Female mice ^{14}C-oleic acid appearance in the feces and the blood (n=7); C, Male mice FA uptake into eWAT, liver, P. Int, D. Int and gastrocnemius muscle (n=6-9); D, Male mice ^{14}C-oleic acid appearance in the feces and the blood (n=8-9). D. Int, distal intestine; eWAT, epididymal white adipose tissue; P. Int, proximal intestine. Data are given as mean±S.E.M, analyzed using Student's t-test. *, $p < 0.05$ and **, $p < 0.01$ for LFABP$^{liv-/-}$ versus LFABP$^{fl/fl}$.

The ablation of liver-LFABP is associated with alterations in the expression of genes involved in hepatic lipid metabolism

It is possible that the absence of LFABP in the liver may result in alterations in the expression of genes related to lipid metabolic pathways. qPCR analysis was used to assess some of the genes involved in hepatic lipid transport and metabolism, i.e. membrane FA uptake, cytosolic LCFA binding/transporting, mitochondrial and peroxisomal LCFA β-oxidation, *de novo* FA synthesis and TG synthesis. In both male and female LFABP$^{liv-/-}$ mice, several changes in the hepatic expression of genes related to lipid uptake, transport, and metabolism were noted, when compared to their respective control mice.

In female mice there was not that much impact of liver-LFABP ablation on genes expression (Fig 3-17A, Table 3-1) compared to the changes in male mice. There was a significant reduction in the expression of glutamic oxaloacetic transaminase (Got1) gene, which was opposed by the up-regulation of CD36 expression, suggesting that these two counter-regulated genes would have no net influence on FA uptake, and that the reduction that was noted in female hepatic FA uptake was mainly due to the ablation of LFABP from the liver. There were no changes in the expression of genes involved in FA synthesis, except for an upregulation of the Scd1 gene, which catalyzes the rate-limiting step in the synthesis of unsaturated FA. Additionally, LFABP ablation was associated with a decreased expression of genes involved in FA oxidation like Cpt1α and acyl-CoA dehydrogenase-long chain (Acadl), however, it was insufficient to reduce FA oxidation to a significant extent. A decreased expression of these genes indicated less FA breakdown which may be related to the decreased availability of intracellular FA.

The ablation of LFABP in male mice (Fig 3-17B, Table 3-1), resulted in down-regulation in the expression of genes involved in LCFA uptake across the plasma and peroxisomal membrane, i.e. CD36 and Fatp2 respectively. There was also a reduction in the mRNA expression of low-density lipoprotein receptor (Ldlr), a gene that is involved in the uptake of cholesterol. Other genes involved in plasma membrane FA uptake showed no change in response to liver-LFABP ablation. There was also a down-regulation in the expression of Acbp which is involved in cytosolic LCFA-CoAs transport. Unlike what was found in McIntosh *et al*. and Martin *et al*. studies [179,214], which reported an increase in the expression of Scp2, both male and female $LFABP^{liv-/-}$ mice had no changes in the expression of this gene.

In male mice the expression of Acc1 and Fasn, genes involved in *de novo* FA synthesis, showed a substantial reduction. There was also a reduction in the expression of Acsl1. Hepatic LFABP ablation also down-regulated hepatic expression of key enzymes involved in mitochondrial LCFA β-oxidation like Cpt2, 3-hydroxy-3-methylglutaryl-CoA synthase (Hmgcs) and peroxisomal FA oxidation like acyl-CoA oxidase-1 (Acox1) and acetyl-CoA acyl transferase 1b (Acaa1b). Hepatic TG lipase (Lipc), which is involved in the hydrolysis of TG, also showed a reduction in expression suggesting that there might be less degradation of TG. The reduced expression of FA oxidation related genes could be a feedback mechanism to balance out the reduced expression of genes involved in FA uptake and synthesis as an attempt to maintain FA homeostasis. Collectively, the results of hepatic expression of genes related to lipid metabolism in male mice suggested that the lack of metabolic responses to liver-LFABP ablation in male mice might be due to these potential alterations in genes expression which are opposing each other, resulting in no net changes in hepatic contents of FA, TG and other lipid species. In both female and male mice there was no effect of LFABP ablation on the expression of Pparα, Hnf1α and

Hnf4α or signaling molecules like fibroblast growth factor (Fgf21). This finding is in agreement with previous work showing that L-FABP is not required for the action of the transcriptional factor Ppar-α [188].

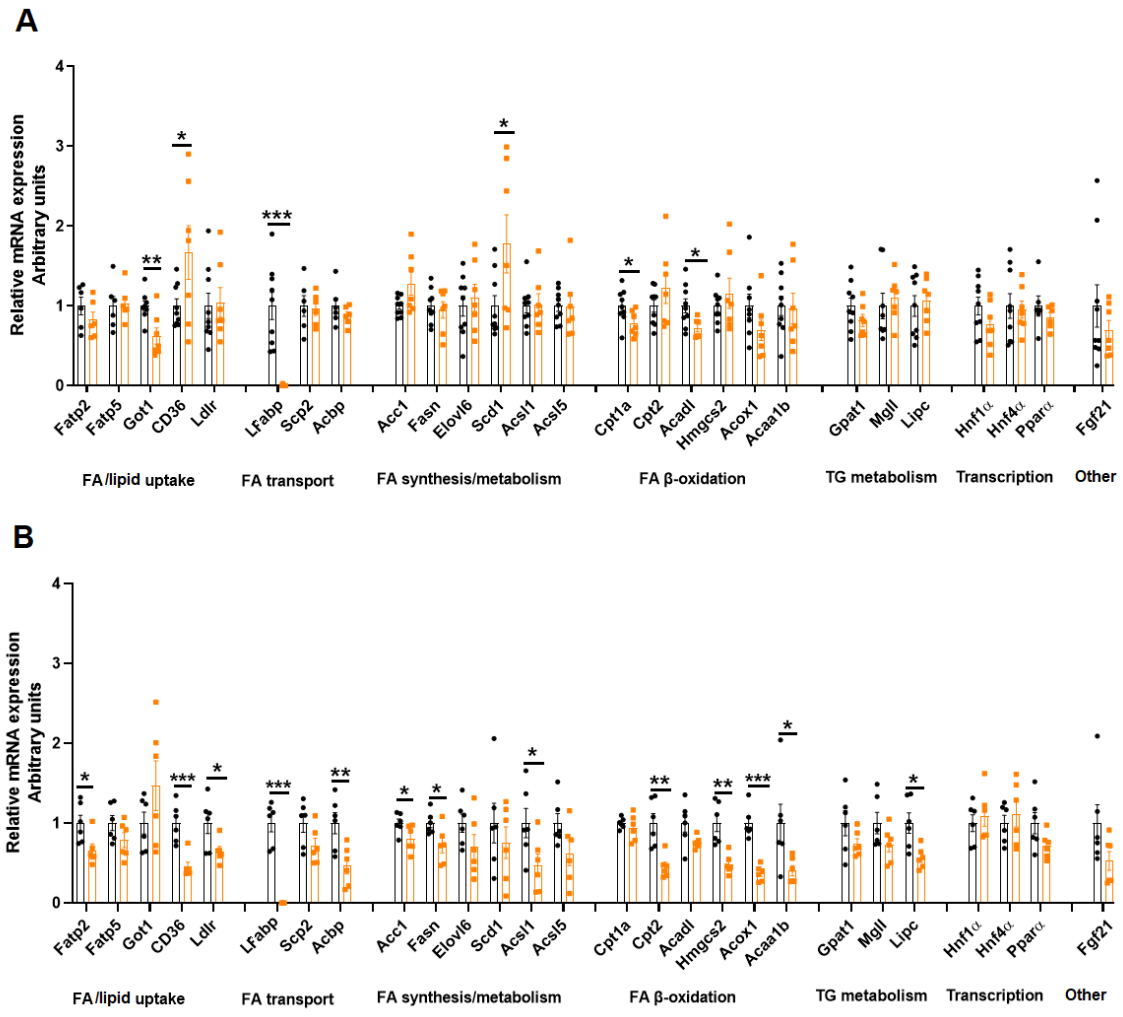

Figure 3-17: Relative quantitation of mRNA expression of genes involved in liver lipid metabolism in 45% Kcal fat HF fed LFABP$^{fl/fl}$ (●) and LFABP$^{liv-/-}$ (■) mice. A, Female mice expression of genes involved in lipid metabolic pathways (n=7-9); B, Male mice expression of genes involved in lipid metabolic pathways (n=6). Data are given as mean±S.E.M., analyzed using Student's t-test. *, $p < 0.05$, **, $p < 0.01$, and ***, $p < 0.001$ for LFABP$^{liv-/-}$ versus LFABP$^{fl/fl}$.

Table 3-7: Alterations of hepatic mRNA expression of genes involve in lipid metabolism in both female and male LFABP$^{liv-/-}$ mice relative to LFABP$^{fl/fl}$ mice.

Bold arrows indicate significant differences (*, p<0.05; **, p<0.01; ***, p<0.001). Light arrows indicate trends. ↑ indicates increase, ↓ indicates decrease, and = indicates no change.

Genes	Female	Male
FA/lipid uptake		
Fatp2	=	**↓***
Fatp5	=	=
Got1	**↓****	↑
CD36	**↑***	**↓*****
Ldlr	=	**↓***
FA transport		
Lfabp	**↓*****	**↓*****
Scp2	=	↓
Acbp	=	**↓****
FA synthesis/metabolism		
Acc1	=	**↓***
Fasn	=	**↓***
Elovl6	=	↓
Scd1	**↑***	↓
Acsl1	=	**↓***
Acsl5	=	↓
FA β-oxidation		
Cpt1α	**↓***	=
Cpt2	=	**↓****
Acadl	**↓***	=
Hmgcs2	=	**↓****
Acox1	=	**↓*****
Acaa1b	=	**↓***
TG metabolism		
Gpat1	=	↓

Mgll	=	↓
Lipc	=	↓*
Transcription factors		
Hnf1α	=	=
Hnf4α	=	=
Pparα	=	↓
Other		
Fgf21	↓	↓

Discussion

LFABP is a member of a large family of low molecular weight lipid binding proteins that are expressed in many tissues. LFABP is abundantly expressed, constituting 2-5% of the total cytoplasmic proteins in the enterocytes and in the hepatocytes and was also found to be expressed in the HSCs of the liver and in the endocrine D cells of the intestine [36,122,166,292]. It is thought to play a pivotal role in the uptake/transport of FA to different intracellular compartments for further hepatic lipid metabolism [158]. Additionally, LFABP is also involved in the regulation of whole-body energy homeostasis [230]. Previously, it has been shown that LFABP$^{-/-}$ male mice gained more body weight and FM upon HF feeding, which was partly due to increased food intake [162]. Despite their obesity, however, LFABP$^{-/-}$ mice were metabolically healthy, being normoglycemic, normoinsulinemic, and normolipidemic [162]. Recently, we found that whole-body KO of LFABP in female mice also results in greater body weight and FM gain compared to their control mice (unpublished data), the same observations as in another study [213]. LFABP$^{-/-}$ mice, despite their obesity, displayed a protection against hepatic steatosis [213]. Additionally, HF fed LFABP$^{-/-}$ mice were more active and had greater exercise endurance than WT mice [162,219]. Here in this study, mice with the ablation of LFABP specifically in the liver were generated to focus on the liver phenotype of LFABP. Furthermore, liver-specific ablation of LFABP will determine if the MHO phenotypes that were observed in the whole-body LFABP null mice are due to liver-LFABP, or if they require the ablation of either the intestinal or both liver and intestinal LFABPs.

Previous studies from our laboratory demonstrated that there are few phenotypic differences between LFABP$^{-/-}$ and WT mice on a chow diet or a low 10% kcal fat diet, and that LFABP$^{-/-}$ mice become heavier than WT mice when challenged with a 45% kcal HFD for 12 weeks [162,163]. As noted above, the higher body weight gain in the LFABP$^{-/-}$ mice

was partly due to increased caloric intake and feeding efficiency [162]. As shown in chapter 2, we recently found that LFABP$^{-/-}$ mice also have slower intestinal transit time and reduced fecal output, indicating that more time is available for nutrients to be absorbed (chapter 2). In HF fed male global LFABP$^{-/-}$ mice, the ratio of VO_2/VCO_2 (RER) was lower compared to the WT control mice suggesting that these mice are depending on lipids as their major source of energy. Additionally, an assessment of their spontaneous activity and their exercise endurance revealed that, despite being obese, LFABP$^{-/-}$ male mice were more active; were able to run double the distance on a treadmill when compared to the WT mice [162,219]. The protection against HFD inducing decline in the exercise endurance activity in the whole-body LFABP$^{-/-}$ was due, at least in part, to the availability of more skeletal muscle energy sources like intramuscular TG and glycogen stores [219].

Similar to what we found in the global LFABP deletion, female LFABP$^{liv-/-}$ mice displayed an obese phenotype, with higher body weight and FM %, when compared to female LFABP$^{fl/fl}$ mice. Obesity usually occurs as a result of excess energy intake, reduced EE, or a combination of both [312]. However, these alterations in body weight and body composition in the female LFABP$^{liv-/-}$ mice, were not due to differences in the amount of energy absorbed, feeding efficiency, RER, or EE. Alterations in intestinal motility are known to accompany obesity [313], and indeed the obese phenotype in the whole-body HF fed LFABP$^{-/-}$ mice was accompanied by a reduction in the amount of total fecal output and an extended intestinal transit time (chapter 2), which could provide more time for efficient digestion and absorption of nutrients. However, this also was not the case in female LFABP$^{liv-/-}$ mice, as their fecal output and intestinal transit times were comparable to the LFABP$^{fl/fl}$ control mice. Overall, it is not clear what are the underlying causes of the increased body weight and FM observed in the female LFABP$^{liv-/-}$ mice are, although a

trend toward higher feed efficiencies were found in both sexes of LFABP$^{liv-/-}$ mice relative to controls.

Despite the heavier body weight, female LFABP$^{liv-/-}$ mice were similar to the whole-body KO mice, displaying higher exercise activity compared to their respective control mice when they were challenged with treadmill running. This finding suggests that the ablation of LFABP specifically in the liver is able to influence exercise activity and induce the same exercise capacity as in the whole-body LFABP ablation [219]. As previously mentioned, the higher endurance exercise capacity in LFABP$^{-/-}$ mice was due to the availability of more intramuscular substrates, utilized as sources of energy, like intramuscular TG and glycogen [219]. Additionally, these mice had higher FA oxidative machinery and greater mitochondrial function, which are necessary for skeletal muscle substrate utilization [219]. LFABP is expressed abundantly in the liver and intestine, but not in the skeletal muscle. Many studies have shown that there is an inter-organ crosstalk that can occur between skeletal muscle and different tissues like gut, liver, bone, brain, and adipose tissue [314,315]. Interestingly, as described in Chapter 2, we recently found that in LFABP$^{-/-}$ mice there is a change in the luminal microbiota towards increased abundance of obesity-associated bacteria. At the same time, there are higher fecal levels of the bacterial SCFA metabolites, including acetate, propionate, butyrate and other SCFAs (chapter 2). Many studies have focused on inter-organ crosstalk between the gut and skeletal muscle via the proposed “gut-muscle axis”, highlighting the beneficial effects of SCFAs in increasing the availability of muscular glycogen and stimulating FA uptake and oxidation, resulting in more efficient energy utilization, and promoting higher exercise activity [64,219,225,276]. It is possible that the liver-specific ablation of LFABP is sufficient to induce the active phenotype via communication between skeletal muscle, intestine, and liver, via alteration in the microbiome and SCFA levels.

There was no change in the body weight and the body composition of male LFABP$^{liv-/-}$ mice, possibly because these mice did not show any differences in amount of energy absorbed, EE, or feeding efficiency. Additionally, there was not any observable change in the intestinal transit time or energy excreted. These findings suggest that the ablation of LFABP in the intestine or in both the liver and the intestine is necessary to induce the body weight, FM and food intake changes that are observed in the male whole-body LFABP$^{-/-}$ mice. Male LFABP$^{liv-/-}$ also were also similar to the whole-body LFABP$^{-/-}$ mice, displayed higher spontaneous activity, and they retained their endurance capacity after treadmill challenge when compared to the LFABP$^{fl/fl}$ mice. This finding indicates that the higher exercise activity of LFABP$^{liv-/-}$ mice was not gender dependent phenotype. However, liver-specific ablation of LFABP did not affect EE or RER, suggesting that the ablation of liver-LFABP in male mice is not enough to shift the whole-body fuel usage towards lipids. Nevertheless, it was enough to induce the same spontaneous activity and exercise endurance phenotypes that were seen in the whole-body LFABP$^{-/-}$ mice.

The phenotypes associated with the MHO phenomenon include normal glucose levels, blood pressure, and lipid levels [294]. Analysis of plasma signals involved in whole-body homeostasis in HF fed LFABP$^{-/-}$ mice revealed no remarkable differences from the WT control mice. [162]. Despite their obese phenotype, the global LFABP$^{-/-}$ mice had fasting glucose, insulin, and lipids levels comparable to those of their leaner WT counterparts. Leptin and leptin index values were strikingly higher in both HF fed obese LFABP$^{-/-}$ and low fat fed lean LFABP$^{-/-}$, indicating that the elevation of plasma leptin was a genotype related effect, primarily due to the ablation of LFABP, and not related to the administration of diet induced obesity. Similarly, in female and male LFABP$^{liv-/-}$ mice, all these plasma parameters were comparable to the LFABP$^{fl/fl}$ control mice. The only exception was leptin,

with higher levels in female LFABP$^{liv-/-}$ mice, however, when leptin level was normalized to the corresponding FM, there were no differences between LFABP$^{liv-/-}$ mice and LFABP$^{fl/fl}$ controls. This indicates that the ablation of intestinal LFABP is likely necessary for the elevated leptin level that was found in the whole-body KO mice. Interestingly, we recently found that mice with intestinal specific ablation of LFABP (LFABP$^{int-/-}$) demonstrated higher body weight and FM but no change in leptin index (unpublished data), suggesting that ablation of both liver and intestinal LFABP is necessary for generating the higher leptin levels in the global LFABP$^{-/-}$ mouse.

LFABP has two ligand binding sites and has been shown to bind two FAs or two MGs [169,170]. It is also known to bind a broad range of other hydrophobic ligands. LFABP binds FA with high affinity and is thought to play a pivotal role in FA uptake, trafficking, and metabolism [169]. Therefore, we hypothesized that ablation of LFABP specifically in the liver would disturb FA uptake and metabolism. While the livers of female LFABP$^{liv-/-}$ mice were larger than those of their control mice, this difference was abrogated when liver weights were normalized to body weight, resulting in a significant reduction relative to the LFABP$^{fl/fl}$ control mice. This indicates a possible protection against hepatic steatosis. Two other groups, working with whole-body LFABP$^{-/-}$ mice, have demonstrated a protection against hepatic steatosis in response to LFABP ablation and concomitant HF feeding, independent of their respective body weight phenotypes. The Davidson group found that female LFABP$^{-/-}$ mice were protected from developing obesity and hepatic steatosis on a high saturated fat diet, and were protected against hepatic steatosis on chow diet. In contrast, this protection was no longer manifested when female LFABP$^{-/-}$ mice were fed with polyunsaturated FA diet [189,212,316,317]. The Binas and Schroeder group demonstrated that male and female LFABP$^{-/-}$ gained more weight and were protected against hepatic steatosis, when pair fed a HFD for 12 weeks [213]. However, *ad libitum*

access to HFD did not result in the same protection against hepatic steatosis in these mice [214].

Obesity is typically associated with non-alcoholic fatty liver disease that is characterized by TG accumulation in lipid droplets (i.e. steatosis), and sometimes accompanied by inflammation and fibrosis (i.e. steatohepatitis) [318]. In our study, despite the obese phenotype, female LFABP$^{liv-/-}$ mice displayed no accumulation of neutral lipids indicative of steatosis, such as TG, CE, and its FA precursors when compared to their controls. The same findings were noted in the whole-body male and female LFABP$^{-/-}$ mice; they displayed no changes in the levels of different hepatic lipid species compared to their controls [213]. This protection could be due to the redistribution of FA into another lipid species or an increased incorporation of TG into new VLDL for export instead of storage. However, the results showed that no significant differences between LFABP$^{liv-/-}$ mice and their controls in FA redistribution, and no alterations in VLDL secretion. This finding in female LFABP$^{liv-/-}$ mice is different from some other studies in the whole-body LFABP$^{-/-}$ mice, where increased hepatic cholesterol, lower TG levels [179,189,212] and lower PL level were reported following HFD feeding [212]. While the reduced VLDL secretion in the whole-body KO mice could not explain the protection against accumulation of hepatic TG in the LFABP whole-body KO, reduced hepatic FA uptake was accounted for this protection [189]

Since LFABP is still expressed in the proximal small intestine where most of intestinal lipid processing occurs, we hypothesized that the observed protection against hepatic steatosis in the female LFABP$^{liv-/-}$ mice might be influenced by compensatory responses in the intestine to the liver-specific ablation of LFABP, such as changes in the intestinal length, alterations in the amount of intestinal lipids, or a change in TG output as

chylomicrons. In female LFABP$^{liv-/-}$ mice the intestinal length was not changed, however, the intestinal mucosa of female LFABP$^{liv-/-}$ mice had higher TG and lower PL concentrations than the control mice. These findings could be due to an up-regulation of the intestinal-LFABP upon its specific ablation from the liver, and we found previously that intestinal-LFABP play a role in incorporating FA into TG more than into PL [162,163]. Interestingly, despite the fact that obesity and HFD are usually associated with a substantial reduction in rates of intestinal TG secretion [217,218], the obese female LFABP$^{liv-/-}$ mice did not show any differences in the rate of TG appearance in the blood after a lipid bolus, relative to their control mice. Since there is more intestinal TG content in female LFABP$^{liv-/-}$ mice, it is possible that it is incorporated into chylomicrons, counteracting the effect of obesity on reducing chylomicron secretion rates, and leading to comparable levels to their control mice. Another suggested mechanism that could prevent the reduction in the output of TG-rich chylomicron caused by obesity and HF feeding, is an up-regulation in the expression of intestinal-LFABP which is involved in the generation of PCTVs from the ER and chylomicron assembly in Golgi apparatus [90,91]. In contrast to our finding in female LFABP$^{liv-/-}$ mice, Schroeder group reported that their whole-body LFABP$^{-/-}$ obese mice tended to have a greater intestinal TG secretion rate than the control mice [162], while Newberry and coworkers reported that their lean LFABP$^{-/-}$ mice showed a substantial decrease in the intestinal TG secretion rate, and a higher TG content in the proximal part of the intestine [212]. This divergence in the results of chylomicron secretion rate is not yet understood. It was noted that the secretion rate of VLDL and chylomicron were higher in the female mice than in the male mice. This increase could be due to the sex hormones differences and also it has been found recently that gut microbioba can modulate sex related differences in lipid metabolism [319,320]

Another mechanism that might explain the protection against hepatic steatosis would be increased oxidation of hepatic FA. Liver FA oxidation was inferred from the levels of $^{14}CO_2$ and ^{14}C-labeled ASM, and in female LFABP$^{liv-/-}$ mice it was found to be slightly lower than the control mice, however, it did not reach statistical significance. Our previous study in the whole-body LFABP$^{-/-}$ mice also showed no changes in the plasma level of β-hydroxybutyrate (unpublished data). These findings are different than those of Newberry and co-workers, where lower plasma levels of β-hydroxybutyrate in the whole-body LFABP$^{-/-}$ mice were used to suggest that there was a reduction of hepatic FA oxidation [189]. It is worth noting that β-hydroxybutyrate may not be the best indicator of hepatic FA oxidation, since it is a product of the ketogenesis pathway and does not necessarily reflect the whole mitochondrial oxidative capacity. Erol *et al.* also showed in their study that there is a reduction in hepatic FA oxidation, however, this reduction occurred only in the intact hepatocytes but not in the liver homogenates of LFABP$^{-/-}$ mice [188] which is in accordance with our finding in this study, and which likely reflects impaired trafficking of the FA to the oxidative machinery rather than a reduction in the oxidative capacity. It is also possible that the liver-LFABP is involved in directing FA towards TG synthetic pathway more than to the oxidative pathway, and therefore its specific ablation from the liver could impact TG levels more than FA oxidation. Studying the intestinal phenotype of LFABP in the whole-body KO mice showed that LFABP has an important role in directing FA to the oxidative pathway [162]. Thus the role of LFABP trafficking of FA to oxidative machinery appears to be similar in the liver and the intestine. Overall, these findings suggess that the resistance to hepatic steatosis is not caused by upreglulation of FA oxidation.

LFABP and other FABPs decrease the unbound FA concentration by being a reservoir for FA, thereby preventing lipotoxicity caused by high levels of FFA, and enhancing FA uptake by maintaining the FA concentration gradient across the plasma membrane [311,321,322].

For this reason, another potential mechanism for protection against hepatic steatosis is the reduction of FA uptake into the liver. We hypothesized that the ablation of LFABP in the liver would impact hepatic FA uptake. Indeed, the results from FA uptake experiments, which measured the activity of the gavaged ^{14}C-oleate in different tissues, demonstrated that this was the case; there was a significant reduction in FA uptake in the liver of female LFABP$^{liv-/-}$ mice relative to the floxed control mice, indicating that there might be a shift of FA trafficking away from the liver, leading to increased availability of FA to be taken up by other tissues such as adipose tissue for storage and/or muscle for use as an energy substrate. The protection against hepatic steatosis in the whole-body LFABP$^{-/-}$ mice was also due to reduced hepatic FA uptake [189]. Examining FA uptake in other tissues of female LFABP$^{liv-/-}$ mice revealed a trend towards higher FA uptake in the adipose tissue with no difference in the muscle when compared to their control mice. This finding suggests that more FA are taken up by adipose tissue for storage as TG, which may partly explain the greater FM that is seen in female LFABP$^{liv-/-}$ mice. However, there was no difference in FA taken up by the muscle. As mentioned previously, in the whole-body LFABP KO, the protection against the decline in the endurance activity was due to higher intramuscular substrates availability such as TG and glycogen. Additionally, there was a greater mitochondrial quantity and activity with higher FA oxidative machinery in the muscle of LFABP$^{-/-}$ mice relative to their WT control mice [219]. Therefore, it is expected that those mechanisms that underlie the greater endurance activity in the whole body LFABP$^{-/-}$ mice could explain, at least in part, the greater endurance activity that was found in LFABP$^{liv-/-}$ mice when compared to their control mice. It is also possible that at the time of tissue collection, the muscle may have taken more FA but at the same time oxidized it, such that no increase in the activity of ^{14}C-oleate was found in the muscle.

Surprisingly, despite the fact that LFABP is still expressed in the intestine of LFABP$^{liv-/-}$ mice, there was significant reduction in FA uptake in the proximal part of the small intestine, and a non-significant reduction in FA uptake in the distal part of the small intestine of female LFABP$^{liv-/-}$ mice when compared to their control floxed mice. Gajda and colleagues found in their study that the intestinal LFABP did not affect intestinal FA uptake, since fecal fat excretion was not altered in LFABP$^{-/-}$ mice [162]. Therefore, there might be other mechanisms leading to the reduction of intestinal FA uptake. For example, alterations in the abundance of other proteins involved in FA uptake, such as CD36 and FATP4, could result in a reduction of intestinal FA uptake. We hypothesize that such reductions in intestinal FA uptake could be a negative feedback mechanism to oppose the surplus availability of FA resulting from lower hepatic uptake of FA. Previous studies also demonstrated a reduction in FA uptake in the livers of whole-body LFABP$^{-/-}$ mice [179,189]. We propose that the reduction of hepatic FA uptake due to the absence of LFABP is associated with reducing hepatic storage of FA in the form of TG, leading to a comparable hepatic lipid droplets accumulation in female LFABP$^{liv-/-}$ mice relative to the control mice despite their obese phenotype. At the same time, there was no effect on FA that were directed to oxidative pathways, to VLDL secretion, or to the synthesis of other lipid species.

While no alterations were found in energy consumption, energy production, or the intestinal transit time that can explain the heavier body weight and FM in the female LFABP$^{liv-/-}$ mice, these phenotypes could be due to the redistribution of FA from liver to adipose tissues for storage. This redistribution of FA also could account for the protection against hepatic steatosis.

In male mice we found that the ablation of hepatic-LFABP did not influence liver weight, hepatic lipid concentrations, and hepatic FA uptake. Additionally, there were no significant

changes in other mechanisms that can influence the supply or the availability of hepatic FA, such as intestinal lipid content, intestinal TG secretion rate, FA uptake to tissue other than the liver such as intestine, muscle and adipose tissue, hepatic FA oxidation, or VLDL secretion.

It is well known that LFABP affects trafficking of FA to the nucleus where it interacts with PPARα and induces the transcription of many genes involved in lipid metabolism. Thus, both male and female $LFABP^{liv-/-}$ mice showed an effect of liver-specific ablation of LFABP on hepatic lipid metabolic pathways, observed mainly in the expression of genes involved with FA transport, FA synthesis, and FA oxidation. However, these transcriptional changes have no discernable effect on lipids levels or the rate of FA oxidation. By binding FAs LFABP functions to generate a FA concentration gradient across the cell membrane, promoting FA uptake upon binding and transporting FFA into various metabolic pathways [321,322]. Ablation of liver-LFABP likely leads to more unbound FA in the cytosol, resulting in higher cytosolic FA concentration, hence, generating an opposite concentration gradient to limit further FA uptake. Therefore, the reduction in the expression of genes involved in FA uptake and synthesis could be a negative feedback mechanism to prevent accumulation of unbound FA. The imbalanced FA concentration that might be caused by decreased uptake and synthesis of FA was also restored by reducing FA degradation as suggested by decreased expression of genes involved in FA oxidation and by trend toward a reduction in the oxidation of ^{14}C-oleate. Overall, these changes appear to lead to a balanced hepatic FA and TG concentrations that were comparable to what was found in $LFABP^{fl/fl}$ control mice. The gene expression data support a pivotal role of LFABP in hepatic FA uptake and transportation and was likely the main cause of the observed reduction of hepatic FA uptake in this study. However, it is worth mentioning that the changes that were observed in lipid metabolic pathways at the transcriptional level do not

necessarily mean that the same trends of changes are occurring at the level of protein abundance, or protein activity; such analyses will be needed to support these interpretations.

In summary liver-LFABP gene ablation in mice resulted in strong body weight and FM phenotypes, with female LFABP$^{liv-/-}$ mice displaying increased values, while male LFABP$^{liv-/-}$ mice displayed little or no alterations, relative to their respective control mice. Metabolic adaptations in response to the ablation of hepatic-LFABP were not profound in male mice, except for the endurance activity which was also higher in male LFABP$^{liv-/-}$ mice than their controls. The female LFABP$^{liv-/-}$ mice were also protected against a HFD induced decline in endurance activity, and in addition they were protected against the development of hepatic steatosis despite their obese phenotype. While there was no redistribution of FA to other hepatic lipid species, no change in VLDL secretion or FA oxidation, the protection against hepatic neutral lipids accumulation was likely due to the reduction in hepatic FA uptake, and the higher adiposity found in female LFABP$^{liv-/-}$ mice is related to the increased FA uptake in other tissues, i.e. adipose tissue. Collectively, these findings suggest that in HF fed LFABP$^{liv-/-}$ female mice, the LCFA are preferentially stored in adipose tissues rather than being taken up by the liver for storage and oxidation. This is in agreement with prior literature where the functions of LFABP were examined in vitro, in cultured transformed cells, cultured primary hepatocytes from the liver of LFABP$^{-/-}$ mice, and in the null mice themselves [182]. Interestingly, it has been found that the expression of hepatic LFABP is higher in female rats than male rats [323]. Thus, the gender dependent metabolic changes in this study could be related to a higher expression of LFABP in the liver of female mice more than in male mice, making the impact of hepatic-LFABP deficiency stronger in female than in male LFABP$^{liv-/-}$ mice.

It is worth mentioning that recently a novel FABP3 inhibitor was developed and found to prevent the spreading and toxicity of α-synuclein which plays a role in some of the neurological diseases such as Parkinson's disease and dementia [324]. Therefore, our findings in these studies may have clinical implications in the future such as developing LFABP inhibitor that can prevent obesity associated physical inactivity and liver steatosis.

In conclusion, hepatic-LFABP ablation in female mice was sufficient to induce the MHO phenotype of the whole body LFABP$^{-/-}$ mice. Conversely, in male LFABP$^{liv-/-}$ mice, it is possible that some of the phenotypic changes require either the ablation of intestine-LFABP alone or the concurrent ablation of both liver- and intestine-LFABP. More studies are required to elucidate the role of LFABP in the intestine and the potential contributors of intestinal-LFABP to the whole-body phenotypes and to the alterations in the liver.

Chapter 4

General Conclusions and Future Directions

The Ablation of enterocyte IFABP and LFABP induces a dramatic alteration in the gut microbiome composition

Western diet, which contains high amounts of fat, has been associated with development of obesity and hypertriglyceridemia, which are major risk factors associated with cardiovascular disease and many other related comorbidities [9]. The intestine is the primary site where the digestion, emulsification, absorption, and secretion of lipids to other peripheral tissues takes place [19]. The central role that the intestine plays in the efficient uptake and processing of dietary lipids requires the presence of several lipid binding proteins in the enterocyte, notably IFABP, LFABP and other proteins, to process the large dietary lipid content of the Western diet.

We have found previously that ablation of LFABP accompanied with HF feeding resulted in higher body weight and FM gain compared with the WT controls in male mice, and recent studies have shown the same results in females as well. These results could be partly attributed to the higher food intake in those mice. However, despite their obesity, LFABP$^{-/-}$ mice displayed plasma glucose, insulin, and lipid levels comparable to those of the WT mice [162]. Additionally, LFABP$^{-/-}$ mice had better stamina and exercise performance when compared to their WT counterparts [219]. On the other hand, ablation of IFABP in HF fed mice resulted in lean mice that were normoglycemic and normoinsulinimic despite the chronic exposure to HFD, relative to WT mice. These findings were partially due to the HF fed IFABP$^{-/-}$ mice consuming less calories than their WT counterparts [162]. More recently, we have shown that the IFABP$^{-/-}$ mice may malabsorb nutrients in general, including lipids. Compared to WT mice, IFABP$^{-/-}$ mice displayed a disruption in their intestinal membrane integrity, where the villi were blunted compared to the control mice. This was accompanied by faster intestinal transit time, and

an increased amount of excreted feces [222]. In LFABP$^{-/-}$ mice, by contrast, there was no effect of the genotype or HFD on the intestinal villi structure (unpublished data).

Many of the phenotypic changes in the IFABP and LFABP KO mice could be related to alterations in the gut microbiota. It has been found that changes in the microbiome composition could impact the body weight, endurance activity, intestinal motility and integrity and other phenotypes [66,254,325]. It is well known that high saturated fat intake may be deleterious and that it leads to distinct microbiota composition, relative to standard chow [66]. The available data on HF fed animals supports the relationship between gut health and microbial composition, and their association with the development of obesity and its metabolic consequences [233].

It is thought that IFABP and LFABP are involved with the efficient uptake of FA into the enterocyte, while also playing a role in trafficking FA into different organelles [204]. Our recent findings have also shown that intestinal motility in IFABP$^{-/-}$ mice was affected [222], and many studies have demonstrated a strong association between gut motility and microbiome composition [254,261]. Changes in intestinal motility in LFABP$^{-/-}$ mice were also observed in this study, with LFABP$^{-/-}$ mice having an opposite phenotype to IFABP$^{-/-}$ mice. LFABP$^{-/-}$ mice had a longer intestinal transit time and a reduced amount of feces excreted compared to the WT control mice. Furthermore, we have found previously that intestinal ECs levels, were affected by the ablation of IFABP or LFABP, with significantly higher levels observed in LFABP$^{-/-}$ mice mucosa, and a trend towards lower levels in IFABP$^{-/-}$ mice [162]. The associations between gut motility and ECs levels on one side [258,259], and gut motility and microbiome composition on the other side are well established [254,261].

For all these reasons we hypothesized that ablation of these proteins will affect the intestinal availability of FA and other lipid ligands and, in turn, impact the intestinal microbial community and their associated production of metabolites. Therefore, our results strongly encouraged us to performed fecal microbiome analysis.

Indeed we found dramatic changes in the bacterial community structure and abundance that are strongly associated with the phenotypes that were observed in both KO mice, with anti-obesity associated bacteria being more abundant and obesity associated bacteria being less in IFABP$^{-/-}$ mice, and obesity associated bacteria being higher in LFABP$^{-/-}$ mice. Additionally, there was a higher bacterial richness in LFABP$^{-/-}$ mice, as indicated by the highest number of bacteria ASVs among the three genotypes; this is probably due to the slower intestinal transit time which reduces the amount of bacteria that are secreted in the feces [254]. Reducing intestinal motility also suggests that there is more time available for the food to be exposed to the gut bacteria, and this probably helps in more efficient food digestion, and results in more nutrients to be extracted. This supports the role of bacterial composition and abundance in contributing to the body weight changes in both IFABP$^{-/-}$ and LFABP$^{-/-}$ mice after chronic HFD feeding.

Recently, we have found that HF fed female LFABP$^{-/-}$ mice also gained more weight than their control mice (unpublished data). Notably, the Schroeder and Binas group, from where we derived our mice, also demonstrated that female LFABP$^{-/-}$ mice gained more weight than their WT control mice [213]. For this reason, it will be important to assess whether HFD fed female whole-body LFABP$^{-/-}$ mice also display the MHO and the intestinal motility phenotypes that have been observed in male LFABP$^{-/-}$ mice.

While our HF fed LFABP$^{-/-}$ mice and Schroeder group HF fed LFABP$^{-/-}$ mice had increased body weight and adiposity compared to their controls [162,213], the Davidson group LFABP$^{-/-}$ mice displayed some differences in phenotype in response to chronic HF feeding; both the male and the female LFABP$^{-/-}$ mice used by the Davidson group were resistant to diet induced obesity [212,317]. These differences could be related to the strategies used in gene ablation, strain background, or it can be due to differences in gut microbiome structure and density [182,326]. Additionally, many of the HFD studies of the Davidson group used diets that were devoid of essential FAs. Here, we found robust alterations in the intestinal microbiome of both IFABP$^{-/-}$ and LFABP$^{-/-}$ male mice. The differences in the microbiome were associated significantly with the phenotypes observed in both genotypes. In regard to the microbiome changes that have been observed in the male mice, and the fact that there may be sexual dimorphic phenotypes in response to the ablation of liver-LFABP, it will be worth to assessing the intestinal microbial composition in female mice as well.

In order to get more depth in understanding the influence of IFABP and LFABP ablation on the gut microbiome composition, future studies should involve microbial transplantation from each KO group of mice into germ-free mice. Additionally, the KO mice should be challenged with chronic antibiotic exposure. These two sets of experimental conditions would assist in determining whether LFABP, IFABP, or the gut microbiome acts as the primary influencer on whole-body energy homeostasis.

The whole-body KO of IFABP or LFABP is associated with changes in the levels of microbial metabolites

In this study we found that there is a dramatic increase in the metabolites that are produced in the colon of mice via bacterial fermentation of indigestible carbohydrates,

namely SCFAs [58]. Many studies have demonstrated the beneficial effects of SCFAs on whole-body energy homeostasis [64,276,325]. Both IFABP$^{-/-}$ and LFABP$^{-/-}$ male mice display a higher fecal levels of SCFAs, which are correlated with some of phenotypic changes that were observed in these mice, such as the lean phenotype in IFABP$^{-/-}$ male mice and the MHO phenotype in LFABP$^{-/-}$ male mice [162]. However, it is unknown whether the increased fecal output of SCFAs is due to reduced SCFAs intestinal absorption, increased SCFAs production, or a combination of both. IFABP$^{-/-}$ mice have a reduced intestinal transit times and increased fecal output which would likely result in a reduction in efficient nutrient absorption [222]. This may partly explain the observed increase in fecal SCFAs levels in the IFABP$^{-/-}$ mice. It is worth noting, however, that the IFABP$^{-/-}$ mice also had a higher density of SCFAs producing bacteria, which may also contribute to the observed increase in fecal SCFAs. While LFABP$^{-/-}$ mice have a lower abundance of SCFAs producing bacteria, the fecal levels of SCFAs are still significantly high when compared to the WT control mice. This could be also either due to less efficient absorption, or more likely, the longer intestinal transit time seen in these mice, leading to the accumulation of more SCFAs in the intestine. In order to unravel this, further studies, including measuring SCFAs intestinal uptake, are necessary to elucidate the extent of SCFAs absorption efficiency.

SCFAs can stimulate the production of gut peptides such as GLP-1 by L-cells [327]. GLP-1 is involved in the regulation of energy balance, glucose homeostasis, and appetite; it promotes satiety and delays gastric emptying [32,34]. Interestingly, Both IFABP$^{-/-}$ and LFABP$^{-/-}$ mice displayed blood glucose and insulin levels that are comparable to the WT control mice [162], and both displayed alterations in intestinal motility, relative to control mice (chapter 2). Therefore, it is possible that SCFAs are involved in these effects by stimulating the release of GLP-1. Preliminary results suggest higher fasting levels of

plasma GLP-1 in both IFABP$^{-/-}$ and LFABP$^{-/-}$ mice. However, it is good to note that although IFABP$^{-/-}$ mice have a higher GLP-1 level, however, their intestinal motility is still faster than the WT control mice. This could be related to the fact that IFABP$^{-/-}$ mice have lower mucosal ECs levels that might have a greater impact on intestinal motility than GLP-1 [162], or it could be related to the shorter villi length in these mice, allowing for faster intestinal motility [222]. Recently we have found that there were reductions in the density of goblet cells in LFABP$^{-/-}$ mice (unpublished data) and in the density of Paneth cells and goblet cells in IFABP$^{-/-}$ mice [222]. Therefore, there might be also alterations in the density of L-cells or other EECs. Future studies should be directed to assess the level of GLP-1 and other enteroendocrine hormones secondary to feeding, quantify and characterize the EECs that secrete these hormones and, further, assess their correlation with the gut microbiome and SCFAs.

Disturbances in gut microbiome can lead to obesity, low grade inflammation, and higher plasma LPS [63]. In the gut/adipose tissue axis, it has been found that LPS, released from gut microbiota, has the ability to control and stimulate the ECs system and thereby increase gut permeability. This consequently leads to the penetration of more LPS into the circulation, resulting in low grade inflammation, adipose tissue expansion and obesity [61,260]. We have shown previously that HF fed lean IFABP$^{-/-}$ mice showed a trend toward lower small intestinal ECs levels, while the MHO LFABP$^{-/-}$ mice had higher mucosal ECs levels [162]. Further research should be directed at elucidating the interplay between host microbiota and the ECs system. In addition to assessing circulating LPS levels, future studies should focus on studying aspects of the colonic and adipose tissue ECs system components, such as cannabinoid receptor expression, colonic ECs concentrations, and their metabolic pathways in LFABP and IFABP KO mice.

Specific ablation of liver-LFABP results in a more dramatic MHO phenotype in female than in male mice

LFABP has a concurrent expression in both the liver and the intestine. Therefore, it is important to study the functions of this protein in each of these tissues individually, to determine how LFABP ablation in the liver or in the intestine contributes to the MHO phenotype of LFABP$^{-/-}$ mice. Whole-body LFABP ablation resulted in body weight and body composition changes, differences in fuel utilization, and changes in the rate of lipid oxidation and lipid distribution [162,163,179,212]. Previously, we found that in male mice the whole-body ablation of LFABP together with HF feeding resulted in a MHO phenotype. Despite being obese, the mice remained normoglycemic, normoinsulinic, normolipidemic, quite active, and also had increased stamina when challenged by exercise bouts, relative to the WT control mice [162,219]. Additionally, others have demonstrated that LFABP$^{-/-}$ mice were protected against hepatic steatosis [64,233,261].

Here, in this study, we have shown that the liver-specific ablation of LFABP in male mice, upon HF feeding, does not result in an obese phenotype, and that in response to a chronic HF feeding, LFABP$^{liv-/-}$ male mice have glucose, insulin and lipids levels comparable to the floxed control mice. Interestingly, however, they have higher exercise capacity compared the LFABP$^{fl/fl}$ control mice; thus the males partially recapitulate characteristics of the MHO phenotype of the whole-body KO mice, though they themselves are not more obese than their WT counterparts. Female LFABP$^{liv-/-}$ mice seem to fully recapitulate the MHO model, displaying greater body weight and adiposity, but at the same time having glucose tolerance, fasting insulin, and fasting lipids levels comparable to the floxed control mice. Additionally, despite their heavier body weight, female LFABP$^{liv-/-}$ mice also display better exercise capacity than the control mice. The differential results of the body weight between

male and female liver-LFABP cKO mice are indicative of sexual dimorphism in response to HF feeding (to be discussed later).

Specific alteration to the liver is associated with dramatic whole-body responses

It is interesting that ablation of LFABP specific to the liver results in resistance to the HF feeding-induced decline in exercise capacity in both the non-obese male mice and most importantly the obese female mice, when compared to control mice. Our previous study indicated that the greater endurance capacity observed in whole-body KO of LFABP in male mice was due to higher availability of intramuscular energy storage such as TG and glycogen, and the more efficient mitochondrial machinery for substrates utilization [219]. Unlike what was found in male LFABP$^{-/-}$ mice [162], and what we found here in male LFABP$^{liv-/-}$, the ability of female LFABP$^{liv-/-}$ mice to retain their exercise capacity in response to chronic HF feeding, seems to be independent of changes in spontaneous activity. Therefore, it is important to also unravel the underlying causes for the better exercise endurance that is seen in the cKO male and female mice relative to their control mice. Recently, we conducted studies on intestinal specific LFABP KO male and female mice (LFABP$^{int-/-}$). The preliminary data show similar results that were found in male and female LFABP$^{liv-/-}$ mice, with male mice having better exercise capacity but only modest changes in body weight and FM, and female mice being a more robust model for the MHO phenotype, with a greater exercise capacity relative to their floxed control mice as well as significantly higher body weight gain and FM (unpublished data). It is important to mention that all of our previous studies with the whole-body ablation of LFABP were on male mice [162,163,219]. Therefore, it will be important to examine the exercise phenotype in female whole-body LFABP$^{-/-}$ mice as well.

These changes in exercise activity and the differential response to the ablation of liver-LFABP under HFD between male and female mice could also result from organ crosstalk, for example the gut/muscle axis. Recently (chapter 2), we have found that variability in gut microbiome composition and abundance can play a fundamental role in the phenotypic changes that were observed in both IFABP$^{-/-}$ and LFABP$^{-/-}$ mice. Therefore, it is also possible that the microbiome composition can play a role in the sexual dimorphism that is seen not only in liver-specific ablation of LFABP (chapter 3) but also in intestine-specific ablation of LFABP (unpublished data). Hence, it will be of interest to assess the microbiome community in both male and female tissues-specific LFABP null mice, and in female whole-body LFABP null mice, to determine the bacterial composition and abundance that may influence the phenotypes that have been observed in these aforementioned groups of mice. In addition to the changes in the gut microbiota the microbiome metabolites, specifically the SCFAs, were found to be higher in both LFABP and IFABP KO mice than their WT control mice. SCFAs were reported to have several beneficial effect such as increasing skeletal muscle glycogen and promoting FA uptake and oxidation [276]. These observations may be related to the higher exercise performance that is seen in whole-body LFABP$^{-/-}$ mice, and it could be the same case in male and female liver-specific LFABP$^{-/-}$ mice. Therefore, in addition to assessing microbiome composition, it will also be important to measure fecal and plasma SCFAs in male and female cKO mice.

Alteration specific to the liver is associated with sexual dimorphism in lipids distribution

Results in this study indicate that liver-specific ablation of LFABP in male mice does not affect the hepatic level of different lipid species, hepatic FA oxidation, hepatic FA uptake, or FA uptake by other tissues. These findings are consistent with other findings in the male

cKO mice in regard to the body weight, body composition, and other measured parameters. HF fed female LFABP$^{liv-/-}$ mice, despite their markedly obese phenotype which is usually associated with hepatic accumulation of TG and FA [318], appeared to be protected against hepatic steatosis. This protection was evident, as the female LFABP$^{liv-/-}$ mice had a lower liver weight/body weight ratio, and a lack of hepatic neutral lipid accumulation when compared to their control LFABP$^{fl/fl}$ mice. Different mechanisms were investigated to determine the underlying cause for the protection against hepatic steatosis. No distribution of FA into other hepatic lipid species, no increase in FA oxidation and no alteration in hepatic VLDL secretion were observed. Assessing FA uptake in different tissues, however, revealed a significant reduction in hepatic FA uptake, and a trend towards a higher FA uptake by the adipose tissue. This suggests that the redistribution of FA into tissues other than the liver, such as adipose tissue, is probably the cause of both the protection against hepatic steatosis and the increased adiposity observed in female LFABP$^{liv-/-}$ mice. These results are in accordance with other studies, supporting the role of LFABP in enhancing FA uptake and facilitating intracellular transport and trafficking [179,189].

Additionally, here we showed that liver-specific ablation of LFABP in both male and female cKO mice results in the alteration of the expression of several genes involved in hepatic lipid metabolism, without affecting hepatic lipid levels. Intestine-specific ablation of LFABP also resulted in alterations of hepatic expression of genes involved in lipid metabolism (unpublished data), supporting the idea of organ crosstalk between the intestine and the liver. In order to confirm this interaction, it is also necessary to measure intestinal expression of genes that are involved in lipid metabolism in liver- and intestine-LFABP null mice. Furthermore, protein abundance and activity should be measured to get more depth

in assessing how alteration in the liver or in the intestine can influence the pathways involved in lipid metabolism.

As mentioned previously, LFABP is expressed in both the liver and the intestine of mice. LFABP$^{liv-/-}$ mice still have the LFABP expressed in the intestine. Therefore, we tested whether ablation of LFABP from the liver affects intestinal lipid metabolism. No changes were found in intestinal FA uptake, mucosal lipids levels, or in TG-rich chylomicron levels in male LFABP$^{liv-/-}$ mice. However, in female cKO mice there was a reduction in intestinal FA uptake. There was also accumulation of intestinal TG at the expense of PL, though this did not affect chylomicron secretion. However, it is possible that the chylomicron composition or size may be altered. Hence, future analysis of chylomicrons composition may reveal changes in the intestine caused by liver-specific ablation of LFABP. In order to unravel the cause of this reduction in intestinal FA uptake and the changes seen in FA distribution between lipid species in female LFABP$^{liv-/-}$ mice, gene expression and protein abundance of different intestinal membrane and intracellular FA uptake/transporters, need to be assessed.

Overall, it is obvious that the liver-specific ablation of LFABP can affect whole-body homeostasis. Furthermore, sexual dimorphism has been observed between male and female LFABP$^{liv-/-}$ in response to chronic HFD feeding, suggesting that sex hormones play an important role as well. It has been found that LFABP expression is influenced by steroid hormone regulation, with its concentration being higher in female compared to male rodents [160]. When castrated male rats were treated with estradiol, hepatic LFABP levels were restored to levels comparable to that in female rats. Conversely, treating ovariectomized female rats with testosterone resulted in hepatic LFABP levels that are comparable to male rats. This suggests that LFABP expression is affected by steroid

hormones [160]. This higher expression in female livers enhances the rate of hepatic transport of FA through the cytoplasm and hence their utilization [160,328]. Perhaps that is why female mice in this study were more affected by liver specific ablation of LFABP relative to their male counterparts. Thus generating ovariectomized female mice or castrated male mice, together with using sex hormones, may help to elucidate the underlying causes of the sexual dimorphism in the phenotypes that were noted between male and female cKO mice.

Acknowledgement of Previous Publications

The results of some of these studies have also been published previously. Sources for reference and background information are numbered throughout the text and listed in the bibliography at the end of this dissertation. Hiba Tawfeeq is the first co-author of chapter 2 and is the writer of all of the other dissertation sections. Other individuals were involved in the research in the previously published work and have been identified here.

Previously published work

Wu, G.*; Tawfeeq, H.R.*; Lackey, A.I.; Zhou, Y.; Sifnakis, Z.; Zacharisen, S.M.; Xu, H.; Doran, J.M.; Sampath, H.; Zhao, L.; Lam, Y.Y.; Storch, J. Gut Microbiota and Phenotypic Changes Induced by Ablation of Liver- and Intestinal-Type Fatty Acid-Binding Proteins. Nutrients 2022, 14, doi:10.3390/nu14091762. **These authors contributed equally to this work.*

Chapter 2 was previously published in the Journal of Nutrients in 2022. Author Contributions: G.W., H.R.T., L.Z., Y.Y.L. and J.S. designed the experiments; H.R.T., A.I.L., Y.Z., Z.S., S.M.Z., H.X. and J.M.D. performed animal procedures and sample collections; G.W. and Y.Y.L. performed fecal DNA and gut microbiota analyses; H.S. performed metabolite analysis. H.R.T., G.W., J.S., L.Z. and Y.Y.L. wrote and edited the manuscript. Reprinting of this article for the dissertation is permitted by the Journal of Nutrients, which maintains ownership of the article content.

Literature Cited

1. Fahy, E.; Subramaniam, S.; Murphy, R.C.; Nishijima, M.; Raetz, C.R.; Shimizu, T.; Spener, F.; van Meer, G.; Wakelam, M.J.; Dennis, E.A. Update of the LIPID MAPS comprehensive classification system for lipids. *Journal of lipid research* **2009**, *50 Suppl*, S9-14, doi:10.1194/jlr.R800095-JLR200.
2. Dyatlovitskaya, E.; Bezuglov, V.J.B.-N.Y.-E.T.o.B. Lipids as bioeffectors. Introduction. **1998**, *63*, 1-3.
3. Petit, V.; Arnould, L.; Martin, P.; Monnot, M.C.; Pineau, T.; Besnard, P.; Niot, I. Chronic high-fat diet affects intestinal fat absorption and postprandial triglyceride levels in the mouse. *Journal of lipid research* **2007**, *48*, 278-287, doi:10.1194/jlr.M600283-JLR200.
4. Bray, G.A.; Nielsen, S.J.; Popkin, B.M. Consumption of high-fructose corn syrup in beverages may play a role in the epidemic of obesity. *The American journal of clinical nutrition* **2004**, *79*, 537-543, doi:10.1093/ajcn/79.4.537.
5. Bray, G.A. How do we get fat? An epidemiologic and metabolic approach. *Clinics in dermatology* **2004**, *22*, 281-288, doi:10.1016/j.clindermatol.2004.01.009.
6. Jéquier, E. Pathways to obesity. *International journal of obesity and related metabolic disorders : journal of the International Association for the Study of Obesity* **2002**, *26 Suppl 2*, S12-17, doi:10.1038/sj.ijo.0802123.
7. Hariri, N.; Thibault, L. High-fat diet-induced obesity in animal models. *Nutrition research reviews* **2010**, *23*, 270-299, doi:10.1017/s0954422410000168.
8. Canbay, A.; Bechmann, L.; Gerken, G. Lipid Metabolism in the Liver. *Z Gastroenterol* **2007**, *45*, 35-41.
9. Pi-Sunyer, X. The medical risks of obesity. *Postgraduate medicine* **2009**, *121*, 21-33, doi:10.3810/pgm.2009.11.2074.
10. World Health Organization. Obesity and overweight. Availabe online: https://www.who.int/news-room/fact-sheets/detail/obesity-and-overweight (accessed on 2021, June 9).
11. Center for Disease Control and Prevention. Overweight & Obesity. Availabe online: https://www.cdc.gov/obesity/data/adult.html (accessed on 2021, June 7).
12. Ogobuiro I, G.J., Tuma F. Physiology, Gastrointestinal. *Treasure Island (FL): StatPearls Publishing;* **2020** https://www.ncbi.nlm.nih.gov/books/NBK537103/, doi:https://www.ncbi.nlm.nih.gov/books/NBK537103/.
13. Lai, W.Y.W.; Chua, J.W.M.; Gill, S.; Brownlee, I.A. Analysis of the Lipolytic Activity of Whole-Saliva and Site-Specific Secretions from the Oral Cavity of Healthy Adults. *Nutrients* **2019**, *11*, doi:10.3390/nu11010191.
14. Hamosh, M. Lingual and gastric lipases. *Nutrition (Burbank, Los Angeles County, Calif.)* **1990**, *6*, 421-428.
15. Keast, R.S.J.; Costanzo, A. Is fat the sixth taste primary? Evidence and implications. *Flavour* **2015**, *4*, 5, doi:10.1186/2044-7248-4-5.
16. Roberts, I.M.; Montgomery, R.K.; Carey, M.C. Rat lingual lipase: partial purification, hydrolytic properties, and comparison with pancreatic lipase. *The American journal of physiology* **1984**, *247*, G385-393, doi:10.1152/ajpgi.1984.247.4.G385.
17. Jensen, R.G.; Clark, R.M.; deJong, F.A.; Hamosh, M.; Liao, T.H.; Mehta, N.R. The lipolytic triad: human lingual, breast milk, and pancreatic lipases: physiological implications of their characteristics in digestion of dietary fats. *Journal of pediatric gastroenterology and nutrition* **1982**, *1*, 243-255, doi:10.1097/00005176-198201020-00016.
18. Hussain, M.M. Intestinal lipid absorption and lipoprotein formation. *Current opinion in lipidology* **2014**, *25*, 200-206, doi:10.1097/mol.0000000000000084.

19. Iqbal, J.; Hussain, M.M. Intestinal lipid absorption. *American journal of physiology. Endocrinology and metabolism* **2009**, *296*, E1183-1194, doi:10.1152/ajpendo.90899.2008.
20. Phan, C.T.; Tso, P. Intestinal lipid absorption and transport. *Frontiers in bioscience : a journal and virtual library* **2001**, *6*, D299-319, doi:10.2741/phan.
21. Erlanson-Albertsson, C. Pancreatic colipase. Structural and physiological aspects. *Biochimica et biophysica acta* **1992**, *1125*, 1-7, doi:10.1016/0005-2760(92)90147-n.
22. Thomson, A.; Tso, P.J.B., Physiological,; Nutrition, M.A.o.H. Overview of digestion and absorption. **2013**, 123-141.
23. Kong, S.; Zhang, Y.H.; Zhang, W. Regulation of Intestinal Epithelial Cells Properties and Functions by Amino Acids. *BioMed Research International* **2018**, *2018*, 2819154, doi:10.1155/2018/2819154.
24. Peterson, L.W.; Artis, D. Intestinal epithelial cells: regulators of barrier function and immune homeostasis. *Nature Reviews Immunology* **2014**, *14*, 141-153, doi:10.1038/nri3608.
25. Williams, J.M.; Duckworth, C.A.; Burkitt, M.D.; Watson, A.J.; Campbell, B.J.; Pritchard, D.M. Epithelial cell shedding and barrier function: a matter of life and death at the small intestinal villus tip. *Veterinary pathology* **2015**, *52*, 445-455, doi:10.1177/0300985814559404.
26. Madsen, K.; Park, H. Chapter 26 - Immunologic Response in the Host. In *The Microbiota in Gastrointestinal Pathophysiology*, Floch, M.H., Ringel, Y., Allan Walker, W., Eds. Academic Press: Boston, 2017; https://doi.org/10.1016/B978-0-12-804024-9.00026-4pp. 233-241.
27. González-Mariscal, L.; Betanzos, A.; Nava, P.; Jaramillo, B.E. Tight junction proteins. *Progress in biophysics and molecular biology* **2003**, *81*, 1-44, doi:10.1016/s0079-6107(02)00037-8.
28. Kim, Y.S.; Ho, S.B. Intestinal goblet cells and mucins in health and disease: recent insights and progress. *Current gastroenterology reports* **2010**, *12*, 319-330, doi:10.1007/s11894-010-0131-2.
29. de Santa Barbara, P.; van den Brink, G.R.; Roberts, D.J. Development and differentiation of the intestinal epithelium. *Cellular and molecular life sciences : CMLS* **2003**, *60*, 1322-1332, doi:10.1007/s00018-003-2289-3.
30. Zhao, Q.; Elson, C.O. Role of the Microbiota in Immune Development. In *Encyclopedia of Immunobiology*, Ratcliffe, M.J.H., Ed. Academic Press: Oxford, 2016; https://doi.org/10.1016/B978-0-12-374279-7.19019-8pp. 109-119.
31. Noah, T.K.; Donahue, B.; Shroyer, N.F. Intestinal development and differentiation. *Experimental cell research* **2011**, *317*, 2702-2710, doi:10.1016/j.yexcr.2011.09.006.
32. Worthington, J.J.; Reimann, F.; Gribble, F.M. Enteroendocrine cells-sensory sentinels of the intestinal environment and orchestrators of mucosal immunity. *Mucosal Immunology* **2018**, *11*, 3-20, doi:10.1038/mi.2017.73.
33. Ye, L.; Liddle, R.A. Gastrointestinal hormones and the gut connectome. *Current opinion in endocrinology, diabetes, and obesity* **2017**, *24*, 9-14, doi:10.1097/med.0000000000000299.
34. Everard, A.; Cani, P.D. Gut microbiota and GLP-1. *Rev Endocr Metab Disord* **2014**, *15*, 189-196, doi:10.1007/s11154-014-9288-6.
35. Gribble, F.M.; Reimann, F. Enteroendocrine Cells: Chemosensors in the Intestinal Epithelium. *Annual review of physiology* **2016**, *78*, 277-299, doi:10.1146/annurev-physiol-021115-105439.

36. Iseki, S.; Kondo, H. An immunocytochemical study on the occurrence of liver fatty-acid-binding protein in the digestive organs of rats: specific localization in the D cells and brush cells. *Acta anatomica* **1990**, *138*, 15-23, doi:10.1159/000146915.
37. Dockray, G.J. Enteroendocrine cell signalling via the vagus nerve. *Current opinion in pharmacology* **2013**, *13*, 954-958, doi:10.1016/j.coph.2013.09.007.
38. Cristino, L.; Becker, T.; Di Marzo, V. Endocannabinoids and energy homeostasis: an update. *BioFactors (Oxford, England)* **2014**, *40*, 389-397, doi:10.1002/biof.1168.
39. Koch, M. Cannabinoid Receptor Signaling in Central Regulation of Feeding Behavior: A Mini-Review. *Frontiers in neuroscience* **2017**, *11*, 293, doi:10.3389/fnins.2017.00293.
40. Wang, J.; Ueda, N. Biology of endocannabinoid synthesis system. *Prostaglandins & other lipid mediators* **2009**, *89*, 112-119, doi:10.1016/j.prostaglandins.2008.12.002.
41. Pertwee, R.G. Targeting the endocannabinoid system with cannabinoid receptor agonists: pharmacological strategies and therapeutic possibilities. *Philosophical transactions of the Royal Society of London. Series B, Biological sciences* **2012**, *367*, 3353-3363, doi:10.1098/rstb.2011.0381.
42. Bass, L.; Wershil, B.K.J.S.; gastrointestinal, F.s.; liver disease. 10th ed. Philadelphia, P.S., Elsevier Inc. Anatomy, histology, embryology and developmental anomalies of the small and large intestine. **2016**, 1649.
43. Parikh, K.; Antanaviciute, A.; Fawkner-Corbett, D.; Jagielowicz, M.; Aulicino, A.; Lagerholm, C.; Davis, S.; Kinchen, J.; Chen, H.H.; Alham, N.K.; Ashley, N.; Johnson, E.; Hublitz, P.; Bao, L.; Lukomska, J.; Andev, R.S.; Björklund, E.; Kessler, B.M.; Fischer, R.; Goldin, R.; Koohy, H.; Simmons, A. Colonic epithelial cell diversity in health and inflammatory bowel disease. *Nature* **2019**, *567*, 49-55, doi:10.1038/s41586-019-0992-y.
44. McCauley, H.A.; Guasch, G. Three cheers for the goblet cell: maintaining homeostasis in mucosal epithelia. *Trends in molecular medicine* **2015**, *21*, 492-503, doi:10.1016/j.molmed.2015.06.003.
45. Thiagarajah, J.R.; Verkman, A.S. Chapter 55 - Water Transport in the Gastrointestinal Tract. In *Physiology of the Gastrointestinal Tract (Sixth Edition)*, Said, H.M., Ed. Academic Press: 2018; https://doi.org/10.1016/B978-0-12-809954-4.00055-4pp. 1249-1272.
46. Brown, E.M.; Sadarangani, M.; Finlay, B.B. The role of the immune system in governing host-microbe interactions in the intestine. *Nature Immunology* **2013**, *14*, 660-667, doi:10.1038/ni.2611.
47. Xiao, L.; Feng, Q.; Liang, S.; Sonne, S.B.; Xia, Z.; Qiu, X.; Li, X.; Long, H.; Zhang, J.; Zhang, D.; Liu, C.; Fang, Z.; Chou, J.; Glanville, J.; Hao, Q.; Kotowska, D.; Colding, C.; Licht, T.R.; Wu, D.; Yu, J.; Sung, J.J.; Liang, Q.; Li, J.; Jia, H.; Lan, Z.; Tremaroli, V.; Dworzynski, P.; Nielsen, H.B.; Bäckhed, F.; Doré, J.; Le Chatelier, E.; Ehrlich, S.D.; Lin, J.C.; Arumugam, M.; Wang, J.; Madsen, L.; Kristiansen, K. A catalog of the mouse gut metagenome. *Nature biotechnology* **2015**, *33*, 1103-1108, doi:10.1038/nbt.3353.
48. Gill, S.R.; Pop, M.; Deboy, R.T.; Eckburg, P.B.; Turnbaugh, P.J.; Samuel, B.S.; Gordon, J.I.; Relman, D.A.; Fraser-Liggett, C.M.; Nelson, K.E. Metagenomic analysis of the human distal gut microbiome. *Science (New York, N.Y.)* **2006**, *312*, 1355-1359, doi:10.1126/science.1124234.
49. Frank, D.N.; St Amand, A.L.; Feldman, R.A.; Boedeker, E.C.; Harpaz, N.; Pace, N.R. Molecular-phylogenetic characterization of microbial community imbalances in human inflammatory bowel diseases. *Proceedings of the National Academy of*

Sciences of the United States of America **2007**, *104*, 13780-13785, doi:10.1073/pnas.0706625104.

50. Ley, R.E.; Bäckhed, F.; Turnbaugh, P.; Lozupone, C.A.; Knight, R.D.; Gordon, J.I. Obesity alters gut microbial ecology. *Proceedings of the National Academy of Sciences of the United States of America* **2005**, *102*, 11070-11075, doi:10.1073/pnas.0504978102.
51. Ley, R.E.; Peterson, D.A.; Gordon, J.I. Ecological and evolutionary forces shaping microbial diversity in the human intestine. *Cell* **2006**, *124*, 837-848, doi:10.1016/j.cell.2006.02.017.
52. Peterson, L.W.; Artis, D. Intestinal epithelial cells: regulators of barrier function and immune homeostasis. *Nature reviews. Immunology* **2014**, *14*, 141-153, doi:10.1038/nri3608.
53. Slack, E.; Hapfelmeier, S.; Stecher, B.; Velykoredko, Y.; Stoel, M.; Lawson, M.A.; Geuking, M.B.; Beutler, B.; Tedder, T.F.; Hardt, W.D.; Bercik, P.; Verdu, E.F.; McCoy, K.D.; Macpherson, A.J. Innate and adaptive immunity cooperate flexibly to maintain host-microbiota mutualism. *Science (New York, N.Y.)* **2009**, *325*, 617-620, doi:10.1126/science.1172747.
54. Cani, P.D.; Amar, J.; Iglesias, M.A.; Poggi, M.; Knauf, C.; Bastelica, D.; Neyrinck, A.M.; Fava, F.; Tuohy, K.M.; Chabo, C.; Waget, A.; Delmée, E.; Cousin, B.; Sulpice, T.; Chamontin, B.; Ferrières, J.; Tanti, J.F.; Gibson, G.R.; Casteilla, L.; Delzenne, N.M.; Alessi, M.C.; Burcelin, R. Metabolic endotoxemia initiates obesity and insulin resistance. *Diabetes* **2007**, *56*, 1761-1772, doi:10.2337/db06-1491.
55. Masood, M.I.; Qadir, M.I.; Shirazi, J.H.; Khan, I.U. Beneficial effects of lactic acid bacteria on human beings. *Critical reviews in microbiology* **2011**, *37*, 91-98, doi:10.3109/1040841x.2010.536522.
56. Anhê, F.F.; Varin, T.V.; Le Barz, M.; Desjardins, Y.; Levy, E.; Roy, D.; Marette, A. Gut Microbiota Dysbiosis in Obesity-Linked Metabolic Diseases and Prebiotic Potential of Polyphenol-Rich Extracts. *Current obesity reports* **2015**, *4*, 389-400, doi:10.1007/s13679-015-0172-9.
57. Canani, R.B.; Costanzo, M.D.; Leone, L.; Pedata, M.; Meli, R.; Calignano, A. Potential beneficial effects of butyrate in intestinal and extraintestinal diseases. *World journal of gastroenterology* **2011**, *17*, 1519-1528, doi:10.3748/wjg.v17.i12.1519.
58. Lozupone, C.A.; Stombaugh, J.I.; Gordon, J.I.; Jansson, J.K.; Knight, R. Diversity, stability and resilience of the human gut microbiota. *Nature* **2012**, *489*, 220-230, doi:10.1038/nature11550.
59. Tedelind, S.; Westberg, F.; Kjerrulf, M.; Vidal, A. Anti-inflammatory properties of the short-chain fatty acids acetate and propionate: a study with relevance to inflammatory bowel disease. *World journal of gastroenterology* **2007**, *13*, 2826-2832, doi:10.3748/wjg.v13.i20.2826.
60. Kostic, A.D.; Xavier, R.J.; Gevers, D. The microbiome in inflammatory bowel disease: current status and the future ahead. *Gastroenterology* **2014**, *146*, 1489-1499, doi:10.1053/j.gastro.2014.02.009.
61. Liu, J.; Bátkai, S.; Pacher, P.; Harvey-White, J.; Wagner, J.A.; Cravatt, B.F.; Gao, B.; Kunos, G. Lipopolysaccharide Induces Anandamide Synthesis in Macrophages via CD14/MAPK/Phosphoinositide 3-Kinase/NF-κB Independently of Platelet-activating Factor*. *Journal of Biological Chemistry* **2003**, *278*, 45034-45039, doi:https://doi.org/10.1074/jbc.M306062200.
62. Mehrpouya-Bahrami, P.; Chitrala, K.N.; Ganewatta, M.S.; Tang, C.; Murphy, E.A.; Enos, R.T.; Velazquez, K.T.; McCellan, J.; Nagarkatti, M.; Nagarkatti, P. Blockade of CB1 cannabinoid receptor alters gut microbiota and attenuates inflammation

and diet-induced obesity. *Scientific reports* **2017**, *7*, 15645, doi:10.1038/s41598-017-15154-6.

63. Muccioli, G.G.; Naslain, D.; Bäckhed, F.; Reigstad, C.S.; Lambert, D.M.; Delzenne, N.M.; Cani, P.D. The endocannabinoid system links gut microbiota to adipogenesis. *Molecular systems biology* **2010**, *6*, 392, doi:10.1038/msb.2010.46.
64. Okamoto, T.; Morino, K.; Ugi, S.; Nakagawa, F.; Lemecha, M.; Ida, S.; Ohashi, N.; Sato, D.; Fujita, Y.; Maegawa, H. Microbiome potentiates endurance exercise through intestinal acetate production. *American journal of physiology. Endocrinology and metabolism* **2019**, *316*, E956-e966, doi:10.1152/ajpendo.00510.2018.
65. Clark, A.; Mach, N. The Crosstalk between the Gut Microbiota and Mitochondria during Exercise. *Frontiers in physiology* **2017**, *8*, 319, doi:10.3389/fphys.2017.00319.
66. Bäckhed, F.; Ding, H.; Wang, T.; Hooper, L.V.; Koh, G.Y.; Nagy, A.; Semenkovich, C.F.; Gordon, J.I. The gut microbiota as an environmental factor that regulates fat storage. *Proceedings of the National Academy of Sciences - PNAS* **2004**, *101*, 15718-15723, doi:10.1073/pnas.0407076101 %J Proceedings of the National Academy of Sciences of the United States of America.
67. Bäckhed, F.; Manchester, J.K.; Semenkovich, C.F.; Gordon, J.I. Mechanisms underlying the resistance to diet-induced obesity in germ-free mice. *Proceedings of the National Academy of Sciences of the United States of America* **2007**, *104*, 979-984, doi:10.1073/pnas.0605374104.
68. Flier, J.S.; Mekalanos, J.J. Gut check: testing a role for the intestinal microbiome in human obesity. *Science translational medicine* **2009**, *1*, 6ps7, doi:10.1126/scitranslmed.3000483.
69. Kim, K.A.; Gu, W.; Lee, I.A.; Joh, E.H.; Kim, D.H. High fat diet-induced gut microbiota exacerbates inflammation and obesity in mice via the TLR4 signaling pathway. *PloS one* **2012**, *7*, e47713, doi:10.1371/journal.pone.0047713.
70. Shen, W.; Wolf, P.G.; Carbonero, F.; Zhong, W.; Reid, T.; Gaskins, H.R.; McIntosh, M.K. Intestinal and systemic inflammatory responses are positively associated with sulfidogenic bacteria abundance in high-fat-fed male C57BL/6J mice. *The Journal of nutrition* **2014**, *144*, 1181-1187, doi:10.3945/jn.114.194332.
71. Ding, S.; Chi, M.M.; Scull, B.P.; Rigby, R.; Schwerbrock, N.M.; Magness, S.; Jobin, C.; Lund, P.K. High-fat diet: bacteria interactions promote intestinal inflammation which precedes and correlates with obesity and insulin resistance in mouse. *PloS one* **2010**, *5*, e12191, doi:10.1371/journal.pone.0012191.
72. Cani, P.D.; Bibiloni, R.; Knauf, C.; Waget, A.; Neyrinck, A.M.; Delzenne, N.M.; Burcelin, R. Changes in gut microbiota control metabolic endotoxemia-induced inflammation in high-fat diet-induced obesity and diabetes in mice. *Diabetes* **2008**, *57*, 1470-1481, doi:10.2337/db07-1403.
73. Brown, K.; DeCoffe, D.; Molcan, E.; Gibson, D.L. Diet-induced dysbiosis of the intestinal microbiota and the effects on immunity and disease. *Nutrients* **2012**, *4*, 1095-1119, doi:10.3390/nu4081095.
74. Schulz, M.D.; Atay, Ç.; Heringer, J.; Romrig, F.K.; Schwitalla, S.; Aydin, B.; Ziegler, P.K.; Varga, J.; Reindl, W.; Pommerenke, C.; Salinas-Riester, G.; Böck, A.; Alpert, C.; Blaut, M.; Polson, S.C.; Brandl, L.; Kirchner, T.; Greten, F.R.; Polson, S.W.; Arkan, M.C. High-fat-diet-mediated dysbiosis promotes intestinal carcinogenesis independently of obesity. *Nature* **2014**, *514*, 508-512, doi:10.1038/nature13398.
75. Jackson, A.D.; McLaughlin, J. Digestion and absorption. *Surgery (Oxford)* **2009**, *27*, 231-236, doi:https://doi.org/10.1016/j.mpsur.2009.03.003.

76. Chiang, J.Y. Bile acid metabolism and signaling. *Comprehensive Physiology* **2013**, *3*, 1191-1212, doi:10.1002/cphy.c120023.
77. Mariadason, J.M.; Nicholas, C.; L'Italien, K.E.; Zhuang, M.; Smartt, H.J.; Heerdt, B.G.; Yang, W.; Corner, G.A.; Wilson, A.J.; Klampfer, L.; Arango, D.; Augenlicht, L.H. Gene expression profiling of intestinal epithelial cell maturation along the crypt-villus axis. *Gastroenterology* **2005**, *128*, 1081-1088, doi:10.1053/j.gastro.2005.01.054.
78. D'Aquila, T.; Hung, Y.H.; Carreiro, A.; Buhman, K.K. Recent discoveries on absorption of dietary fat: Presence, synthesis, and metabolism of cytoplasmic lipid droplets within enterocytes. *Biochimica et biophysica acta* **2016**, *1861*, 730-747, doi:10.1016/j.bbalip.2016.04.012.
79. Mansbach, C.M., 2nd; Gorelick, F. Development and physiological regulation of intestinal lipid absorption. II. Dietary lipid absorption, complex lipid synthesis, and the intracellular packaging and secretion of chylomicrons. *American journal of physiology. Gastrointestinal and liver physiology* **2007**, *293*, G645-650, doi:10.1152/ajpgi.00299.2007.
80. Ho, S.Y.; Storch, J. Common mechanisms of monoacylglycerol and fatty acid uptake by human intestinal Caco-2 cells. *American journal of physiology. Cell physiology* **2001**, *281*, C1106-1117, doi:10.1152/ajpcell.2001.281.4.C1106.
81. Murota, K.; Storch, J. Uptake of micellar long-chain fatty acid and sn-2-monoacylglycerol into human intestinal Caco-2 cells exhibits characteristics of protein-mediated transport. *The Journal of nutrition* **2005**, *135*, 1626-1630, doi:10.1093/jn/135.7.1626.
82. Binnert, C.; Pachiaudi, C.; Beylot, M.; Croset, M.; Cohen, R.; Riou, J.P.; Laville, M. Metabolic fate of an oral long-chain triglyceride load in humans. *The American journal of physiology* **1996**, *270*, E445-450, doi:10.1152/ajpendo.1996.270.3.E445.
83. Caspary, W.F. Physiology and pathophysiology of intestinal absorption. *The American journal of clinical nutrition* **1992**, *55*, 299s-308s, doi:10.1093/ajcn/55.1.299s.
84. Storch, J.; Thumser, A.E. Tissue-specific functions in the fatty acid-binding protein family. *The Journal of biological chemistry* **2010**, *285*, 32679-32683, doi:10.1074/jbc.R110.135210.
85. Mashek, D.G.; Li, L.O.; Coleman, R.A. Rat long-chain acyl-CoA synthetase mRNA, protein, and activity vary in tissue distribution and in response to diet. *Journal of lipid research* **2006**, *47*, 2004-2010, doi:10.1194/jlr.M600150-JLR200.
86. Milger, K.; Herrmann, T.; Becker, C.; Gotthardt, D.; Zickwolf, J.; Ehehalt, R.; Watkins, P.A.; Stremmel, W.; Füllekrug, J. Cellular uptake of fatty acids driven by the ER-localized acyl-CoA synthetase FATP4. **2006**, *119*, 4678-4688, doi:10.1242/jcs.03280 %J Journal of Cell Science.
87. Coleman, R.A.; Haynes, E.B. Monoacylglycerol acyltransferase. Evidence that the activities from rat intestine and suckling liver are tissue-specific isoenzymes. *The Journal of biological chemistry* **1986**, *261*, 224-228.
88. Yen, C.L.; Nelson, D.W.; Yen, M.I. Intestinal triacylglycerol synthesis in fat absorption and systemic energy metabolism. *Journal of lipid research* **2015**, *56*, 489-501, doi:10.1194/jlr.R052902.
89. Yen, C.L.; Stone, S.J.; Koliwad, S.; Harris, C.; Farese, R.V., Jr. Thematic review series: glycerolipids. DGAT enzymes and triacylglycerol biosynthesis. *Journal of lipid research* **2008**, *49*, 2283-2301, doi:10.1194/jlr.R800018-JLR200.
90. Siddiqi, S.; Saleem, U.; Abumrad, N.A.; Davidson, N.O.; Storch, J.; Siddiqi, S.A.; Mansbach, C.M., 2nd. A novel multiprotein complex is required to generate the

prechylomicron transport vesicle from intestinal ER. *Journal of lipid research* **2010**, *51*, 1918-1928, doi:10.1194/jlr.M005611.

91. Neeli, I.; Siddiqi, S.A.; Siddiqi, S.; Mahan, J.; Lagakos, W.S.; Binas, B.; Gheyi, T.; Storch, J.; Mansbach, C.M., 2nd. Liver fatty acid-binding protein initiates budding of pre-chylomicron transport vesicles from intestinal endoplasmic reticulum. *The Journal of biological chemistry* **2007**, *282*, 17974-17984, doi:10.1074/jbc.M610765200.
92. Mansbach, C.M.; Siddiqi, S.A. The biogenesis of chylomicrons. *Annual review of physiology* **2010**, *72*, 315-333, doi:10.1146/annurev-physiol-021909-135801.
93. Auclair, N.; Melbouci, L.; St-Pierre, D.; Levy, E. Gastrointestinal factors regulating lipid droplet formation in the intestine. *Experimental cell research* **2018**, *363*, 1-14, doi:10.1016/j.yexcr.2017.12.031.
94. Harayama, T.; Riezman, H. Understanding the diversity of membrane lipid composition. *Nature Reviews Molecular Cell Biology* **2018**, *19*, 281-296, doi:10.1038/nrm.2017.138.
95. Storch, J.; Zhou, Y.X.; Lagakos, W.S. Metabolism of apical versus basolateral sn-2-monoacylglycerol and fatty acids in rodent small intestine. *Journal of lipid research* **2008**, *49*, 1762-1769, doi:10.1194/jlr.M800116-JLR200.
96. Gangl, A.; Ockner, R.K.J.T.J.o.c.i. Intestinal metabolism of plasma free fatty acids. Intracellular compartmentation and mechanisms of control. **1975**, *55*, 803-813.
97. Varga, T.; Czimmerer, Z.; Nagy, L. PPARs are a unique set of fatty acid regulated transcription factors controlling both lipid metabolism and inflammation. *Biochimica et Biophysica Acta (BBA) - Molecular Basis of Disease* **2011**, *1812*, 1007-1022, doi:https://doi.org/10.1016/j.bbadis.2011.02.014.
98. Gupta, A. Digestion and Absorption of Lipids. In *Comprehensive Biochemistry for Dentistry: Textbook for Dental Students*, Springer Singapore: Singapore, 2019; 10.1007/978-981-13-1035-5_16pp. 441-450.
99. Olivecrona, G. Role of lipoprotein lipase in lipid metabolism. *Current opinion in lipidology* **2016**, *27*, 233-241, doi:10.1097/mol.0000000000000297.
100. Goldberg, I.J.; Ginsberg, H.N. Ins and outs modulating hepatic triglyceride and development of nonalcoholic fatty liver disease. *Gastroenterology* **2006**, *130*, 1343-1346, doi:10.1053/j.gastro.2006.02.040.
101. Bloemen, J.G.; Venema, K.; van de Poll, M.C.; Olde Damink, S.W.; Buurman, W.A.; Dejong, C.H. Short chain fatty acids exchange across the gut and liver in humans measured at surgery. *Clinical nutrition (Edinburgh, Scotland)* **2009**, *28*, 657-661, doi:10.1016/j.clnu.2009.05.011.
102. Schönfeld, P.; Wojtczak, L. Short- and medium-chain fatty acids in energy metabolism: the cellular perspective. *Journal of lipid research* **2016**, *57*, 943-954, doi:10.1194/jlr.R067629.
103. Mitra, V.; Metcalf, J. Metabolic functions of the liver. *Anaesthesia & Intensive Care Medicine* **2012**, *13*, 54-55, doi:https://doi.org/10.1016/j.mpaic.2011.11.006.
104. Ben-Moshe, S.; Itzkovitz, S. Spatial heterogeneity in the mammalian liver. *Nature Reviews Gastroenterology & Hepatology* **2019**, *16*, 395-410, doi:10.1038/s41575-019-0134-x.
105. Kalra, A.; Yetiskul, E.; Wehrle, C.J.; Tuma, F.J.S. Physiology, liver. **2020**.
106. Krishna, M. Microscopic anatomy of the liver. *Clinical liver disease* **2013**, *2*, S4-s7, doi:10.1002/cld.147.
107. Naito, M.; Hasegawa, G.; Ebe, Y.; Yamamoto, T.J.M.E.M. Differentiation and function of Kupffer cells. **2004**, *37*, 16-28.
108. Wang, Y.; Zhang, C. The Roles of Liver-Resident Lymphocytes in Liver Diseases. **2019**, *10*, doi:10.3389/fimmu.2019.01582.

109. Blaner, W.S.; O'Byrne, S.M.; Wongsiriroj, N.; Kluwe, J.; D'Ambrosio, D.M.; Jiang, H.; Schwabe, R.F.; Hillman, E.M.C.; Piantedosi, R.; Libien, J. Hepatic stellate cell lipid droplets: A specialized lipid droplet for retinoid storage. *Biochimica et Biophysica Acta (BBA) - Molecular and Cell Biology of Lipids* **2009**, *1791*, 467-473, doi:https://doi.org/10.1016/j.bbalip.2008.11.001.
110. Friedman, S.L. Mechanisms of hepatic fibrogenesis. *Gastroenterology* **2008**, *134*, 1655-1669, doi:10.1053/j.gastro.2008.03.003.
111. Berlanga, A.; Guiu-Jurado, E.; Porras, J.A.; Auguet, T. Molecular pathways in non-alcoholic fatty liver disease. *Clinical and experimental gastroenterology* **2014**, *7*, 221-239, doi:10.2147/ceg.S62831.
112. Enjoji, M.; Kohjima, M.; Nakamuta, M. Lipid Metabolism and the Liver. In *The Liver in Systemic Diseases*, Ohira, H., Ed. Springer Japan: Tokyo, 2016; 10.1007/978-4-431-55790-6_6pp. 105-122.
113. Chabowski, A.; Górski, J.; Luiken, J.J.; Glatz, J.F.; Bonen, A. Evidence for concerted action of FAT/CD36 and FABPpm to increase fatty acid transport across the plasma membrane. *Prostaglandins, leukotrienes, and essential fatty acids* **2007**, *77*, 345-353, doi:10.1016/j.plefa.2007.10.017.
114. Ibrahimi, A.; Abumrad, N.A. Role of CD36 in membrane transport of long-chain fatty acids. *Current opinion in clinical nutrition and metabolic care* **2002**, *5*, 139-145, doi:10.1097/00075197-200203000-00004.
115. Isola, L.M.; Zhou, S.L.; Kiang, C.L.; Stump, D.D.; Bradbury, M.W.; Berk, P.D. 3T3 fibroblasts transfected with a cDNA for mitochondrial aspartate aminotransferase express plasma membrane fatty acid-binding protein and saturable fatty acid uptake. *Proceedings of the National Academy of Sciences of the United States of America* **1995**, *92*, 9866-9870, doi:10.1073/pnas.92.21.9866.
116. Donnelly, K.L.; Smith, C.I.; Schwarzenberg, S.J.; Jessurun, J.; Boldt, M.D.; Parks, E.J. Sources of fatty acids stored in liver and secreted via lipoproteins in patients with nonalcoholic fatty liver disease. *The Journal of clinical investigation* **2005**, *115*, 1343-1351, doi:10.1172/jci23621.
117. Sanders, F.W.; Griffin, J.L. De novo lipogenesis in the liver in health and disease: more than just a shunting yard for glucose. *Biological reviews of the Cambridge Philosophical Society* **2016**, *91*, 452-468, doi:10.1111/brv.12178.
118. Wolf, G. Nutritional and hormonal regulation of fatty acid synthase. *Nutrition reviews* **1996**, *54*, 122-123, doi:10.1111/j.1753-4887.1996.tb03886.x.
119. Martin, G.G.; Huang, H.; Atshaves, B.P.; Binas, B.; Schroeder, F. Ablation of the liver fatty acid binding protein gene decreases fatty acyl CoA binding capacity and alters fatty acyl CoA pool distribution in mouse liver. *Biochemistry* **2003**, *42*, 11520-11532, doi:10.1021/bi0346749.
120. Burrier, R.E.; Manson, C.R.; Brecher, P. Binding of acyl-CoA to liver fatty acid binding protein: effect on acyl-CoA synthesis. *Biochimica et biophysica acta* **1987**, *919*, 221-230, doi:10.1016/0005-2760(87)90261-x.
121. Hubbell, T.; Behnke, W.D.; Woodford, J.K.; Schroeder, F. Recombinant liver fatty acid binding protein interacts with fatty acyl-coenzyme A. *Biochemistry* **1994**, *33*, 3327-3334, doi:10.1021/bi00177a025.
122. Ockner, R.K.; Manning, J.A.; Poppenhausen, R.B.; Ho, W.K. A binding protein for fatty acids in cytosol of intestinal mucosa, liver, myocardium, and other tissues. *Science (New York, N.Y.)* **1972**, *177*, 56-58, doi:10.1126/science.177.4043.56.
123. Frolov, A.; Cho, T.H.; Billheimer, J.T.; Schroeder, F. Sterol carrier protein-2, a new fatty acyl coenzyme A-binding protein. *The Journal of biological chemistry* **1996**, *271*, 31878-31884, doi:10.1074/jbc.271.50.31878.

124. Knebel, B.; Fahlbusch, P.; Dille, M.; Wahlers, N.; Hartwig, S.; Jacob, S.; Kettel, U.; Schiller, M.; Herebian, D.; Koellmer, C.; Lehr, S.; Müller-Wieland, D.; Kotzka, J. Fatty Liver Due to Increased de novo Lipogenesis: Alterations in the Hepatic Peroxisomal Proteome. **2019**, *7*, doi:10.3389/fcell.2019.00248.
125. Listenberger, L.L.; Han, X.; Lewis, S.E.; Cases, S.; Farese, R.V.; Ory, D.S.; Schaffer, J.E. Triglyceride accumulation protects against fatty acid-induced lipotoxicity. **2003**, *100*, 3077-3082, doi:10.1073/pnas.0630588100 %J Proceedings of the National Academy of Sciences.
126. Alves-Bezerra, M.; Cohen, D.E. Triglyceride Metabolism in the Liver. *Comprehensive Physiology* **2017**, *8*, 1-8, doi:10.1002/cphy.c170012.
127. Coleman, R.A.; Lewin, T.M.; Van Horn, C.G.; Gonzalez-Baró, M.R. Do long-chain acyl-CoA synthetases regulate fatty acid entry into synthetic versus degradative pathways? *The Journal of nutrition* **2002**, *132*, 2123-2126, doi:10.1093/jn/132.8.2123.
128. Mashek, D.G.; Li, L.O.; Coleman, R.A. Long-chain acyl-CoA synthetases and fatty acid channeling. *Future lipidology* **2007**, *2*, 465-476, doi:10.2217/17460875.2.4.465.
129. Yan, S.; Yang, X.F.; Liu, H.L.; Fu, N.; Ouyang, Y.; Qing, K. Long-chain acyl-CoA synthetase in fatty acid metabolism involved in liver and other diseases: an update. *World journal of gastroenterology* **2015**, *21*, 3492-3498, doi:10.3748/wjg.v21.i12.3492.
130. Reshef, L.; Olswang, Y.; Cassuto, H.; Blum, B.; Croniger, C.M.; Kalhan, S.C.; Tilghman, S.M.; Hanson, R.W. Glyceroneogenesis and the triglyceride/fatty acid cycle. *The Journal of biological chemistry* **2003**, *278*, 30413-30416, doi:10.1074/jbc.R300017200.
131. Yang, M.; Nickels, J.T. MOGAT2: A New Therapeutic Target for Metabolic Syndrome. *Diseases (Basel, Switzerland)* **2015**, *3*, 176-192, doi:10.3390/diseases3030176.
132. Ipsen, D.H.; Lykkesfeldt, J.; Tveden-Nyborg, P. Molecular mechanisms of hepatic lipid accumulation in non-alcoholic fatty liver disease. *Cellular and molecular life sciences : CMLS* **2018**, *75*, 3313-3327, doi:10.1007/s00018-018-2860-6.
133. Fisher, E.A.; Ginsberg, H.N. Complexity in the secretory pathway: the assembly and secretion of apolipoprotein B-containing lipoproteins. *The Journal of biological chemistry* **2002**, *277*, 17377-17380, doi:10.1074/jbc.R100068200.
134. Yao, Z.; Wang, Y. Apolipoprotein C-III and hepatic triglyceride-rich lipoprotein production. *Current opinion in lipidology* **2012**, *23*, 206-212, doi:10.1097/MOL.0b013e328352dc70.
135. Cohen, D.E.; Fisher, E.A. Lipoprotein metabolism, dyslipidemia, and nonalcoholic fatty liver disease. *Seminars in liver disease* **2013**, *33*, 380-388, doi:10.1055/s-0033-1358519.
136. Merkel, M.; Kako, Y.; Radner, H.; Cho, I.S.; Ramasamy, R.; Brunzell, J.D.; Goldberg, I.J.; Breslow, J.L. Catalytically inactive lipoprotein lipase expression in muscle of transgenic mice increases very low density lipoprotein uptake: direct evidence that lipoprotein lipase bridging occurs in vivo. *Proceedings of the National Academy of Sciences of the United States of America* **1998**, *95*, 13841-13846, doi:10.1073/pnas.95.23.13841.
137. Diraison, F.; Moulin, P.; Beylot, M. Contribution of hepatic de novo lipogenesis and reesterification of plasma non esterified fatty acids to plasma triglyceride synthesis during non-alcoholic fatty liver disease. *Diabetes & Metabolism* **2003**, *29*, 478-485, doi:https://doi.org/10.1016/S1262-3636(07)70061-7.

138. Schonfeld, G.; Pfleger, B. Utilization of exogenous free fatty acids for the production of very low density lipoprotein triglyceride by livers of carbohydrate-fed rats. *Journal of lipid research* **1971**, *12*, 614-621.
139. Wiegman, C.H.; Bandsma, R.H.; Ouwens, M.; van der Sluijs, F.H.; Havinga, R.; Boer, T.; Reijngoud, D.J.; Romijn, J.A.; Kuipers, F. Hepatic VLDL production in ob/ob mice is not stimulated by massive de novo lipogenesis but is less sensitive to the suppressive effects of insulin. *Diabetes* **2003**, *52*, 1081-1089, doi:10.2337/diabetes.52.5.1081.
140. Bandsma, R.H.; Wiegman, C.H.; Herling, A.W.; Burger, H.J.; ter Harmsel, A.; Meijer, A.J.; Romijn, J.A.; Reijngoud, D.J.; Kuipers, F. Acute inhibition of glucose-6-phosphate translocator activity leads to increased de novo lipogenesis and development of hepatic steatosis without affecting VLDL production in rats. *Diabetes* **2001**, *50*, 2591-2597, doi:10.2337/diabetes.50.11.2591.
141. Begriche, K.; Igoudjil, A.; Pessayre, D.; Fromenty, B. Mitochondrial dysfunction in NASH: causes, consequences and possible means to prevent it. *Mitochondrion* **2006**, *6*, 1-28, doi:10.1016/j.mito.2005.10.004.
142. Wanders, R.J.A.; Waterham, H.R.; Ferdinandusse, S. Metabolic Interplay between Peroxisomes and Other Subcellular Organelles Including Mitochondria and the Endoplasmic Reticulum. **2016**, *3*, doi:10.3389/fcell.2015.00083.
143. Schrader, M.; Costello, J.; Godinho, L.F.; Islinger, M. Peroxisome-mitochondria interplay and disease. *Journal of inherited metabolic disease* **2015**, *38*, 681-702, doi:10.1007/s10545-015-9819-7.
144. Grevengoed, T.J.; Klett, E.L.; Coleman, R.A. Acyl-CoA metabolism and partitioning. *Annual review of nutrition* **2014**, *34*, 1-30, doi:10.1146/annurev-nutr-071813-105541.
145. Hardwick, J.P. Cytochrome P450 omega hydroxylase (CYP4) function in fatty acid metabolism and metabolic diseases. *Biochemical Pharmacology* **2008**, *75*, 2263-2275, doi:https://doi.org/10.1016/j.bcp.2008.03.004.
146. Hostetler, H.A.; McIntosh, A.L.; Atshaves, B.P.; Storey, S.M.; Payne, H.R.; Kier, A.B.; Schroeder, F. L-FABP directly interacts with PPARalpha in cultured primary hepatocytes. *Journal of lipid research* **2009**, *50*, 1663-1675, doi:10.1194/jlr.M900058-JLR200.
147. Lefebvre, P.; Chinetti, G.; Fruchart, J.C.; Staels, B. Sorting out the roles of PPAR alpha in energy metabolism and vascular homeostasis. *The Journal of clinical investigation* **2006**, *116*, 571-580, doi:10.1172/jci27989.
148. Lewis, G.F.; Carpentier, A.; Adeli, K.; Giacca, A. Disordered fat storage and mobilization in the pathogenesis of insulin resistance and type 2 diabetes. *Endocrine reviews* **2002**, *23*, 201-229, doi:10.1210/edrv.23.2.0461.
149. Postic, C.; Girard, J. Contribution of de novo fatty acid synthesis to hepatic steatosis and insulin resistance: lessons from genetically engineered mice. *The Journal of clinical investigation* **2008**, *118*, 829-838, doi:10.1172/jci34275.
150. Ockner, R.K.; Manning, J.A. Fatty acid-binding protein in small intestine. Identification, isolation, and evidence for its role in cellular fatty acid transport. *The Journal of clinical investigation* **1974**, *54*, 326-338, doi:10.1172/jci107768.
151. Coe, N.R.; Bernlohr, D.A. Physiological properties and functions of intracellular fatty acid-binding proteins. *Biochimica et biophysica acta* **1998**, *1391*, 287-306, doi:10.1016/s0005-2760(97)00205-1.
152. Banaszak, L.; Winter, N.; Xu, Z.; Bernlohr, D.A.; Cowan, S.; Jones, T.A. Lipid-binding proteins: a family of fatty acid and retinoid transport proteins. *Advances in protein chemistry* **1994**, *45*, 89-151, doi:10.1016/s0065-3233(08)60639-7.

153. Bass, N.M. Cellular binding proteins for fatty acids and retinoids: similar or specialized functions? *Molecular and cellular biochemistry* **1993**, *123*, 191-202, doi:10.1007/bf01076492.
154. Börchers, T.; Spener, F. Fatty acid binding proteins. *Current topics in membranes* **1994**, *40*, 261-294.
155. Hertzel, A.V.; Bernlohr, D.A. The mammalian fatty acid-binding protein multigene family: molecular and genetic insights into function. *Trends in endocrinology and metabolism: TEM* **2000**, *11*, 175-180, doi:10.1016/s1043-2760(00)00257-5.
156. Furuhashi, M.; Hotamisligil, G.S. Fatty acid-binding proteins: role in metabolic diseases and potential as drug targets. *Nature Reviews Drug Discovery* **2008**, *7*, 489-503, doi:10.1038/nrd2589.
157. Makowski, L.; Hotamisligil, G.S. Fatty acid binding proteins--the evolutionary crossroads of inflammatory and metabolic responses. *The Journal of nutrition* **2004**, *134*, 2464s-2468s, doi:10.1093/jn/134.9.2464S.
158. Storch, J.; Corsico, B. The emerging functions and mechanisms of mammalian fatty acid-binding proteins. *Annual review of nutrition* **2008**, *28*, 73-95, doi:10.1146/annurev.nutr.27.061406.093710.
159. Storch, J.; Herr, F. Nutritional Regulation of Fatty Acid Transport Protein Expression. 2001; 10.1201/9781420039108-6pp. 101-130.
160. Ockner, R.K.; Lysenko, N.; Manning, J.A.; Monroe, S.E.; Burnett, D.A. Sex steroid modulation of fatty acid utilization and fatty acid binding protein concentration in rat liver. *The Journal of clinical investigation* **1980**, *65*, 1013-1023, doi:10.1172/jci109753.
161. Ockner, R.K.; Burnett, D.A.; Lysenko, N.; Manning, J.A. Sex differences in long chain fatty acid utilization and fatty acid binding protein concentration in rat liver. *The Journal of clinical investigation* **1979**, *64*, 172-181, doi:10.1172/jci109437.
162. Gajda, A.M.; Zhou, Y.X.; Agellon, L.B.; Fried, S.K.; Kodukula, S.; Fortson, W.; Patel, K.; Storch, J. Direct comparison of mice null for liver or intestinal fatty acid-binding proteins reveals highly divergent phenotypic responses to high fat feeding. *The Journal of biological chemistry* **2013**, *288*, 30330-30344, doi:10.1074/jbc.M113.501676.
163. Lagakos, W.S.; Gajda, A.M.; Agellon, L.; Binas, B.; Choi, V.; Mandap, B.; Russnak, T.; Zhou, Y.X.; Storch, J. Different functions of intestinal and liver-type fatty acid-binding proteins in intestine and in whole body energy homeostasis. *American journal of physiology. Gastrointestinal and liver physiology* **2011**, *300*, G803-814, doi:10.1152/ajpgi.00229.2010.
164. Mishkin, S.; Stein, L.; Gatmaitan, Z.; Arias, I.M. The binding of fatty acids to cytoplasmic proteins: binding to Z protein in liver and other tissues of the rat. *Biochemical and biophysical research communications* **1972**, *47*, 997-1003, doi:10.1016/0006-291x(72)90931-x.
165. Newberry, E.P.; Xie, Y.; Lodeiro, C.; Solis, R.; Moritz, W.; Kennedy, S.; Barron, L.; Onufer, E.; Alpini, G.; Zhou, T.; Blaner, W.S.; Chen, A.; Davidson, N.O. Hepatocyte and stellate cell deletion of liver fatty acid binding protein reveals distinct roles in fibrogenic injury. *FASEB journal : official publication of the Federation of American Societies for Experimental Biology* **2019**, *33*, 4610-4625, doi:10.1096/fj.201801976R.
166. Chen, A.; Tang, Y.; Davis, V.; Hsu, F.F.; Kennedy, S.M.; Song, H.; Turk, J.; Brunt, E.M.; Newberry, E.P.; Davidson, N.O. Liver fatty acid binding protein (L-Fabp) modulates murine stellate cell activation and diet-induced nonalcoholic fatty liver disease. *Hepatology (Baltimore, Md.)* **2013**, *57*, 2202-2212, doi:10.1002/hep.26318.

167. Pelsers, M.M.A.L.; Namiot, Z.; Kisielewski, W.; Namiot, A.; Januszkiewicz, M.; Hermens, W.T.; Glatz, J.F.C. Intestinal-type and liver-type fatty acid-binding protein in the intestine. Tissue distribution and clinical utility. *Clinical Biochemistry* **2003**, *36*, 529-535, doi:https://doi.org/10.1016/S0009-9120(03)00096-1.
168. Lowe, J.B.; Sacchettini, J.C.; Laposata, M.; McQuillan, J.J.; Gordon, J.I. Expression of rat intestinal fatty acid-binding protein in Escherichia coli. Purification and comparison of ligand binding characteristics with that of Escherichia coli-derived rat liver fatty acid-binding protein. *The Journal of biological chemistry* **1987**, *262*, 5931-5937.
169. Richieri, G.V.; Ogata, R.T.; Kleinfeld, A.M. Equilibrium constants for the binding of fatty acids with fatty acid-binding proteins from adipocyte, intestine, heart, and liver measured with the fluorescent probe ADIFAB. *The Journal of biological chemistry* **1994**, *269*, 23918-23930.
170. Lagakos, W.S.; Guan, X.; Ho, S.Y.; Sawicki, L.R.; Corsico, B.; Kodukula, S.; Murota, K.; Stark, R.E.; Storch, J. Liver fatty acid-binding protein binds monoacylglycerol in vitro and in mouse liver cytosol. *The Journal of biological chemistry* **2013**, *288*, 19805-19815, doi:10.1074/jbc.M113.473579.
171. Huang, H.; McIntosh, A.L.; Martin, G.G.; Landrock, D.; Chung, S.; Landrock, K.K.; Dangott, L.J.; Li, S.; Kier, A.B.; Schroeder, F. FABP1: A Novel Hepatic Endocannabinoid and Cannabinoid Binding Protein. *Biochemistry* **2016**, *55*, 5243-5255, doi:10.1021/acs.biochem.6b00446.
172. Thumser, A.E.; Voysey, J.E.; Wilton, D.C. The binding of lysophospholipids to rat liver fatty acid-binding protein and albumin. *The Biochemical journal* **1994**, *301 (Pt 3)*, 801-806, doi:10.1042/bj3010801.
173. Thumser, A.E.; Wilton, D.C. The binding of cholesterol and bile salts to recombinant rat liver fatty acid-binding protein. *The Biochemical journal* **1996**, *320 (Pt 3)*, 729-733, doi:10.1042/bj3200729.
174. Wolfrum, C.; Börchers, T.; Sacchettini, J.C.; Spener, F. Binding of Fatty Acids and Peroxisome Proliferators to Orthologous Fatty Acid Binding Proteins from Human, Murine, and Bovine Liver. *Biochemistry* **2000**, *39*, 1469-1474, doi:10.1021/bi991638u.
175. Hsu, K.T.; Storch, J. Fatty acid transfer from liver and intestinal fatty acid-binding proteins to membranes occurs by different mechanisms. *The Journal of biological chemistry* **1996**, *271*, 13317-13323, doi:10.1074/jbc.271.23.13317.
176. Ockner, R.K.; Manning, J.A.; Kane, J.P. Fatty acid binding protein. Isolation from rat liver, characterization, and immunochemical quantification. *The Journal of biological chemistry* **1982**, *257*, 7872-7878.
177. Atshaves, B.P.; McIntosh, A.M.; Lyuksyutova, O.I.; Zipfel, W.; Webb, W.W.; Schroeder, F. Liver fatty acid-binding protein gene ablation inhibits branched-chain fatty acid metabolism in cultured primary hepatocytes. *The Journal of biological chemistry* **2004**, *279*, 30954-30965, doi:10.1074/jbc.M313571200.
178. Atshaves, B.P.; Storey, S.M.; Huang, H.; Schroeder, F. Liver fatty acid binding protein expression enhances branched-chain fatty acid metabolism. *Molecular and cellular biochemistry* **2004**, *259*, 115-129, doi:10.1023/b:mcbi.0000021357.97765.f2.
179. Martin, G.G.; Danneberg, H.; Kumar, L.S.; Atshaves, B.P.; Erol, E.; Bader, M.; Schroeder, F.; Binas, B. Decreased liver fatty acid binding capacity and altered liver lipid distribution in mice lacking the liver fatty acid-binding protein gene. *The Journal of biological chemistry* **2003**, *278*, 21429-21438, doi:10.1074/jbc.M300287200.

180. Murphy, E.J.; Prows, D.R.; Jefferson, J.R.; Schroeder, F. Liver fatty acid-binding protein expression in transfected fibroblasts stimulates fatty acid uptake and metabolism. *Biochimica et biophysica acta* **1996**, *1301*, 191-198, doi:10.1016/0005-2760(96)00024-0.
181. Jolly, C.A.; Hubbell, T.; Behnke, W.D.; Schroeder, F. Fatty acid binding protein: stimulation of microsomal phosphatidic acid formation. *Archives of biochemistry and biophysics* **1997**, *341*, 112-121, doi:10.1006/abbi.1997.9957.
182. Atshaves, B.P.; Martin, G.G.; Hostetler, H.A.; McIntosh, A.L.; Kier, A.B.; Schroeder, F. Liver fatty acid-binding protein and obesity. *The Journal of nutritional biochemistry* **2010**, *21*, 1015-1032, doi:10.1016/j.jnutbio.2010.01.005.
183. Tan, N.S.; Shaw, N.S.; Vinckenbosch, N.; Liu, P.; Yasmin, R.; Desvergne, B.; Wahli, W.; Noy, N. Selective cooperation between fatty acid binding proteins and peroxisome proliferator-activated receptors in regulating transcription. *Molecular and cellular biology* **2002**, *22*, 5114-5127, doi:10.1128/mcb.22.14.5114-5127.2002.
184. Hughes, M.L.; Liu, B.; Halls, M.L.; Wagstaff, K.M.; Patil, R.; Velkov, T.; Jans, D.A.; Bunnett, N.W.; Scanlon, M.J.; Porter, C.J. Fatty Acid-binding Proteins 1 and 2 Differentially Modulate the Activation of Peroxisome Proliferator-activated Receptor α in a Ligand-selective Manner. *The Journal of biological chemistry* **2015**, *290*, 13895-13906, doi:10.1074/jbc.M114.605998.
185. McIntosh, A.L.; Atshaves, B.P.; Hostetler, H.A.; Huang, H.; Davis, J.; Lyuksyutova, O.I.; Landrock, D.; Kier, A.B.; Schroeder, F. Liver type fatty acid binding protein (L-FABP) gene ablation reduces nuclear ligand distribution and peroxisome proliferator-activated receptor-alpha activity in cultured primary hepatocytes. *Archives of biochemistry and biophysics* **2009**, *485*, 160-173, doi:10.1016/j.abb.2009.03.004.
186. McIntosh, A.L.; Petrescu, A.D.; Hostetler, H.A.; Kier, A.B.; Schroeder, F. Liver-type fatty acid binding protein interacts with hepatocyte nuclear factor 4α. *FEBS letters* **2013**, *587*, 3787-3791, doi:10.1016/j.febslet.2013.09.043.
187. Babeu, J.P.; Boudreau, F. Hepatocyte nuclear factor 4-alpha involvement in liver and intestinal inflammatory networks. *World journal of gastroenterology* **2014**, *20*, 22-30, doi:10.3748/wjg.v20.i1.22.
188. Erol, E.; Kumar, L.S.; Cline, G.W.; Shulman, G.I.; Kelly, D.P.; Binas, B. Liver fatty acid binding protein is required for high rates of hepatic fatty acid oxidation but not for the action of PPARalpha in fasting mice. *FASEB journal : official publication of the Federation of American Societies for Experimental Biology* **2004**, *18*, 347-349, doi:10.1096/fj.03-0330fje.
189. Newberry, E.P.; Xie, Y.; Kennedy, S.; Han, X.; Buhman, K.K.; Luo, J.; Gross, R.W.; Davidson, N.O. Decreased hepatic triglyceride accumulation and altered fatty acid uptake in mice with deletion of the liver fatty acid-binding protein gene. *The Journal of biological chemistry* **2003**, *278*, 51664-51672, doi:10.1074/jbc.M309377200.
190. Wang, G.; Gong, Y.; Anderson, J.; Sun, D.; Minuk, G.; Roberts, M.S.; Burczynski, F.J. Antioxidative function of L-FABP in L-FABP stably transfected Chang liver cells. **2005**, *42*, 871-879, doi:https://doi.org/10.1002/hep.20857.
191. Agellon, L.B.; Toth, M.J.; Thomson, A.B. Intracellular lipid binding proteins of the small intestine. *Molecular and cellular biochemistry* **2002**, *239*, 79-82.
192. Alpers, D.H.; Bass, N.M.; Engle, M.J.; DeSchryver-Kecskemeti, K. Intestinal fatty acid binding protein may favor differential apical fatty acid binding in the intestine. *Biochimica et biophysica acta* **2000**, *1483*, 352-362, doi:10.1016/s1388-1981(99)00200-0.

193. Mansbach, C.M., 2nd; Siddiqi, S. Control of chylomicron export from the intestine. *American journal of physiology. Gastrointestinal and liver physiology* **2016**, *310*, G659-668, doi:10.1152/ajpgi.00228.2015.
194. Martin, G.G.; McIntosh, A.L.; Huang, H.; Gupta, S.; Atshaves, B.P.; Landrock, K.K.; Landrock, D.; Kier, A.B.; Schroeder, F. The human liver fatty acid binding protein T94A variant alters the structure, stability, and interaction with fibrates. *Biochemistry* **2013**, *52*, 9347-9357, doi:10.1021/bi401014k.
195. Peng, X.E.; Wu, Y.L.; Lu, Q.Q.; Hu, Z.J.; Lin, X. Two genetic variants in FABP1 and susceptibility to non-alcohol fatty liver disease in a Chinese population. *Gene* **2012**, *500*, 54-58, doi:10.1016/j.gene.2012.03.050.
196. McIntosh, A.L.; Huang, H.; Storey, S.M.; Landrock, K.K.; Landrock, D.; Petrescu, A.D.; Gupta, S.; Atshaves, B.P.; Kier, A.B.; Schroeder, F.J.A.J.o.P.-G.; Physiology, L. Human FABP1 T94A variant impacts fatty acid metabolism and PPAR-α activation in cultured human female hepatocytes. *Am J Physiol-Gastr L* **2014**, *307*, G164-G176.
197. Brouillette, C.; Bossé, Y.; Pérusse, L.; Gaudet, D.; Vohl, M.C. Effect of liver fatty acid binding protein (FABP) T94A missense mutation on plasma lipoprotein responsiveness to treatment with fenofibrate. *Journal of human genetics* **2004**, *49*, 424-432, doi:10.1007/s10038-004-0171-2.
198. Le, T.; Gong, Y.; Davies, N.M.; Lillico, R.; Lakowski, T.; Roberts, M.S.; Burczynski, F.J. The Antioxidant Activity of Recombinant Rat Hepatic Fatty Acid Binding Protein T94A Variant. *Journal of pharmacy & pharmaceutical sciences : a publication of the Canadian Society for Pharmaceutical Sciences, Societe canadienne des sciences pharmaceutiques* **2018**, *21*, 309s-324s, doi:10.18433/jpps30246.
199. Veerkamp, J.H.; Paulussen, R.J.A.; Peeters, R.A.; Maatman, R.G.H.J.; van Moerkerk, H.T.B.; van Kuppevelt, T.H.M.S.M. Detection, tissue distribution and (sub)cellular localization of fatty acid-binding protein types. *Molecular and cellular biochemistry* **1990**, *98*, 11-18, doi:10.1007/BF00231362.
200. Sacchettini, J.C.; Hauft, S.M.; Van Camp, S.L.; Cistola, D.P.; Gordon, J.I. Developmental and structural studies of an intracellular lipid binding protein expressed in the ileal epithelium. *The Journal of biological chemistry* **1990**, *265*, 19199-19207.
201. Shields, H.M.; Bates, M.L.; Bass, N.M.; Best, C.J.; Alpers, D.H.; Ockner, R.K. Light microscopic immunocytochemical localization of hepatic and intestinal types of fatty acid-binding proteins in rat small intestine. *Journal of lipid research* **1988**, *27*, 549-557, doi:https://doi.org/10.1016/S0022-2275(20)35193-2.
202. Richieri, G.V.; Ogata, R.T.; Zimmerman, A.W.; Veerkamp, J.H.; Kleinfeld, A.M. Fatty acid binding proteins from different tissues show distinct patterns of fatty acid interactions. *Biochemistry* **2000**, *39*, 7197-7204, doi:10.1021/bi000314z.
203. Lai, M.P.; Katz, F.S.; Bernard, C.; Storch, J.; Stark, R.E. Two fatty acid-binding proteins expressed in the intestine interact differently with endocannabinoids. *Protein science : a publication of the Protein Society* **2020**, *29*, 1606-1617, doi:10.1002/pro.3875.
204. Besnard, P.; Niot, I.; Poirier, H.; Clément, L.; Bernard, A. New insights into the fatty acid-binding protein (FABP) family in the small intestine. *Molecular and cellular biochemistry* **2002**, *239*, 139-147, doi:10.1023/A:1020505512364.
205. Baier, L.J.; Sacchettini, J.C.; Knowler, W.C.; Eads, J.; Paolisso, G.; Tataranni, P.A.; Mochizuki, H.; Bennett, P.H.; Bogardus, C.; Prochazka, M. An amino acid substitution in the human intestinal fatty acid binding protein is associated with

increased fatty acid binding, increased fat oxidation, and insulin resistance. *The Journal of clinical investigation* **1995**, *95*, 1281-1287, doi:10.1172/jci117778.

206. Levy, E.; Ménard, D.; Delvin, E.; Stan, S.; Mitchell, G.; Lambert, M.; Ziv, E.; Feoli-Fonseca, J.C.; Seidman, E. The polymorphism at codon 54 of the FABP2 gene increases fat absorption in human intestinal explants. *The Journal of biological chemistry* **2001**, *276*, 39679-39684, doi:10.1074/jbc.M105713200.
207. Baier, L.J.; Bogardus, C.; Sacchettini, J.C. A Polymorphism in the Human Intestinal Fatty Acid Binding Protein Alters Fatty Acid Transport across Caco-2 Cells (∗). *Journal of Biological Chemistry* **1996**, *271*, 10892-10896, doi:https://doi.org/10.1074/jbc.271.18.10892.
208. Khattab, S.A.; Abo-Elmatty, D.M.; Ghattas, M.H.; Mesbah, N.M.; Mehanna, E.T. Intestinal fatty acid binding protein Ala54Thr polymorphism is associated with peripheral atherosclerosis combined with type 2 diabetes mellitus. *Journal of diabetes* **2017**, *9*, 821-826, doi:10.1111/1753-0407.12496.
209. Guedj, K.; Uzzan, M.; Soudan, D.; Trichet, C.; Nicoletti, A.; Weiss, E.; Manceau, H.; Nuzzo, A.; Corcos, O.; Treton, X.; Peoc'h, K. I-FABP is decreased in COVID-19 patients, independently of the prognosis. *PloS one* **2021**, *16*, e0249799, doi:10.1371/journal.pone.0249799.
210. Reisinger, K.W.; Elst, M.; Derikx, J.P.M.; Nikkels, P.G.J.; de Vries, B.; Adriaanse, M.P.M.; Jellema, R.K.; Kramer, B.W.W.; Wolfs, T.G.A.M. Intestinal fatty acid–binding protein: a possible marker for gut maturation. *Pediatric Research* **2014**, *76*, 261-268, doi:10.1038/pr.2014.89.
211. Ng, E.W.; Poon, T.C.; Lam, H.S.; Cheung, H.M.; Ma, T.P.; Chan, K.Y.; Wong, R.P.; Leung, K.T.; Lam, M.M.; Li, K.; Ng, P.C. Gut-associated biomarkers L-FABP, I-FABP, and TFF3 and LIT score for diagnosis of surgical necrotizing enterocolitis in preterm infants. *Annals of surgery* **2013**, *258*, 1111-1118, doi:10.1097/SLA.0b013e318288ea96.
212. Newberry, E.P.; Xie, Y.; Kennedy, S.M.; Luo, J.; Davidson, N.O. Protection against Western diet-induced obesity and hepatic steatosis in liver fatty acid-binding protein knockout mice. *Hepatology (Baltimore, Md.)* **2006**, *44*, 1191-1205, doi:10.1002/hep.21369.
213. Atshaves, B.P.; McIntosh, A.L.; Storey, S.M.; Landrock, K.K.; Kier, A.B.; Schroeder, F. High dietary fat exacerbates weight gain and obesity in female liver fatty acid binding protein gene-ablated mice. *Lipids* **2010**, *45*, 97-110, doi:10.1007/s11745-009-3379-2.
214. McIntosh, A.L.; Atshaves, B.P.; Landrock, D.; Landrock, K.K.; Martin, G.G.; Storey, S.M.; Kier, A.B.; Schroeder, F. Liver fatty acid binding protein gene-ablation exacerbates weight gain in high-fat fed female mice. *Lipids* **2013**, *48*, 435-448, doi:10.1007/s11745-013-3777-3.
215. Atshaves, B.P.; McIntosh, A.L.; Payne, H.R.; Mackie, J.; Kier, A.B.; Schroeder, F. Effect of branched-chain fatty acid on lipid dynamics in mice lacking liver fatty acid binding protein gene. *American journal of physiology. Cell physiology* **2005**, *288*, C543-558, doi:10.1152/ajpcell.00359.2004.
216. Vassileva, G.; Huwyler, L.; Poirier, K.; Agellon, L.B.; Toth, M.J. The intestinal fatty acid binding protein is not essential for dietary fat absorption in mice. *FASEB journal : official publication of the Federation of American Societies for Experimental Biology* **2000**, *14*, 2040-2046, doi:10.1096/fj.99-0959com.
217. Douglass, J.D.; Malik, N.; Chon, S.H.; Wells, K.; Zhou, Y.X.; Choi, A.S.; Joseph, L.B.; Storch, J. Intestinal mucosal triacylglycerol accumulation secondary to decreased lipid secretion in obese and high fat fed mice. *Frontiers in physiology* **2012**, *3*, 25, doi:10.3389/fphys.2012.00025.

218. Uchida, A.; Whitsitt, M.C.; Eustaquio, T.; Slipchenko, M.N.; Leary, J.F.; Cheng, J.X.; Buhman, K.K. Reduced triglyceride secretion in response to an acute dietary fat challenge in obese compared to lean mice. *Frontiers in physiology* **2012**, *3*, 26, doi:10.3389/fphys.2012.00026.
219. Xu, H.; Gajda, A.M.; Zhou, Y.X.; Panetta, C.; Sifnakis, Z.; Fatima, A.; Henderson, G.C.; Storch, J. Muscle metabolic reprogramming underlies the resistance of liver fatty acid-binding protein (LFABP)-null mice to high-fat feeding-induced decline in exercise capacity. *The Journal of biological chemistry* **2019**, *294*, 15358-15372, doi:10.1074/jbc.RA118.006684.
220. Gonçalves, C.G.; Glade, M.J.; Meguid, M.M. Metabolically healthy obese individuals: Key protective factors. *Nutrition (Burbank, Los Angeles County, Calif.)* **2016**, *32*, 14-20, doi:10.1016/j.nut.2015.07.010.
221. Primeau, V.; Coderre, L.; Karelis, A.D.; Brochu, M.; Lavoie, M.E.; Messier, V.; Sladek, R.; Rabasa-Lhoret, R. Characterizing the profile of obese patients who are metabolically healthy. *Int J Obes (Lond)* **2011**, *35*, 971-981, doi:10.1038/ijo.2010.216.
222. Lackey, A.I.; Chen, T.; Zhou, Y.X.; Bottasso Arias, N.M.; Doran, J.M.; Zacharisen, S.M.; Gajda, A.M.; Jonsson, W.O.; Córsico, B.; Anthony, T.G.; Joseph, L.B.; Storch, J. Mechanisms underlying reduced weight gain in intestinal fatty acid-binding protein (IFABP) null mice. *American journal of physiology. Gastrointestinal and liver physiology* **2020**, *318*, G518-g530, doi:10.1152/ajpgi.00120.2019.
223. Cani, P.D.; Van Hul, M.; Lefort, C.; Depommier, C.; Rastelli, M.; Everard, A. Microbial regulation of organismal energy homeostasis. *Nat Metab* **2019**, *1*, 34-46, doi:10.1038/s42255-018-0017-4.
224. Ghazalpour, A.; Cespedes, I.; Bennett, B.J.; Allayee, H. Expanding role of gut microbiota in lipid metabolism. *Current opinion in lipidology* **2016**, *27*, 141-147, doi:10.1097/MOL.0000000000000278.
225. Ticinesi, A.; Lauretani, F.; Milani, C.; Nouvenne, A.; Tana, C.; Del Rio, D.; Maggio, M.; Ventura, M.; Meschi, T. Aging Gut Microbiota at the Cross-Road between Nutrition, Physical Frailty, and Sarcopenia: Is There a Gut-Muscle Axis? *Nutrients* **2017**, *9*, doi:10.3390/nu9121303.
226. Tang, J.; Wu, Q.; Li, Y.; Wu, X.; Wang, Y.; Zhu, L.; Shi, Y.; Bu, H.; Bao, J.; Xie, M. Construction of a general albumin promoter reporter system for real-time monitoring of the differentiation status of functional hepatocytes from stem cells in mouse, rat and human. *Biomedical reports* **2017**, *6*, 627-632, doi:10.3892/br.2017.905.
227. Zimmerman, A.W.; Veerkamp, J.H. New insights into the structure and function of fatty acid-binding proteins. *Cellular and molecular life sciences : CMLS* **2002**, *59*, 1096-1116, doi:10.1007/s00018-002-8490-y.
228. Gordon, J.I.; Elshourbagy, N.; Lowe, J.B.; Liao, W.S.; Alpers, D.H.; Taylor, J.M. Tissue specific expression and developmental regulation of two genes coding for rat fatty acid binding proteins. *The Journal of biological chemistry* **1985**, *260*, 1995-1998.
229. He, Y.; Yang, X.; Wang, H.; Estephan, R.; Francis, F.; Kodukula, S.; Storch, J.; Stark, R.E. Solution-state molecular structure of apo and oleate-liganded liver fatty acid-binding protein. *Biochemistry* **2007**, *46*, 12543-12556, doi:10.1021/bi701092r.
230. Gajda, A.M.; Storch, J. Enterocyte fatty acid-binding proteins (FABPs): different functions of liver and intestinal FABPs in the intestine. *Prostaglandins, leukotrienes, and essential fatty acids* **2015**, *93*, 9-16, doi:10.1016/j.plefa.2014.10.001.

231. Schoeler, M.; Caesar, R. Dietary lipids, gut microbiota and lipid metabolism. *Rev Endocr Metab Disord* **2019**, *20*, 461-472, doi:10.1007/s11154-019-09512-0.
232. Caesar, R.; Tremaroli, V.; Kovatcheva-Datchary, P.; Cani, P.D.; Backhed, F. Crosstalk between Gut Microbiota and Dietary Lipids Aggravates WAT Inflammation through TLR Signaling. *Cell Metab* **2015**, *22*, 658-668, doi:10.1016/j.cmet.2015.07.026.
233. Lam, Y.Y.; Ha, C.W.Y.; Hoffmann, J.M.A.; Oscarsson, J.; Dinudom, A.; Mather, T.J.; Cook, D.I.; Hunt, N.H.; Caterson, I.D.; Holmes, A.J.; Storlien, L.H. Effects of dietary fat profile on gut permeability and microbiota and their relationships with metabolic changes in mice. *Obesity* **2015**, *23*, 1429-1439, doi:10.1002/oby.21122.
234. Devkota, S.; Wang, Y.W.; Musch, M.W.; Leone, V.; Fehlner-Peach, H.; Nadimpalli, A.; Antonopoulos, D.A.; Jabri, B.; Chang, E.B. Dietary-fat-induced taurocholic acid promotes pathobiont expansion and colitis in Il10(-/-) mice. *Nature* **2012**, *487*, 104-+, doi:10.1038/nature11225.
235. Singh, R.K.; Chang, H.W.; Yan, D.; Lee, K.M.; Ucmak, D.; Wong, K.; Abrouk, M.; Farahnik, B.; Nakamura, M.; Zhu, T.H.; Bhutani, T.; Liao, W. Influence of diet on the gut microbiome and implications for human health. *J Transl Med* **2017**, *15*, doi:ARTN 73

10.1186/s12967-017-1175-y.
236. Org, E.; Parks, B.W.; Joo, J.W.; Emert, B.; Schwartzman, W.; Kang, E.Y.; Mehrabian, M.; Pan, C.; Knight, R.; Gunsalus, R.; Drake, T.A.; Eskin, E.; Lusis, A.J. Genetic and environmental control of host-gut microbiota interactions. *Genome Res* **2015**, *25*, 1558-1569, doi:10.1101/gr.194118.115.
237. Nagakura, Y.; Ito, H.; Kiso, T.; Naitoh, Y.; Miyata, K. The selective 5-hydroxytryptamine (5-HT)4-receptor agonist RS67506 enhances lower intestinal propulsion in mice. *Japanese journal of pharmacology* **1997**, *74*, 209-212, doi:10.1254/jjp.74.209.
238. Kelly, J.R.; Borre, Y.; C, O.B.; Patterson, E.; El Aidy, S.; Deane, J.; Kennedy, P.J.; Beers, S.; Scott, K.; Moloney, G.; Hoban, A.E.; Scott, L.; Fitzgerald, P.; Ross, P.; Stanton, C.; Clarke, G.; Cryan, J.F.; Dinan, T.G. Transferring the blues: Depression-associated gut microbiota induces neurobehavioural changes in the rat. *Journal of psychiatric research* **2016**, *82*, 109-118, doi:10.1016/j.jpsychires.2016.07.019.
239. Parada, A.E.; Needham, D.M.; Fuhrman, J.A. Every base matters: assessing small subunit rRNA primers for marine microbiomes with mock communities, time series and global field samples. *Environ Microbiol* **2016**, *18*, 1403-1414, doi:10.1111/1462-2920.13023.
240. Apprill, A.; McNally, S.; Parsons, R.; Weber, L. Minor revision to V4 region SSU rRNA 806R gene primer greatly increases detection of SAR11 bacterioplankton. *Aqaut Microb Ecol* **2015**, *75*, 129-137.
241. Martin, M. Cutadapt removes adapter sequences from high-throughput sequencing reads. *EMBnet. journal* **2011**, *17*, 10-12.
242. Bolyen, E.; Rideout, J.R.; Dillon, M.R.; Bokulich, N.A.; Abnet, C.C.; Al-Ghalith, G.A.; Alexander, H.; Alm, E.J.; Arumugam, M.; Asnicar, F.; Bai, Y.; Bisanz, J.E.; Bittinger, K.; Brejnrod, A.; Brislawn, C.J.; Brown, C.T.; Callahan, B.J.; Caraballo-Rodriguez, A.M.; Chase, J.; Cope, E.K.; Da Silva, R.; Diener, C.; Dorrestein, P.C.; Douglas, G.M.; Durall, D.M.; Duvallet, C.; Edwardson, C.F.; Ernst, M.; Estaki, M.; Fouquier, J.; Gauglitz, J.M.; Gibbons, S.M.; Gibson, D.L.; Gonzalez, A.; Gorlick, K.; Guo, J.; Hillmann, B.; Holmes, S.; Holste, H.; Huttenhower, C.; Huttley, G.A.; Janssen, S.; Jarmusch, A.K.; Jiang, L.; Kaehler, B.D.; Kang, K.B.; Keefe, C.R.;

Keim, P.; Kelley, S.T.; Knights, D.; Koester, I.; Kosciolek, T.; Kreps, J.; Langille, M.G.I.; Lee, J.; Ley, R.; Liu, Y.X.; Loftfield, E.; Lozupone, C.; Maher, M.; Marotz, C.; Martin, B.D.; McDonald, D.; McIver, L.J.; Melnik, A.V.; Metcalf, J.L.; Morgan, S.C.; Morton, J.T.; Naimey, A.T.; Navas-Molina, J.A.; Nothias, L.F.; Orchanian, S.B.; Pearson, T.; Peoples, S.L.; Petras, D.; Preuss, M.L.; Pruesse, E.; Rasmussen, L.B.; Rivers, A.; Robeson, M.S., 2nd; Rosenthal, P.; Segata, N.; Shaffer, M.; Shiffer, A.; Sinha, R.; Song, S.J.; Spear, J.R.; Swafford, A.D.; Thompson, L.R.; Torres, P.J.; Trinh, P.; Tripathi, A.; Turnbaugh, P.J.; Ul-Hasan, S.; van der Hooft, J.J.J.; Vargas, F.; Vazquez-Baeza, Y.; Vogtmann, E.; von Hippel, M.; Walters, W.; Wan, Y.; Wang, M.; Warren, J.; Weber, K.C.; Williamson, C.H.D.; Willis, A.D.; Xu, Z.Z.; Zaneveld, J.R.; Zhang, Y.; Zhu, Q.; Knight, R.; Caporaso, J.G. Reproducible, interactive, scalable and extensible microbiome data science using QIIME 2. *Nature biotechnology* **2019**, *37*, 852-857, doi:10.1038/s41587-019-0209-9.

243. Callahan, B.J.; McMurdie, P.J.; Rosen, M.J.; Han, A.W.; Johnson, A.J.; Holmes, S.P. DADA2: High-resolution sample inference from Illumina amplicon data. *Nature methods* **2016**, *13*, 581-583, doi:10.1038/nmeth.3869.
244. Wang, J.; Zhang, Q.; Wu, G.; Zhang, C.; Zhang, M.; Zhao, L. Minimizing spurious features in 16S rRNA gene amplicon sequencing. *PeerJ Preprints* **2018**, 10.7287/peerj.preprints.26872v1, 2167-9843, doi:10.7287/peerj.preprints.26872v1.
245. Bokulich, N.A.; Kaehler, B.D.; Rideout, J.R.; Dillon, M.; Bolyen, E.; Knight, R.; Huttley, G.A.; Gregory Caporaso, J. Optimizing taxonomic classification of marker-gene amplicon sequences with QIIME 2's q2-feature-classifier plugin. *Microbiome* **2018**, *6*, 90, doi:10.1186/s40168-018-0470-z.
246. Quast, C.; Pruesse, E.; Yilmaz, P.; Gerken, J.; Schweer, T.; Yarza, P.; Peplies, J.; Glockner, F.O. The SILVA ribosomal RNA gene database project: improved data processing and web-based tools. *Nucleic acids research* **2013**, *41*, D590-596, doi:10.1093/nar/gks1219.
247. Paradis, E.; Claude, J.; Strimmer, K. APE: Analyses of Phylogenetics and Evolution in R language. *Bioinformatics* **2004**, *20*, 289-290, doi:10.1093/bioinformatics/btg412 %J Bioinformatics.
248. Liaw, A.W., M. . Classification and regression by randomForest. *R news* **2002**, *2*, 18-22.
249. Wickham, H. ggplot2: elegant graphics for data analysis. *Springer* **2016**, 10.18637/jss.v077.b02, doi:10.18637/jss.v077.b02.
250. Kolde, R. pheatmap: Pretty Heatmaps. *R package version 1.0. 8* **2015**.
251. Bland, J.M.; Altman, D.G. Calculating correlation coefficients with repeated observations: Part 1--Correlation within subjects. *BMJ* **1995**, *310*, 446, doi:10.1136/bmj.310.6977.446.
252. Wu, G.; Zhao, N.; Zhang, C.; Lam, Y.Y.; Zhao, L. Guild-based analysis for understanding gut microbiome in human health and diseases. *Genome Med* **2021**, *13*, 22, doi:10.1186/s13073-021-00840-y.
253. García-Villalba, R.; Giménez-Bastida, J.A.; García-Conesa, M.T.; Tomás-Barberán, F.A.; Carlos Espín, J.; Larrosa, M. Alternative method for gas chromatography-mass spectrometry analysis of short-chain fatty acids in faecal samples. *Journal of separation science* **2012**, *35*, 1906-1913, doi:10.1002/jssc.201101121.
254. Muller, M.; Hermes, G.D.A.; Canfora, E.E.; Smidt, H.; Masclee, A.A.M.; Zoetendal, E.G.; Blaak, E.E. Distal colonic transit is linked to gut microbiota diversity and

microbial fermentation in humans with slow colonic transit. *Am J Physiol-Gastr L* **2020**, *318*, G361-G369, doi:10.1152/ajpgi.00283.2019.

255. Faust, K.; Raes, J. Microbial interactions: from networks to models. *Nat Rev Microbiol* **2012**, *10*, 538-550, doi:10.1038/nrmicro2832.
256. Simberloff, D.; Dayan, T. The guild concept and the structure of ecological communities. *Annual review of ecology and systematics* **1991**, *22*, 115-143.
257. Kaczocha, M.; Glaser, S.T.; Deutsch, D.G. Identification of intracellular carriers for the endocannabinoid anandamide. *Proceedings of the National Academy of Sciences of the United States of America* **2009**, *106*, 6375-6380, doi:10.1073/pnas.0901515106.
258. Partosoedarso, E.R.; Abrahams, T.P.; Scullion, R.T.; Moerschbaecher, J.M.; Hornby, P.J. Cannabinoid1 receptor in the dorsal vagal complex modulates lower oesophageal sphincter relaxation in ferrets. *The Journal of physiology* **2003**, *550*, 149-158, doi:10.1113/jphysiol.2003.042242.
259. Vianna, C.R.; Donato, J., Jr.; Rossi, J.; Scott, M.; Economides, K.; Gautron, L.; Pierpont, S.; Elias, C.F.; Elmquist, J.K. Cannabinoid receptor 1 in the vagus nerve is dispensable for body weight homeostasis but required for normal gastrointestinal motility. *The Journal of neuroscience : the official journal of the Society for Neuroscience* **2012**, *32*, 10331-10337, doi:10.1523/jneurosci.4507-11.2012.
260. DiPatrizio, N.V. Endocannabinoids in the Gut. *Cannabis and cannabinoid research* **2016**, *1*, 67-77, doi:10.1089/can.2016.0001.
261. Roager, H.M.; Hansen, L.B.S.; Bahl, M.I.; Frandsen, H.L.; Carvalho, V.; Gobel, R.J.; Dalgaard, M.D.; Plichta, D.R.; Sparholt, M.H.; Vestergaard, H.; Hansen, T.; Sicheritz-Ponten, T.; Nielsen, H.B.; Pedersen, O.; Lauritzen, L.; Kristensen, M.; Gupta, R.; Licht, T.R. Colonic transit time is related to bacterial metabolism and mucosal turnover in the gut. *Nat Microbiol* **2016**, *1*, doi:Artn 16093

10.1038/Nmicrobiol.2016.93.

262. Xu, Y.; Wang, N.; Tan, H.Y.; Li, S.; Zhang, C.; Feng, Y.B. Function of Akkermansia muciniphila in Obesity: Interactions With Lipid Metabolism, Immune Response and Gut Systems. *Front Microbiol* **2020**, *11*, doi:ARTN 219

10.3389/fmicb.2020.00219.

263. Heeney, D.D.; Gareau, M.G.; Marco, M.L. Intestinal Lactobacillus in health and disease, a driver or just along for the ride? *Curr Opin Biotechnol* **2018**, *49*, 140-147, doi:10.1016/j.copbio.2017.08.004.
264. Wang, P.; Li, D.; Ke, W.; Liang, D.; Hu, X.; Chen, F. Resveratrol-induced gut microbiota reduces obesity in high-fat diet-fed mice. *Int J Obes (Lond)* **2020**, *44*, 213-225, doi:10.1038/s41366-019-0332-1.
265. Zhou, L.; Ni, Z.X.; Yu, J.; Cheng, W.; Cai, Z.L.; Yu, C.Q. Correlation Between Fecal Metabolomics and Gut Microbiota in Obesity and Polycystic Ovary Syndrome. *Front Endocrinol* **2020**, *11*, doi:ARTN 628

10.3389/fendo.2020.00628.

266. Chen, L.W.; Xu, J.; Soh, S.E.; Aris, I.M.; Tint, M.T.; Gluckman, P.D.; Tan, K.H.; Shek, L.P.C.; Chong, Y.S.; Yap, F.; Godfrey, K.M.; Gilbert, J.A.; Karnani, N.; Lee, Y.S. Implication of gut microbiota in the association between infant antibiotic exposure and childhood obesity and adiposity accumulation. *Int J Obesity* **2020**, *44*, 1508-1520, doi:10.1038/s41366-020-0572-0.
267. Won, S.M.; Chen, S.; Lee, S.Y.; Lee, K.E.; Park, K.W.; Yoon, J.H. Lactobacillus sakei ADM14 Induces Anti-Obesity Effects and Changes in Gut Microbiome in High-Fat Diet-Induced Obese Mice. *Nutrients* **2020**, *12*, doi:10.3390/nu12123703.

268. Wang, J.; Tang, H.; Zhang, C.; Zhao, Y.; Derrien, M.; Rocher, E.; van-Hylckama Vlieg, J.E.; Strissel, K.; Zhao, L.; Obin, M.; Shen, J. Modulation of gut microbiota during probiotic-mediated attenuation of metabolic syndrome in high fat diet-fed mice. *ISME J* **2015**, *9*, 1-15, doi:10.1038/ismej.2014.99.
269. Naudin, C.R.; Maner-Smith, K.; Owens, J.A.; Wynn, G.M.; Robinson, B.S.; Matthews, J.D.; Reedy, A.R.; Luo, L.; Wolfarth, A.A.; Darby, T.M.; Ortlund, E.A.; Jones, R.M. Lactococcus lactis Subspecies cremoris Elicits Protection Against Metabolic Changes Induced by a Western-Style Diet. *Gastroenterology* **2020**, *159*, 639-651 e635, doi:10.1053/j.gastro.2020.03.010.
270. Loubinoux, J.; Bronowicki, J.P.; Pereira, I.A.C.; Mougenel, J.L.; Le Faou, A.E. Sulfate-reducing bacteria in human feces and their association with inflammatory bowel diseases. *Fems Microbiol Ecol* **2002**, *40*, 107-112, doi:PII S0168-6496(02)00201-5

DOI 10.1111/j.1574-6941.2002.tb00942.x.
271. Zhang, C.H.; Zhang, M.H.; Wang, S.Y.; Han, R.J.; Cao, Y.F.; Hua, W.Y.; Mao, Y.J.; Zhang, X.J.; Pang, X.Y.; Wei, C.C.; Zhao, G.P.; Chen, Y.; Zhao, L.P. Interactions between gut microbiota, host genetics and diet relevant to development of metabolic syndromes in mice (vol 4, pg 232, 2010). *Isme Journal* **2010**, *4*, 312-313, doi:10.1038/ismej.2009.144.
272. Li, J.; Pang, B.; Shao, D.; Jiang, C.; Hu, X.; Shi, J. Artemisia sphaerocephala Krasch polysaccharide mediates lipid metabolism and metabolic endotoxaemia in associated with the modulation of gut microbiota in diet-induced obese mice. *Int J Biol Macromol* **2020**, *147*, 1008-1017, doi:10.1016/j.ijbiomac.2019.10.069.
273. Allen, J.M.; Mailing, L.J.; Niemiro, G.M.; Moore, R.; Cook, M.D.; White, B.A.; Holscher, H.D.; Woods, J.A. Exercise Alters Gut Microbiota Composition and Function in Lean and Obese Humans. *Med Sci Sports Exerc* **2018**, *50*, 747-757, doi:10.1249/MSS.0000000000001495.
274. Barton, W.; Penney, N.C.; Cronin, O.; Garcia-Perez, I.; Molloy, M.G.; Holmes, E.; Shanahan, F.; Cotter, P.D.; O'Sullivan, O. The microbiome of professional athletes differs from that of more sedentary subjects in composition and particularly at the functional metabolic level. *Gut* **2018**, *67*, 625-633, doi:10.1136/gutjnl-2016-313627.
275. Grosicki, G.J.; Fielding, R.A.; Lustgarten, M.S. Gut Microbiota Contribute to Age-Related Changes in Skeletal Muscle Size, Composition, and Function: Biological Basis for a Gut-Muscle Axis. *Calcified Tissue Int* **2018**, *102*, 433-442, doi:10.1007/s00223-017-0345-5.
276. Frampton, J.; Murphy, K.G.; Frost, G.; Chambers, E.S. Short-chain fatty acids as potential regulators of skeletal muscle metabolism and function. *Nature Metabolism* **2020**, *2*, 840-848, doi:10.1038/s42255-020-0188-7.
277. Morita, H.; Kano, C.; Ishii, C.; Kagata, N.; Ishikawa, T.; Uchiyama, Y.; Hara, S.; Nakamura, T.; Fukuda, S.J.b. Bacteroides uniformis enhances endurance exercise performance through gluconeogenesis. **2020**.
278. den Besten, G.; Bleeker, A.; Gerding, A.; van Eunen, K.; Havinga, R.; van Dijk, T.H.; Oosterveer, M.H.; Jonker, J.W.; Groen, A.K.; Reijngoud, D.J.; Bakker, B.M. Short-Chain Fatty Acids Protect Against High-Fat Diet-Induced Obesity via a PPARγ-Dependent Switch From Lipogenesis to Fat Oxidation. *Diabetes* **2015**, *64*, 2398-2408, doi:10.2337/db14-1213.
279. Lu, Y.; Fan, C.; Li, P.; Lu, Y.; Chang, X.; Qi, K. Short Chain Fatty Acids Prevent High-fat-diet-induced Obesity in Mice by Regulating G Protein-coupled Receptors and Gut Microbiota. *Scientific reports* **2016**, *6*, 37589, doi:10.1038/srep37589.

280. Gao, Z.; Yin, J.; Zhang, J.; Ward, R.E.; Martin, R.J.; Lefevre, M.; Cefalu, W.T.; Ye, J. Butyrate improves insulin sensitivity and increases energy expenditure in mice. *Diabetes* **2009**, *58*, 1509-1517, doi:10.2337/db08-1637.
281. Wong, J.M.; de Souza, R.; Kendall, C.W.; Emam, A.; Jenkins, D.J. Colonic health: fermentation and short chain fatty acids. *J Clin Gastroenterol* **2006**, *40*, 235-243, doi:10.1097/00004836-200603000-00015.
282. Tottey, W.; Feria-Gervasio, D.; Gaci, N.; Laillet, B.; Pujos, E.; Martin, J.F.; Sebedio, J.L.; Sion, B.; Jarrige, J.F.; Alric, M.; Brugere, J.F. Colonic Transit Time Is a Driven Force of the Gut Microbiota Composition and Metabolism: In Vitro Evidence. *Journal of neurogastroenterology and motility* **2017**, *23*, 124-134, doi:10.5056/jnm16042.
283. Kopp, W. How Western Diet And Lifestyle Drive The Pandemic Of Obesity And Civilization Diseases. *Diabetes, metabolic syndrome and obesity : targets and therapy* **2019**, *12*, 2221-2236, doi:10.2147/dmso.S216791.
284. Kaplan, L.M.J.G. Leptin, obesity, and liver disease. **1998**, *115*, 997-1001.
285. San-Cristobal, R.; Navas-Carretero, S.; Martínez-González, M.Á.; Ordovas, J.M.; Martínez, J.A. Contribution of macronutrients to obesity: implications for precision nutrition. *Nature Reviews Endocrinology* **2020**, *16*, 305-320, doi:10.1038/s41574-020-0346-8.
286. Hruby, A.; Hu, F.B.J.P. The epidemiology of obesity: a big picture. **2015**, *33*, 673-689.
287. Canbay, A.; Bechmann, L.; Gerken, G.J.Z.f.G. Lipid metabolism in the liver. **2007**, *45*, 35-41.
288. Berlanga, A.; Guiu-Jurado, E.; Porras, J.A.; Auguet, T.J.C.; gastroenterology, e. Molecular pathways in non-alcoholic fatty liver disease. **2014**, *7*, 221.
289. Frohnert, B.I.; Jacobs, D.R., Jr.; Steinberger, J.; Moran, A.; Steffen, L.M.; Sinaiko, A.R. Relation between serum free fatty acids and adiposity, insulin resistance, and cardiovascular risk factors from adolescence to adulthood. *Diabetes* **2013**, *62*, 3163-3169, doi:10.2337/db12-1122.
290. Zhang, J.; Zhao, Y.; Xu, C.; Hong, Y.; Lu, H.; Wu, J.; Chen, Y. Association between serum free fatty acid levels and nonalcoholic fatty liver disease: a cross-sectional study. *Scientific reports* **2014**, *4*, 5832, doi:10.1038/srep05832.
291. Nguyen, P.; Leray, V.; Diez, M.; Serisier, S.; Bloc'h, J.L.; Siliart, B.; Dumon, H.J.J.o.a.p.; nutrition, a. Liver lipid metabolism. **2008**, *92*, 272-283.
292. Sweetser, D.A.; Birkenmeier, E.H.; Hoppe, P.C.; McKeel, D.W.; Gordon, J.I. Mechanisms underlying generation of gradients in gene expression within the intestine: an analysis using transgenic mice containing fatty acid binding protein-human growth hormone fusion genes. *Genes & development* **1988**, *2*, 1318-1332, doi:10.1101/gad.2.10.1318.
293. Nemecz, G.; Schroeder, F. Selective binding of cholesterol by recombinant fatty acid binding proteins. *The Journal of biological chemistry* **1991**, *266*, 17180-17186.
294. Stefan, N.; Kantartzis, K.; Machann, J.; Schick, F.; Thamer, C.; Rittig, K.; Balletshofer, B.; Machicao, F.; Fritsche, A.; Häring, H.U. Identification and characterization of metabolically benign obesity in humans. *Archives of internal medicine* **2008**, *168*, 1609-1616, doi:10.1001/archinte.168.15.1609.
295. Blüher, M. Metabolically Healthy Obesity. *Endocrine reviews* **2020**, *41*, 405-420, doi:10.1210/endrev/bnaa004.
296. Seruggia, D.; Montoliu, L. The new CRISPR-Cas system: RNA-guided genome engineering to efficiently produce any desired genetic alteration in animals. *Transgenic research* **2014**, *23*, 707-716, doi:10.1007/s11248-014-9823-y.

297. Wang, H.; Yang, H.; Shivalila, C.S.; Dawlaty, M.M.; Cheng, A.W.; Zhang, F.; Jaenisch, R. One-step generation of mice carrying mutations in multiple genes by CRISPR/Cas-mediated genome engineering. *Cell* **2013**, *153*, 910-918, doi:10.1016/j.cell.2013.04.025.
298. Jinek, M.; Chylinski, K.; Fonfara, I.; Hauer, M.; Doudna, J.A.; Charpentier, E. A programmable dual-RNA-guided DNA endonuclease in adaptive bacterial immunity. *Science (New York, N.Y.)* **2012**, *337*, 816-821, doi:10.1126/science.1225829.
299. Zhan, T.; Rindtorff, N.; Betge, J.; Ebert, M.P.; Boutros, M. CRISPR/Cas9 for cancer research and therapy. *Seminars in Cancer Biology* **2019**, *55*, 106-119, doi:https://doi.org/10.1016/j.semcancer.2018.04.001.
300. Harno, E.; Cottrell, Elizabeth C.; White, A. Metabolic Pitfalls of CNS Cre-Based Technology. *Cell Metab* **2013**, *18*, 21-28, doi:https://doi.org/10.1016/j.cmet.2013.05.019.
301. McLean, J.A.; Tobin, G. *Animal and Human Calorimetry*; Cambridge University Press: Cambridge, **1988**; DOI: 10.1017/CBO9780511663161.
302. Nagakura, Y.; Naitoh, Y.; Kamato, T.; Yamano, M.; Miyata, K. Compounds possessing 5-HT3 receptor antagonistic activity inhibit intestinal propulsion in mice. *European journal of pharmacology* **1996**, *311*, 67-72, doi:10.1016/0014-2999(96)00403-7.
303. Ma, X.; Hamadeh, M.J.; Christie, B.R.; Foster, J.A.; Tarnopolsky, M.A. Impact of treadmill running and sex on hippocampal neurogenesis in the mouse model of amyotrophic lateral sclerosis. *PloS one* **2012**, *7*, e36048, doi:10.1371/journal.pone.0036048.
304. Tanner, C.B.; Madsen, S.R.; Hallowell, D.M.; Goring, D.M.; Moore, T.M.; Hardman, S.E.; Heninger, M.R.; Atwood, D.R.; Thomson, D.M. Mitochondrial and performance adaptations to exercise training in mice lacking skeletal muscle LKB1. *American journal of physiology. Endocrinology and metabolism* **2013**, *305*, E1018-1029, doi:10.1152/ajpendo.00227.2013.
305. Bradford, M.M. A rapid and sensitive method for the quantitation of microgram quantities of protein utilizing the principle of protein-dye binding. *Analytical biochemistry* **1976**, *72*, 248-254, doi:10.1006/abio.1976.9999.
306. Folch, J.; Lees, M.; Sloane Stanley, G.H. A simple method for the isolation and purification of total lipides from animal tissues. *The Journal of biological chemistry* **1957**, *226*, 497-509.
307. Huynh, F.K.; Green, M.F.; Koves, T.R.; Hirschey, M.D. Measurement of fatty acid oxidation rates in animal tissues and cell lines. *Methods in enzymology* **2014**, *542*, 391-405, doi:10.1016/b978-0-12-416618-9.00020-0.
308. Coburn, C.T.; Knapp, F.F., Jr.; Febbraio, M.; Beets, A.L.; Silverstein, R.L.; Abumrad, N.A. Defective uptake and utilization of long chain fatty acids in muscle and adipose tissues of CD36 knockout mice. *The Journal of biological chemistry* **2000**, *275*, 32523-32529, doi:10.1074/jbc.M003826200.
309. Hagberg, C.E.; Falkevall, A.; Wang, X.; Larsson, E.; Huusko, J.; Nilsson, I.; van Meeteren, L.A.; Samen, E.; Lu, L.; Vanwildemeersch, M.; Klar, J.; Genove, G.; Pietras, K.; Stone-Elander, S.; Claesson-Welsh, L.; Ylä-Herttuala, S.; Lindahl, P.; Eriksson, U. Vascular endothelial growth factor B controls endothelial fatty acid uptake. *Nature* **2010**, *464*, 917-921, doi:10.1038/nature08945.
310. van Diepen, J.A.; Stienstra, R.; Vroegrijk, I.O.; van den Berg, S.A.; Salvatori, D.; Hooiveld, G.J.; Kersten, S.; Tack, C.J.; Netea, M.G.; Smit, J.W.; Joosten, L.A.; Havekes, L.M.; van Dijk, K.W.; Rensen, P.C. Caspase-1 deficiency in mice

reduces intestinal triglyceride absorption and hepatic triglyceride secretion. *Journal of lipid research* **2013**, *54*, 448-456, doi:10.1194/jlr.M031963.

311. Bass, N.M. Function and regulation of hepatic and intestinal fatty acid binding proteins. *Chemistry and physics of lipids* **1985**, *38*, 95-114, doi:10.1016/0009-3084(85)90060-x.
312. Hruby, A.; Hu, F.B. The Epidemiology of Obesity: A Big Picture. *PharmacoEconomics* **2015**, *33*, 673-689, doi:10.1007/s40273-014-0243-x.
313. Gallagher, T.K.; Geoghegan, J.G.; Baird, A.W.; Winter, D.C. Implications of Altered Gastrointestinal Motility in Obesity. *Obesity Surgery* **2007**, *17*, 1399-1407, doi:10.1007/s11695-007-9221-0.
314. Severinsen, M.C.K.; Pedersen, B.K. Muscle-Organ Crosstalk: The Emerging Roles of Myokines. *Endocrine reviews* **2020**, *41*, 594-609, doi:10.1210/endrev/bnaa016.
315. Bay, M.L.; Pedersen, B.K. Muscle-Organ Crosstalk: Focus on Immunometabolism. *Frontiers in physiology* **2020**, *11*, 567881, doi:10.3389/fphys.2020.567881.
316. Newberry, E.P.; Kennedy, S.M.; Xie, Y.; Sternard, B.T.; Luo, J.; Davidson, N.O. Diet-induced obesity and hepatic steatosis in L-Fabp / mice is abrogated with SF, but not PUFA, feeding and attenuated after cholesterol supplementation. *American journal of physiology. Gastrointestinal and liver physiology* **2008**, *294*, G307-314, doi:10.1152/ajpgi.00377.2007.
317. Newberry, E.P.; Kennedy, S.M.; Xie, Y.; Luo, J.; Davidson, N.O. Diet-induced alterations in intestinal and extrahepatic lipid metabolism in liver fatty acid binding protein knockout mice. *Molecular and cellular biochemistry* **2009**, *326*, 79-86, doi:10.1007/s11010-008-0002-4.
318. Fabbrini, E.; Sullivan, S.; Klein, S. Obesity and nonalcoholic fatty liver disease: biochemical, metabolic, and clinical implications. *Hepatology (Baltimore, Md.)* **2010**, *51*, 679-689, doi:10.1002/hep.23280.
319. Link, J.C.; Reue, K. Genetic Basis for Sex Differences in Obesity and Lipid Metabolism. *Annual review of nutrition* **2017**, *37*, 225-245, doi:10.1146/annurev-nutr-071816-064827.
320. Baars, A.; Oosting, A.; Lohuis, M.; Koehorst, M.; El Aidy, S.; Hugenholtz, F.; Smidt, H.; Mischke, M.; Boekschoten, M.V.; Verkade, H.J.; Garssen, J.; van der Beek, E.M.; Knol, J.; de Vos, P.; van Bergenhenegouwen, J.; Fransen, F. Sex differences in lipid metabolism are affected by presence of the gut microbiota. *Scientific reports* **2018**, *8*, 13426, doi:10.1038/s41598-018-31695-w.
321. Weisiger, R.A. Cytoplasmic transport of lipids: Role of binding proteins. *Comparative Biochemistry and Physiology Part B: Biochemistry and Molecular Biology* **1996**, *115*, 319-331, doi:https://doi.org/10.1016/S0305-0491(96)00179-4.
322. Chmurzyńska, A. The multigene family of fatty acid-binding proteins (FABPs): Function, structure and polymorphism. *Journal of Applied Genetics* **2006**, *47*, 39-48, doi:10.1007/BF03194597.
323. Bass, N.M. Fatty acid-binding protein expression in the liver: its regulation and relationship to the zonation of fatty acid metabolism. *Molecular and cellular biochemistry* **1990**, *98*, 167-176, doi:10.1007/BF00231381.
324. Yabuki, Y.; Matsuo, K.; Kawahata, I.; Fukui, N.; Mizobata, T.; Kawata, Y.; Owada, Y.; Shioda, N.; Fukunaga, K. Fatty Acid Binding Protein 3 Enhances the Spreading and Toxicity of α-Synuclein in Mouse Brain. *International journal of molecular sciences* **2020**, *21*, doi:10.3390/ijms21062230.
325. Morita, H.; Kano, C.; Ishii, C.; Kagata, N.; Ishikawa, T.; Uchiyama, Y.; Hara, S.; Nakamura, T.; Fukuda, S. Bacteroides enhances endurance exercise performance

through gluconeogenesis. *bioRxiv* **2020**, 10.1101/2020.03.04.975730, 2020.2003.2004.975730, doi:10.1101/2020.03.04.975730.

326. Newberry, E.P.; Kennedy, S.; Xie, Y.; Luo, J.; Jiang, H.; Ory, D.S.; Davidson, N.O. Phenotypic divergence in two lines of L-Fabp-/- mice reflects substrain differences and environmental modifiers. *American journal of physiology. Gastrointestinal and liver physiology* **2015**, *309*, G648-G661, doi:10.1152/ajpgi.00170.2015.
327. Massimino, S.P.; McBurney, M.I.; Field, C.J.; Thomson, A.B.R.; Keelan, M.; Hayek, M.G.; Sunvold, G.D. Fermentable Dietary Fiber Increases GLP-1 Secretion and Improves Glucose Homeostasis Despite Increased Intestinal Glucose Transport Capacity in Healthy Dogs. *The Journal of nutrition* **1998**, *128*, 1786-1793, doi:10.1093/jn/128.10.1786 %J The Journal of Nutrition.
328. Luxon, B.A.; Weisiger, R.A. Sex differences in intracellular fatty acid transport: role of cytoplasmic binding proteins. *The American journal of physiology* **1993**, *265*, G831-841, doi:10.1152/ajpgi.1993.265.5.G831.